UNIVERSIDADE ESTADUAL PAULISTA – UNESP

CAMPUS DE JABOTICABAL

XAC4296: A multidomain and exclusive *Xanthomonadaceae* protein related to chromosome segregation, cell division, and bacterial fitness

Amanda Carolina Paulino de Oliveira

Bióloga

2021

UNIVERSIDADE ESTADUAL PAULISTA – UNESP

CAMPUS DE JABOTICABAL

XAC4296: A multidomain and exclusive *Xanthomonadaceae* protein related to chromosome segregation, cell division, and bacterial fitness

Discente: Amanda Carolina Paulino de Oliveira

Orientador: Dr. Alessandro de Mello Varani

Coorientador: Prof. Dr. Henrique Ferreira

Coorientador: Dr. Rafael Marini Ferreira

Tese apresentada à Faculdade de Ciências Agrárias e Veterinárias – Unesp, Câmpus de Jaboticabal, como parte das exigências para a obtenção do título de Doutor em Microbiologia Agropecuária

2021

Ficha catalográfica

O48x

Oliveira, Amanda Carolina Paulino de

XAC4296: A multidomain and exclusive Xanthomonadaceae protein related to chromosome segregation, cell division, and bacterial fitness / Amanda Carolina Paulino de Oliveira. -- Jaboticabal, 2022

142 p. : il., tabs., fotos

Tese (doutorado) - Universidade Estadual Paulista (Unesp), Faculdade de Ciências Agrárias e Veterinárias, Jaboticabal

Orientador: Alessandro de Mello Varani

Coorientador: Rafael Marini Ferreira

1. Biologia molecular. 2. Microbiologia. 3. Genética microbiana. 4. Cancro (Fitopatologia). I. Título.

Sistema de geração automática de fichas catalográficas da Unesp. Biblioteca da Faculdade de Ciências Agrárias e Veterinárias, Jaboticabal. Dados fornecidos pelo autor(a).

unesp

UNIVERSIDADE ESTADUAL PAULISTA

Câmpus de Jaboticabal

CERTIFICADO DE APROVAÇÃO

TÍTULO DA TESE: XAC4296: A MULTIDOMAIN AND EXCLUSIVE *Xanthomonadaceae* PROTEIN RELATED TO CHROMOSOME SEGREGATION, CELL DIVISION, AND BACTERIAL *fitness*

AUTORA: AMANDA CAROLINA PAULINO DE OLIVEIRA
ORIENTADOR: ALESSANDRO DE MELLO VARANI
COORIENTADOR: RAFAEL MARINI FERREIRA
COORIENTADOR: HENRIQUE FERREIRA

Aprovada como parte das exigências para obtenção do Título de Doutora em MICROBIOLOGIA AGROPECUÁRIA, pela Comissão Examinadora:

Prof. Dr. ALESSANDRO DE MELLO VARANI (Participaçao Virtual)
Departamento de Biotecnologia Agropecuaria e Ambiental / FCAV UNESP Jaboticabal

Profa. Dra. ALESSANDRA ALVES DE SOUZA (Participaçao Virtual)
Instituto Agronômico de Campinas / Cordeirópolis/SP

Prof. Dr. JACKSON ANTONIO MARCONDES DE SOUZA (Participaçao Virtual)
Departamento de Biologia / FCAV / UNESP - Jaboticabal

Pós-Doutoranda FLÁVIA CAMPOS (Participaçao Virtual)
Microbiology and Plant Pathology Department - University of California / Riverside/EUA

Prof. Dr. LEANDRO MOREIRA (Participaçao Virtual)
Departamento de Ciências Biológicas da Universidade Federal de Ouro Preto / Ouro Preto/MG

Jaboticabal, 13 de maio de 2022

CURRICULAR DATA OF THE AUTHOR

AMANDA CAROLINA PAULINO DE OLIVEIRA - born on February 18, 1993 in Santa Adelia, São Paulo, Brazil. Bachelor's degree in Biology at the Faculty of Agricultural and Veterinary Sciences - Unesp/FCAV, Jaboticabal Campus (2012-2015). Participated in the "Intralab" extension project related to chemical waste management (2012). Developed the scientific research at the Laboratory of Biochemistry and Molecular Biology (LBM): "PATHOGENICITY AND VIRULENCE EVALUATION FOR THE MUTANT *mlt* and *mltB* OF *Xanthomonas citri* subsp. *citri*" under the supervision of Prof. Dr. Jesus Aparecido Ferro (2013-2015). In 2016, joined the Agricultural and Livestock Microbiology Graduation Program, Faculty of Agricultural and Veterinary Sciences - Unesp/FCAV at the Technology Department, Laboratory of Biochemistry and Molecular Biology (LBM) under the supervision of Prof. Dr. Alessandro de Mello Varani and Dr. Rafael Marini Ferreira. The dissertation project was developed as a fellow at the Coordination for the Improvement of Higher Education Personnel (CAPES). Participated as a collaborator of the "BIGA PROJECT" (Bioinformatics, Genomic and Associated - CAPES). In the same period, joined a science degree in Biology from the Faculty of Agricultural and Veterinary Sciences - Unesp/FCAV, FCAV (2016-2018). In August 2018, Joined the doctorate in the Agricultural and Livestock Microbiology Graduation Program, Faculty of Agricultural and Veterinary Sciences - Unesp/FCAV at the Department of Agricultural and Environmental Biotechnology, Laboratory of Biochemistry and Molecular Biology (LBM) under the supervision of Prof. Dr. Alessandro de Mello Varani, Prof. Dr. Henrique Ferreira and Dr. Rafael Marini Ferreira. Participated as a collaborator in research projects at the Laboratory of Bacterial Genetics (LGB), Biochemistry and Microbiology Department, Instituto de Biociências, Universidade Estadual Paulista, Rio Claro, Brazil. The thesis project was developed as a fellow at the Coordination for the Improvement of Higher Education Personnel (CAPES).

Acknowledgments

To God for the beautiful life, for the possibilities in my life, and for guiding me in all choices.

To my wonderful family for the love and support in my choices. Thanks for never measuring efforts to conclude my studies. For belief in my dreams and my potential.

To my fiancé Túlio and his family for the patience and incentive for this work.

To my advisors, Dr. Alessandro de Mello Varani, Rafael Marini Ferreira, and Dr. Henrique Ferreira, for the opportunity, patience, and support for this work. Thank you for teaching me and for providing my personal and professional development.

To the professors Dr. Jesus Aparecido Ferro and Dra. Maria Inês Tiraboschi Ferro for the access to the Laboratory of Biochemistry and Molecular Biology and contribution for this work.

To all Unesp/FCAV employees to execute my project. The excellent graduation program "Agricultural and Livestock Microbiology Graduation Program" for accepting me as a course council member.

To my friends of the Laboratory of Biochemistry and Molecular Biology and Technology Department, for the coffees, brunch, company, making my day.

To Dr. Henrique Ferreira for the opportunity and for teaching me. Thank you for being disponible to the laboratory dependences and contributing to this work.

To the Centro de Recursos Biológicos (CREBIO) to contribute to my experience, personal and professional, and help conclude this work.

To all who contributed directly or indirectly to the execution of this work. Those long years would not be easy without you. My most sincere thank you.

This study was financed in part by the Coordenação de Aperfeiçoamento de Pessoal de Nível Superior - Brasil (CAPES) - Finance Code 001.

Certificado da Comissão Interna de Biossegurança

A Comissão Técnica Nacional de Biossegurança aprovou o desenvolvimento do projeto intitulado “XAC4296: A multidomain and exclusive *Xanthomonadaceae* protein related to chromosome segregation, cell division, and bacterial fitness”

RESUMO

Os micro-organismos apresentam um repertório limitado e extremamente adaptável de genes. Muitos destes genes codificam para proteínas contendo um único domínio ou multidomínios proteicos variáveis, sendo que em ambos os casos, esses domínios proteicos podem ser combinados de diferentes maneiras, e assim formar o repertório enzimático total de um genoma. A bactéria fitopatogênica *Xanthomonas citri* subsp. *citri* 306 (*X. citri*), agente etiológico do cancro cítrico tipo A (CC) e considerada uma das doenças mais devastadoras da citricultura, apresenta um repertório de proteínas multidomínios ainda pouco explorado. Neste sentido, estudos recentes demonstraram que as proteínas multidomínios pertencentes a superfamília das Transglicosilases Líticas (LTs), apresentam um papel importante para a biologia de *X. citri*. As LTs, estão relacionadas com o metabolismo do peptidoglicano, portanto, apresentando uma função importante relacionada com a síntese, remodelagem e degradação da parede celular bacteriana. Em particular, dentre as 14 LTs presentes no genoma de *X. citri,* uma é exclusiva para este gênero, e não caracterizada experimentalmente, denominada XAC4296 (XAC_RS21660). Neste trabalho, empregamos métodos *in-silico*, mutação sítio dirigida e caracterização funcional, com a finalidade avaliar o papel que XAC4296 pode desempenhar em *X. citri*. Nossos resultados indicam que a proteína XAC4296 apresenta uma estrutura multidomíno, formada por dois módulos estruturalmente distintos: o primeiro módulo transglicosilase (PG_binding1, SLT_2), e o segundo módulo epimerase (aldose-1-epimerase). Análises filogenéticas e de contexto genômico indicam que XAC4296 provavelmente foi originada por um evento de fusão gênica a partir do ancestral comum para *Xanthomonas*, *Stenotrophomonas* e *Pseudoxanthomonas*. Análises funcionais indicam que o gene XAC4296 é expresso durante a interação patógeno-hospedeiro, porém, não é essencial para *X. citri* ou desenvolvimento do CC, mas influi no ‘fitness’ bacteriano. Além disso, cepas de *X. citri* sem o gene XAC4296 apresentaram células filamentosas e em formato de correntes, com sua massa cromossômica dispersa, porém, ainda apresentando a formação de constrição de septo, desta forma, sugerindo, primeiro o erro de segregação cromossômica e, consequentemente, divisão celular, indicando que a função LT presente neste

gene possa estar relacionada com este fenótipo observado. Em contrapartida, este fenótipo mutante foi completamente restaurado utilizando sacarose como fonte de carbono, e ácido glutâmico, como fonte de nitrogênio, sugerindo que o módulo epimerase da proteína XAC4296 possa contribuir para o metabolismo basal, impactando paralelamente, na divisão celular. Neste sentido foi possível elaborar a hipótese que, na ausência do gene XAC4296 e de precursores das vias metabólicas basais, a produção de piruvato é alterada, levando ao colapso dos mecanismos de segregação cromossômica e divisão celular. Além disso, o fenótipo mutante foi intensificado na presença do antibiótico ampicilina, atingindo 100% das células, sugerindo que como função adicional, a proteína XAC4296 contribui para a resistência a antibióticos β-lactâmicos em *X. citri*. A expressão da fusão mCherry-XAC4296 mostrou a proteína em ambiente citoplasmático, porém a presença de peptídeo sinal sugere uma localização secundária no periplasma, corroborando a hipótese de multifuncionalidade. Esses dados ressaltam o papel das proteínas multidomínio como mecanismo de geração de diversidade enzimática, aumentando sua funcionalidade sem ocasionar expansão genômica, trazendo novos conhecimentos sobre o papel que enzimas multidomínios podem desempenhar em *X. citri.*

Palavras chave: Cancro cítrico, proteínas multidomínios, transglicosilases, epimerase, mCherry.

ABSTRACT

Microorganisms have a limited and highly adaptable repertoire of genes capable of encoding proteins containing a single or variable multi-domains that can be combined in different ways to form the enzymatic repertoire. The phytopathogenic bacteria *Xanthomonas citri* subsp. *citri* (*X. citri*) (*Xanthomonadaceae* family), the etiological agent of Citrus Canker (CC), presents a collection of multi-domain and multi-functional enzymes (MFEs) that remains to be explored. For instance, recent studies have shown that multi-domain proteins belonging to the superfamily of Lytic Transglycosylases (LTs) play an essential role in *X. citri* biology. The LT are enzymes that act on the metabolism of the peptidoglycan and bacterial cell wall. In particular, among the 14 LTs present in the genome of *X. citri*, one is exclusive to this genus and has not yet been experimentally characterized, called XAC4296 (XAC_RS21660), and apart from the Transglycosylase SLT_2 and Peptidoglycan binding-like domains, contains an unexpected epimerase domain linked to the central metabolism; therefore, resembling a canonical MFE. In this work, we experimentally characterized XAC4296 revealing its role as an MFE in *X. citri*, demonstrating their probable gene fusion origin before the closely-related *Xanthomonadaceae* members, *Xanthomonas*, *Xyella*, *Stenotrophomonas*, and *Pseudoxanthomonas* genera differentiation. Interestingly, it is likely that due to the extensive genome reduction, the *Xyella* genus have lost its XAC4296 homolog. In *X. citri*, the XAC4296 is expressed during plant-pathogen interaction, and the Δ4296 shows an impact on CC progression. Moreover, the Δ4296 exhibited chromosome segregation and cell division errors, and sensitivity to ampicillin, suggesting not only the LT activity but also that XAC4296 may also contribute to resistance to β-lactams. However, both Δ4296 phenotypes are partially or wholly restored when the mutant is supplemented with sucrose or glutamic acid as a carbon and nitrogen source, respectively, supporting the epimerase domain's functional relationship with the central carbon and cell wall metabolism. In this sense, it was possible to hypothesize that, when there is a “lack” of the XAC4296 gene and precursors of the basal metabolic pathways, the production of pyruvate is altered, leading to the collapse of the mechanisms of chromosomal segregation and cell division. Furthermore, The expression of the mCherry-XAC4296 fusion showed the

protein in a cytoplasmic environment, but the presence of a signal peptide suggests a secondary location in the periplasm, corroborating the hypothesis of multifunctionality. Taken together, these results elucidate the role of XAC4296 as an MFE in *X. citri*, also bringing new insights into the evolution of multi-domain proteins and antimicrobial resistance in the *Xanthomonadaceae* family.

Keywords: Citrus canker, multidomain protein, transglycosylase, epimerase, mCherry.

LIST OF ABBREVIATIONS

ampC	adenosine monophosphate
Bp	Base pairs
CC	Citrus Canker
DPI	Days post inoculation
Embden-Meyerhof-Parnas	EM
Entner-Doudoroff	ED
Fructose 6-phosphate	F6P
ftsZ	Filamenting temperature-sensitive
galE	UDPgalactose-4-epimerase
gdhZ	Glutamate dehydrogenase
galK	Galactokinase
galM	Aldose-1-epimerase
galT	Galactose-1-phosphateuridylyl transferase
Glucose-6-phosphate	G6P
GMP	5'-guanylic acid
GTFs	Peptidoglycan glycosyltransferases
kidO	NADH-binding oxidoreductase
LB	Luria-Bertani
Lipid II	[GlcNAc-(1,4)-MurNAc-(pentapeptide)-pyrophosphoril-undecaprenol]
LTs	LyticTransglycosylases
manA	mannose-6-phosphate isomerase
MFEs	Multifunctional enzymes
NA	Nutrient agar
NAG	N-acetylmuramic acid
NAM	N-acetylglucosamine
O.D.	Optical density
opgH	Glucans biosynthesis glucosyltransferase H,
PBPs	Penicillin-Binding Proteins

PEP	Phosphoenolpyruvate
PG	Peptidoglycan
pgcA	Phosphoglucomutase,
pgm	Phosphoglycerate mutase,
pykA	Pyruvate kinase
PG_Binding1	Peptidoglycan-binding
SLT_2	Transglycosylase SLT domain
Sma	*Stenotrophomonas maltophilia*
T3SS	Type 3 secretion system
T4SS	Type 4 secretion system
T6SS	Type 6 secretion system
UDP-GalNAc	uridine-diphosphate-N-acetylgalactosamine
ugtP	Diacylglycerol glucosyltransferase,
X. citri	*Xanthomonas citri* subsp. *citri* 306
XfaB	*Xanthomonas fuscans* subsp. *aurantifolii* strain B
XfaC	Xanthomonas fuscans subsp. aurantifolii strain C
XMP	5'-xanthylic acid
3-phosphoglycerate	3PG
2-phosphoglycerate	2PG

LIST OF TABLES

LIST OF FIGURES

APPENDIX

1. Introduction

The *Xanthomonadaceae* order contains many gram-negative phytopathogens relevant to agriculture (An et al., 2019). A critical species in this group is the phytopathogen *Xanthomonas citri* subsp. *citri* 306 wild type (*X. citri*), the causal agent of citrus canker (CC) (Rodriguez-r et al., 2012). CC is a severe disease that affects citrus crops and decreases fruit production, leading to economic losses (Gottwald et al., 2002). Many efforts to understand the CC mechanisms were made since the disease was discovered in the early 1900s (Boch and Bonas, 2010). One of the hallmarks that led to several new insights into the plant-pathogen mechanisms was related to the analyses of the *X. citri* genome, revealing the genetic basis of bacterial pathogenicity (Ryan et al., 2011). Since then, most studies are focused on *Xanthomonas* pathogenicity mechanisms, like the regulation and secretion of virulence factors, such as the Type 3 Secretion System (Büttner and Bonas, 2010; Ryan et al., 2011). Moreover, genetics studies were also conducted to understand chromosome segregation and cell division mechanism, aiming to better picture the cellular biology of this phytopathogen(Ucci et al., 2014; Lacerda et al., 2017). However, other possible genetic mechanisms related to *Xanthomonas* pathogenicity remain unknown. For instance, the multidomain and multifunctional enzymes (MFEs) role towards bacterial cellular biology, virulence, and fitness.

The MFEs are ubiquitous in prokaryotes (Sriram et al., 2005). These proteins generally harbor more than one domain, each exhibiting a distinct function (Hult and Berglund, 2007). Therefore, the MFEs may perform multiple physiologically biochemical or biophysical functions simultaneously in the cell (Moore, 2004; Vogel et al., 2004), and these numerous functionalities might provide evolutionary advantages for the cell (Aharoni et al., 2005). For instance, combining multiple functions enables the enzyme to catalyze different steps of a single metabolic pathway (Jeffery, 2003). In addition, the MFEs can be considered a clever strategy for generating complexity from existing proteins without expanding the genome (Aharoni et al., 2005).

One example of MFEs is the cardiolipin phosphatidylethanolamine synthase (CL/PEs), which is involved in unusual phospholipid biosynthesis pathways in the *Xanthomonas campestris* (Moser et al., 2014). While the CL/PEs produces cardiolipin (CL) using phosphatidylglycerol and cytidine diphosphate diacylglycerol (CDP-DAG) like a typical ‘eukaryotic’ cardiolipin synthases (Cls), this enzyme can also condense

ethanolamine (EA) and CDP-DAG to phosphatidylethanolamine (PE), representing an unusual PE biosynthesis mechanism in bacteria (Moser et al., 2014). Indeed, the MFEs emerged during species evolution and how they gained their multiple functions by gene fusion or other recombination events is not yet wholly established (Cheng et al., 2012).

In sharp contrast to the MFEs, one interesting class of enzymes has gained attention by their relation to bacterial fitness and virulence. These are the Lytic Transglycosylases (LTs), which are related to cell-wall recycling and cell-wall-antibiotic detection (Dik et al., 2017). LTs are also ubiquitous in prokaryotes, showing involvement with the peptidoglycan biosynthesis and recycling, cell division, septum division allowing cell separation, and insertion of protein complexes like secretion systems, flagella, and pili (Höltje, 1995; Koraimann, 2003; Scheurwater and Clarke, 2008; Uehara and Park, 2008; Scheurwater and Burrows, 2011; Alcorlo et al., 2017; Dik et al., 2017). Due to these features, LTs may also play a relevant role in the pathogenesis and fitness of many bacterial species, such as *Neisseria gonorrhoeae* (Chan et al., 2012), *Burkholderia pseudomallei* (Jenkins et al., 2019), and *Xanthomonas citri* (*X. citri*) (Oliveira et al., 2018).

Recently, we described the LT's arsenal present in the *X. citri* genome (16 LTs from different families) (Oliveira et al., 2018). Among those, we functionally revealed that two LTs from the 3B family: MltB2.1 and MltB2.2, are directly implicated in *X. citri* fitness (Oliveira et al., 2018). We also identified another 3B-like LT, named as XAC4296 (NCBI locus_tag: XAC_RS21660). Notably, apart from the Transglycosylase SLT 2 (IPR031304) and Peptidoglycan binding-like (IPR002477) domains, XAC4296 contains an additional and unexpected aldose 1-epimerase domain (IPR015443) linked to carbohydrate metabolism, and potentially showing involvement with the bacterial cell wall metabolism and biosynthesis of a variety of cell surface polysaccharides (Sala et al., 1996) (Figure 1). Interestingly, the XAC4296 gene was previously identified exclusively in the *Xanthomonas* genus (Oliveira et al., 2018). Moreover, *in silico* analyses revealed that XAC4296 appears to have been formed by a previous gene fusion event, originated by two independent genes (a 3B family LT and D-hexose-6-phosphate mutarotase gene), commonly separated in distinct loci in other non-*Xanthomonas* species (Oliveira et al., 2018). Therefore, XAC4296 resembles a canonical MFEs, showing a multi-domain architecture.

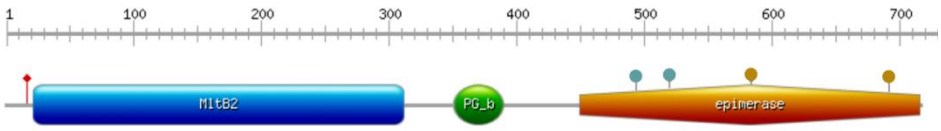

Figure 1. Domain architecture of XAC4296 (WP_011052877), showing the LTs domain associated with 3B family: MltB2 (pfam13406) and Peptidoglycan binding (pfam01471) domains, and the Aldose 1-epimerase (pfam01263) domain. The Lipoprotein signal peptide (Sec/SPII) is shown as a red diamond. The phosphate-binding residues and catalytic residues are shown as green and orange circles on the epimerase domain. This figure was generated using the Prosite MyDomains tool (https://prosite.expasy.org/cgi-bin/prosite/mydomains/).

In this work, we performed an *in silico*, fluorescence microscopy and pathogenicity assays to investigate the evolution and role of XAC4296 as a putative MFE. We also evaluated XAC4296 as a potential *X. citri* virulence and pathogenicity factor. Our results indicate that XAC4296 functions resemble a typical LT, mainly related to peptidoglycan biosynthesis. We also unveiled an additional role related to carbohydrate metabolism, compatible with epimerase domain, and chromosome segregation during cell division. Taken together, these results demonstrate that XAC4296 behaves like a classic MFE, showing at least two unrelated and mechanistically different roles: a primary role related to enzymatic catalysis and a secondary role related to cell structural function.

2. LITERATURE REVIEW

2.1. *Xanthomonas* genus

Xanthomonas genus (from greek, xanthos = yellow; monas = entity) comprises more than 200 bacterial species belonging to the Gammaproteobacteria class. *Xanthomonas* are obligate aerobic, rod-shaped bacteria (1.5–2.0 × 0.5–0.75 µm), presenting a single polar flagellum and yellow coloration once cultivated due to the production of xanthomonadin (He et al., 2020) (Figure 2).

Figure 2. Colonies of *Xanthomonas citri* spp. cultivated in the laboratory. Colonies are usually yellow due to 'xanthomonadin' pigment production. Source: https://www.apsnet.org/edcenter/disandpath/prokaryote/pdlessons/Pages/CitrusCanker.aspx

Bacteria belonging to this genus infect economically important monocot and dicot cultures and presents many hosts, such as *Citrus* spp. (lemons, sweet oranges, sour oranges, grapefruits, among others), *Oryza* ssp. (rice), crucifers (broccoli, cauliflower, lettuce, radish, and *Arabidopsis thaliana*) and *Manihot esculenta* (cassava) (Ryan et al., 2011). However, they still possess too high host specificity, therefore, each member usually infects only a few or even a single host (Jacques et al., 2016). Furthermore, *Xanthomonas* can epiphytically survive in soil, seeds, and harvest remains, interacting with insects and hosts or non-host plants (An et al., 2019). Therefore, these bacteria can be disseminated during agricultural practices, such as

pruning, nebulization, rainwater, contaminated soil, and insects (e.g., “Citrus leafminer” - *Phyllocnistis citrella*).

The *Xanthomonas* possess several invasion strategies to enter into plant tissues: initially, bacteria cells adhere to the host surface using its adhesins, gaining access through wounds or hydathodes, systematically spreading on the vascular system, or penetrating through stomata, colonizing leaf mesophyll (Ference et al., 2018).

Many functional and comparative genomics studies have been developed to elucidate the mechanisms related to the adaptation and evolution of *Xanthomonas,* given the vast diversity of plant hosts and host tissues (Lam et al., 2009)(An et al., 2019). Among the species of the *Xanthomonas* genus, different species and strains can infect citrus plants (e.g., *Citrus sinensis*). The most common is *Xanthomonas fuscans* subsp. *aurantifolii* strain B (XfaB) and C (XfaC), both the etiologic agents of the citrus cancrosis; *Xanthomonas alfalfae* subsp. *citrumelonis* (Xacm) causing citrus bacterial spot (Vauterin et al., 1995; Schaad et al., 2006), and *X. citri*, causal agent of the citrus canker (CC) disease (Da Silva et al., 2002).

2.2. *Xanthomonas citri* and Citrus canker

X. citri is the causal agent of citrus canker (CC) type A, a globally significant disease that affects all *Citrus* varieties, compromising the commerce of fruits and sub-products worldwide (Gottwald et al., 2002). CC severity varies according to the citrus species. In general, while the kumquats (*Fortunella* spp.) are resistant, the sweet oranges (*Citrus sinensis* L. Osbeck) ‘Bahia’, ‘Hamlin’, ‘Valencia’ and ‘Pera’ shows intermediate levels of susceptibility, whereas the ‘Mexican’ lime (*Citrus aurantifolia* (Christm.) Swingle) are considered susceptible to CC (Ferrasa et al., 2020) (Figure 3). Therefore, millions of dollars are spent annually on prevention, quarantines, and eradication programs for disease control (USDA, 2021).

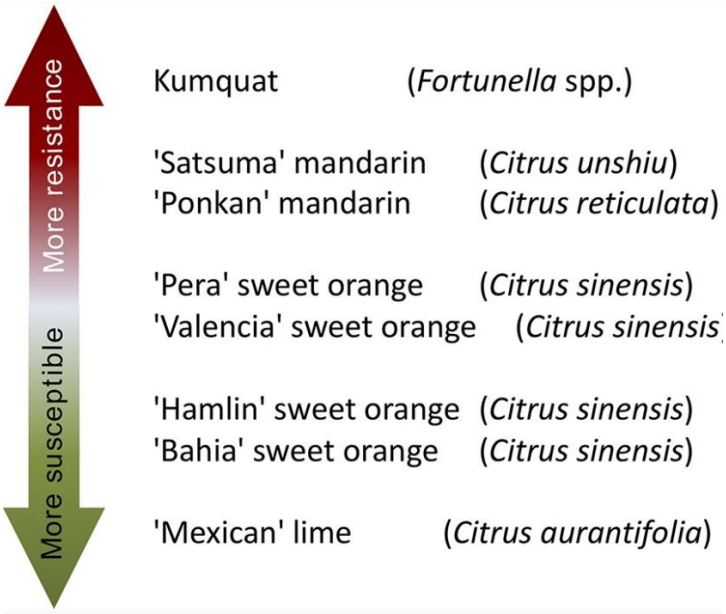

Figure 3. Citrus genotypes resistance and susceptibility scale to citrus canker A. Source: Ferrasa et al., 2020.

The CC infection starts when *X. citri* attaches to the host tissue (Graham, 1992). The pathogen enters the host tissue through wounds or stomatal openings (Figure 4A). The CC symptoms start as pinpoint spots. After approximately ten days, young leaves show pustules. Eventually, the leaves become corky and crateriform with a raised margin, surrounded by a yellow halo, a process known as waker-soaking (Figure 4B) (Schubert and Sun, 2003). The CC lesions are readily observable as cork-like lesions on both leaf faces, in branches, leaves, and fruits (Figure 4 C, D, and E) (Gottwald et al., 2002).

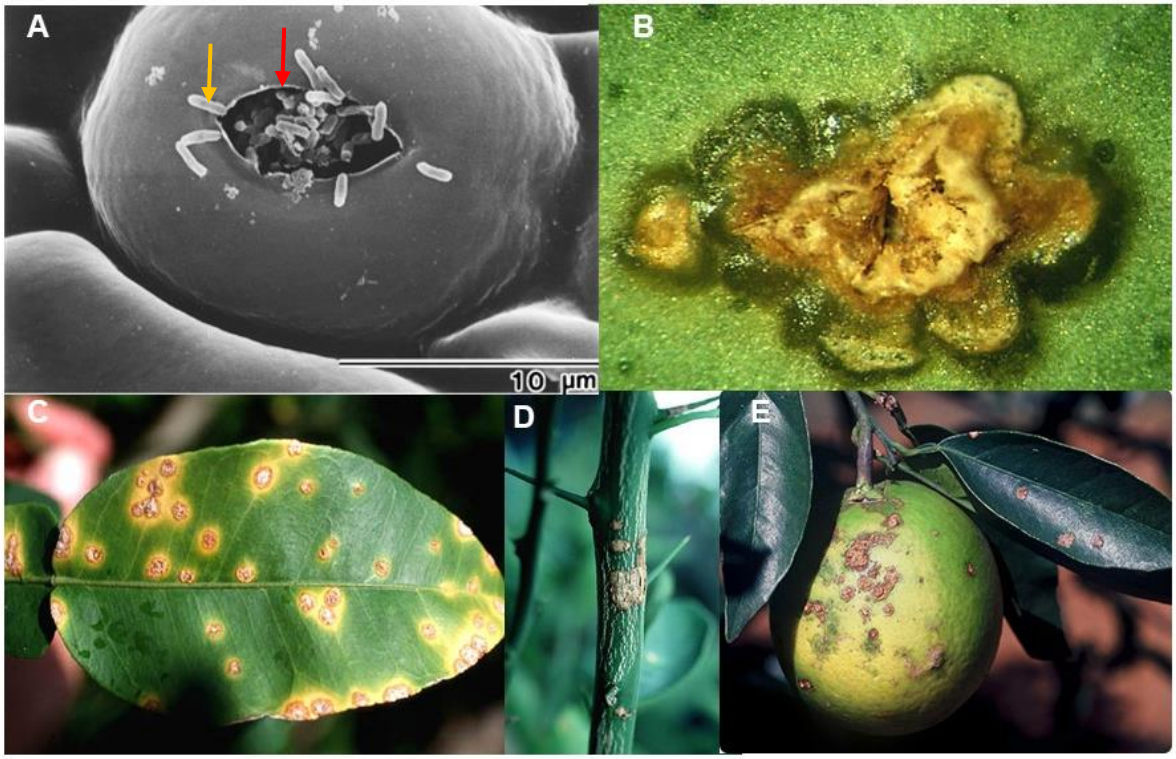

Figure 4. Citrus canker disease infection and symptoms. **A:** Scanning electron microscopy of infections by *Xanthomonas citri* (*X. citri*) on the abaxial leaf surface of grapefruit (*Citrus paradisi*). Bacterial egress from a stomatal opening. Yellow arrows indicate *X. citri*; red arrows indicate stomatal opening. **B:** Citrus canker lesions are raised with a cork-like appearance, surrounded by a yellow halo. **C:** Citrus canker symptoms in leaves (**C**), branches (**D**), and fruits (**E**) of citric plants. Source: Graham et al., 2003 and Fundecitrus (https://www.fundecitrus.com.br/doencas/cancro).

The spread of CC occurs by wind or raindrops, always respecting short distances within neighboring trees or by contaminated agricultural instruments. In general, the disease develops more severely on the side of the tree exposed to wind-driven rain (Gottwald and Timmer, 1995). In addition, leafminer infestations caused by *Phyllocnistis citrella* can also contribute to the *X. citri* dissemination (Gottwald et al., 2002).

Epidemiological, genomic, and evolutionary studies indicate that CC was originated in Southeast Asia (Patané et al., 2019). Nowadays, the disease is also present in Japan, Central Africa, South America (Brazil and Argentina), and the United States of America (Florida) (Schubert and Sun, 2003; Canteros et al., 2017).

CC notably affects the American continent (Schubert and Sun, 2003). For instance, Brazil is responsible for the largest orange production globally, producing at least 14% of the global orange fruits (3.6 million metric tons), and has the most

extensive orange juice production, corresponding to 17% of the global orange juice, equivalent to 1.8 million tons (USDA, 2021). Indeed, Brazilian citriculture is one of the most important agricultural activities for the country, with production concentrated in São Paulo and Minas Gerais states. However, CC infection rate was estimated at 17.26% in Sao Paulo and Minas Gerais orchards (USDA, 2021), making the country one of the centers of CC (Behlau, 2021).

Unfortunately, there is no treatment for CC, and management and sanitation are the only ways to control the disease (Ismail and Zhang, 2004). However, it is still not easy to manage the disease in the production fields. For example, one alternative to CC control relies on copper-based antimicrobial products; however, indiscriminate use gives rise to resistant *X. citri* strains (Voloudakis et al., 2005; Richard et al., 2017). Conversely, copper is considered hazardous to human health and the environment (Behlau et al., 2013). Other promising alternatives to control CC, such as alkyl gallates (Savietto et al., 2018) and even transgenic citrus varieties (Jia and Wang, 2020; Martins et al., 2021) are under scrutiny and development.

2.3. The main *Xanthomonas* Virulence factors

Virulence factors are molecules encoded in the pathogen genome which are secreted to enable infection or damage in the host tissue (Casadevall and Pirofski, 2009). In *Xanthomonas*, secretion systems (1 to 6) are associated with virulence factors related to disease development (Büttner and Bonas, 2010; Alvarez-martinez et al., 2021). Moreover, other virulence factors, like adhesins, extracellular polysaccharides (EPS), lipopolysaccharides (LPS), and degradative enzymes, such as proteases, lipases, and cell wall-degrading enzymes, are also part of the *Xanthomonas* arsenal to ensure efficient multiplication and disease progression (Büttner and Bonas, 2010).

The *Xanthomonas* pathogenicity is mainly determined by the Type 3 Secretion System (T3SS), also called injectisome (Cornelis, 2006; Saijo and Schulze-lefert, 2008). The T3SS appears as a needle-like structure capable of penetrating the plant cell wall, connecting the bacterial cell to the cytosol of the plant cell (Wagner et al., 2018). The main role of T3SS is to inject effector proteins directly into the host cell

cytosol to manipulate plant cellular processes such as basal defense for the benefit of the pathogen (Büttner and Bonas, 2010).

Several effector proteins are involved with CC disease development (Ference et al., 2018), such as Xop effectors (*Xanthomonas* outer proteins) (Jalan et al., 2013), and the Transcription activation-like effectors (TALEs), also known as AvrBs3/PthA (avirulence and pathogenicity proteins). Both effectors are injected by the T3SS machinery into the plant cell. Of those, however, TALEs migrates to the cell nucleus and binds to a specific DNA sequence (Boch et al., 2009), acting as a classic transcription factor, modulating the host gene expression, presumably by direct interaction with the host transcription machinery (Boch and Bonas, 2010; Bogdanove et al., 2010). Indeed, TALEs genes are essential for full CC induction, activating host susceptibility genes (An et al., 2019).

X. citri also uses other virulence factors for bacterial survival during epiphytic and endophytic growth (Rigano et al., 2007). These are related to the biosynthesis of lipopolysaccharides (LPS), extracellular polysaccharides (EPS), and biofilm formation (Büttner and Bonas, 2010).

LPS protects the bacteria against antimicrobial compounds and other external stresses, being a component of the outer membrane (Kummerfeld and Teichmann, 2005). In addition, during the plant-pathogen interactions, the LPS may also protect the bacterial cell acting as a PAMP (“Pathogen-Associated Molecular Pattern”), controlling the plant defense responses such as pathogenesis-related gene expression, oxidative burst, and thickening of the plant cell wall (Dow m., 2000).

The EPS or xanthan gum is a main feature of the *Xanthomonas* species, leading to the bacterial colonies a mucoid appearance (Becker et al., 1998). The gum gene cluster directs xanthan gum production (12 genes: *gumB* to *gumM*), a polymer of repeating pentasaccharide units with cellulose and trisaccharide side chains (Becker et al., 1998; Katzen et al., 1998). The role of xanthan gum is different among *Xanthomonas* strains and hosts (Kemp et al., 2004; Dunger et al., 2007; Rigano et al., 2007). In *X. citri*, the xanthan gum is necessary for initial states of CC development, displaying direct involvement with bacterial adhesion to host cells and protecting against environmental stresses (Rigano et al., 2007; Facincani et al., 2014). In contrast, for *X. campestris*, the xanthan gum induces plant susceptibility by suppressing callose deposition (Oa et al., 2006). In addition, xanthan gum might increase bacterial colonization in the host since it affects the motility by flagellum-

independent movement, the so-called “sliding motility”, and is one of the main components of biofilm matrix (Dunger et al., 2007; Malamud et al., 2013).

Biofilms are a dense surface-associated microorganisms community connected to the cell through an extracellular polymeric substance matrix composed of LPS, proteins, and nucleic acids, important for greater resistance to antibiotics and host immune effectors (Costerton, 1995). In *Xanthomonas*, the biofilm is formed after the initial attachment to the host. This primary function is to protect bacteria against abiotic stress, acting as a defense mechanism (An et al., 2019). Biofilms structure, assembly, and dispersal are mediated by the quorum-sensing signal molecule diffusible signal factor (DSF) (Rigano et al., 2007).

2.4. The possible role of XAC4296 in the *Xanthomonas* carbohydrate metabolism

Procaryotes have three main metabolic pathways to degrade monosaccharides: the Embden-Meyerhof-Parnas (EM or glycolysis), the Entner-Doudoroff (ED), and the pentose phosphate pathways (Chubukov et al., 2014) (Figure 5). Glycolysis takes place in the cytosol of the cell and occurs in two phases: the investment phase, where adenosine triphosphate (ATP) is consumed and glucose is broken down into two three-carbon compounds, generating pyruvic acid as a product. The yield phase, where the free energy produced in this process is used to form pyruvate. In this process, the cell produces four high-energy ATP molecules and two nicotinamide adenine dinucleotide (NADH). Each reaction in glycolysis is catalyzed by many enzymes, producing intermediate metabolites (Bender, 2013).

Some organisms do not have the glycolysis pathway or show some variances to the classical glycolytic pathways, such as the ED pathway. ED was first discovered in *Pseudomonas saccharophila* (1952) (Entner and Douroff, 1952) and later in *E. coli* (1967) (Eisenberg and Dobrogosz, 1967), then, it was discovered in all domains (Eukarya, Bacteria, and Archaea), but most notably in Gram-negative bacteria (Conway, 1992). Subsequently, studies performed in *Xylella fastidiosa* 9a5c showed that the ED pathway prevails over the glycolysis pathway in carbohydrate metabolism (Facincani et al., 2003). In *X. campestris* pv. *campestris*, the central metabolism was elucidated using ^{13}C-based metabolic flux and NMR-based isotopologue profiling,

showing the prevalent role of ED pathway over glycolysis and pentose phosphate pathways (Schatschneider et al., 2014).

The ED metabolic pathway converts glucose into pyruvate using alternative enzymes and, has a net yield of one ATP, one NADH, and one NADPH per glucose molecule processed (Figure 6) (Romano and Conway, 1996). In many cases, bacteria perform the ED pathway using gluconate as a carbon source (Conway, 1992).

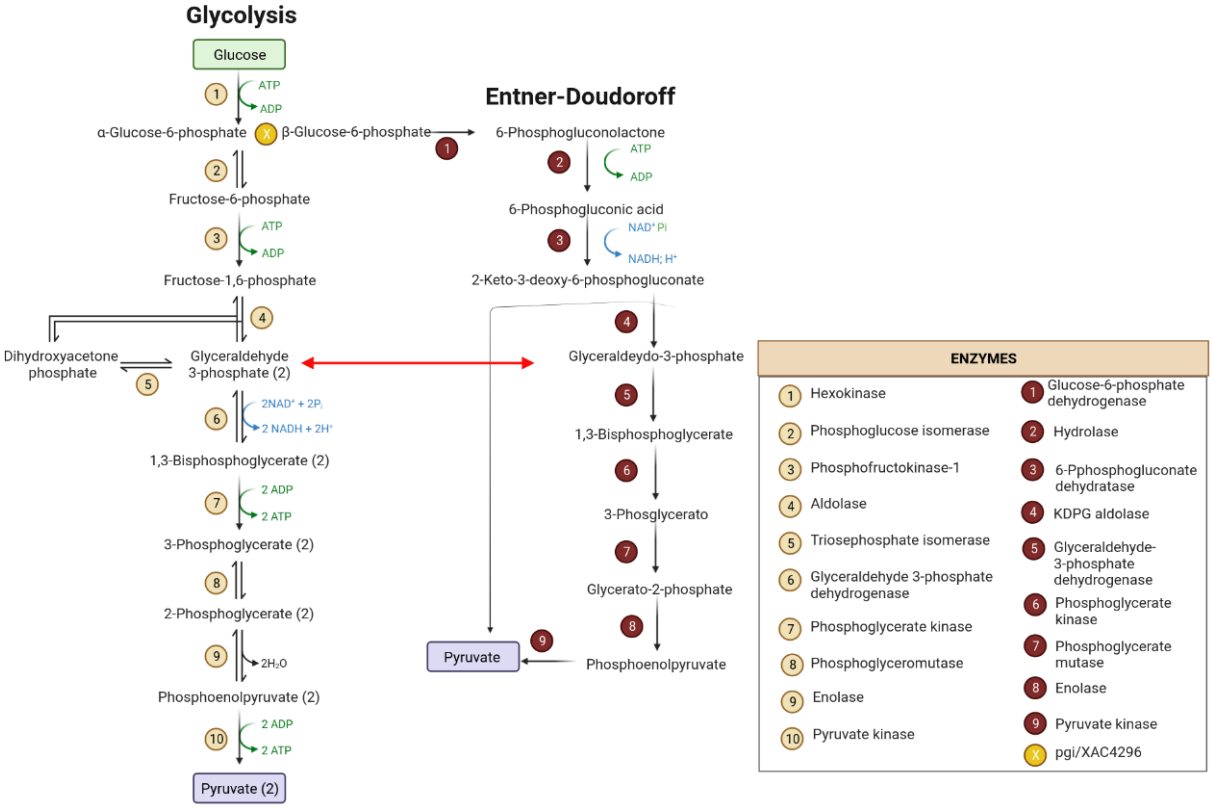

Figure 5. Glycolytic pathways from bacteria: Embden-Meyerhof-Parnas (EM or glycolysis) and Entner-Doudoroff. The red arrow shows the link between the EM and ED pathways.

Many enzymes catalyze specific steps in these metabolic pathways, such as the glucose phosphate isomerase (*pgi*) which converts glucose-6-phosphate (G6P) into fructose 6-phosphate (F6P) in the EM pathway, which is related to the carbohydrate degradation (Rose, 1975). The phosphoglycerate mutase isomerases convert 3-phosphoglycerate (3PG) to 2-phosphoglycerate (2PG) through a 2,3-bisphosphoglycerate intermediate, in the glycolysis via ED and EM pathways, respectively (Figure 5, enzyme number 8). Curiously, the *X. citri* XAC4296 protein (the main focus of this study) contains an aldose 1-epimerase (pfam01263) domain,

belonging to the “Isomerases family”, which catalyzes the conversion of one isomeric form of a chemical compound to another within one molecule (McDonald et al., 2015). Therefore, it is tempting to speculate that the *X. citri* XAC4296 protein may have a role as a pgi-like enzyme, and presumably contribute to EM and ED pathways (Figure 5).

2.5. Epimerases enzymes and their connection to XAC4296

As stated in the previous topic, the *X. citri* XAC4296 contains an epimerase domain. The Epimerases are an important class of isomerases, enzymes that performs the interconversion of an isomeric form of a chemical compound into another (McDonald et al., 2015). The isomerases comprises the following families: Isomerases cis-trans (EC 5.2); intramolecular oxidoreductases (EC 5.3); intramolecular transferases (EC5.4); and intramolecular lyases (EC 5.5) (McDonald et al., 2015). This enzyme catalyzes the inversion of the configuration of an asymmetrically substituted carbon in linear or cyclic sugars (Figure 6).

The epimerases are abundant in procaryotes and the microorganisms might benefit from using these enzymes to produce complex carbohydrate polymers, using them as biosynthetic building blocks in their cell wall (McNeil et al., 1990).

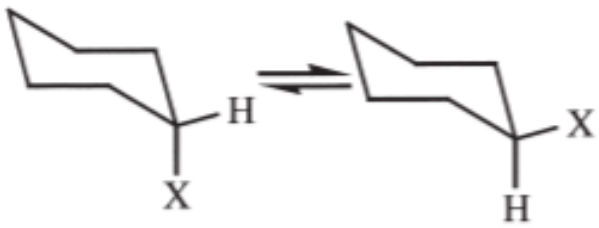

Figure 6. Epimerization reaction catalyzes the interconversion of alpha (α) and beta (β)-anomers of sugars: the inversion of the configuration of an asymmetrical substitution on carbon in sugars. X corresponds to groups -OH or NH. Source: Allard, 2001.

Epimerases are usually involved in metabolic pathways such as inversion of D-alanine and D-glutamate for bacterial cell wall metabolism (Sala et al., 1996), biosynthesis of a variety of cell surface polysaccharides, biosynthesis of heparin and heparin sulfate (Li et al., 2001), biosynthesis of LPS and capsular sugar precursors

(McNeil et al., 1990) and complex biosynthetic pathways, such as Embden-Meyerhof-Parnas pathway (Glycolysis) (Figure 6), Entner-Doudoroff (Figure 5), Leloir and others that present several chemical steps (Nowitzki et al., 1995; Teige et al., 1995).

Epimerases are also involved in many chemical steps, such as oxidation, acetylation, dehydration and carbohydrate reduction (Allard et al., 2001). The carbohydrate epimerization occurs in five ways, as described below (reviewed by Allard et al., 2001).

a) Epimerization employing a transitory keto intermediate.

The UDP-galactose 4-epimerase is the most common example of an enzyme with this type of epimerization. It catalyzes UDP-glucose and UDP-galactose interconversion by inverting the stereochemistry at the C4 position, utilized in *de novo* biosynthesis of sugar (Figure 7) (Carnell, 1999). In addition, this enzyme performs the biological interconversion of galactose and glucose in the Leloir Pathway (Frey, 1996).

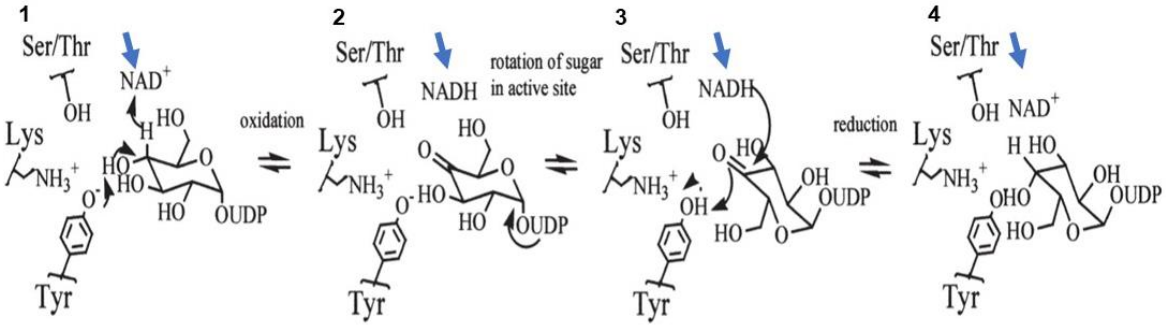

Figure 7. UDP-galactose 4-epimerase (GALE gene) epimerization by a transient keto intermediate.**1**. At the first step occurs the abctraction of the 4-hydroxyl proton by an enzymatic base and an abstraction of a hydride from the C4 position of the sugar to the C4 position on NAD+. **2**. NADH is formed. **3**. A proton shuttle mechanism is created, from serine (Ser124) to Tyr149 and a transient keto sugar is formed but it has no chirality at the C4 position. **4.** The keto sugar is not released by the enzyme and remains bound, the NADH transfers the hydride back to the C4 of the sugar, but this time to the opposite face, with inversion of configuration at C4 of the sugar. The proton extracted by Tyr149 (or Ser124) is transferred back to the sugar. Blue arrows indicate NAD+ reactions. Source: Allard et al. (2001).

b) Epimerization by abstraction/protons addition

The enzyme D-ribulose-5-phosphate 3-epimerase is found in the oxidative pentose phosphate pathway. This enzyme catalyzes the conversion of D-ribulose 5-

phosphate to D-xylulose 5-phosphate. In these reactions, the keto group is located on the C2 carbon, and the stereocenter in the C3 is inverted. This mechanism involves deprotonation and reprotonation and occurs via an enediolate intermediate (Figure 8) (Kopp et al., 1999).

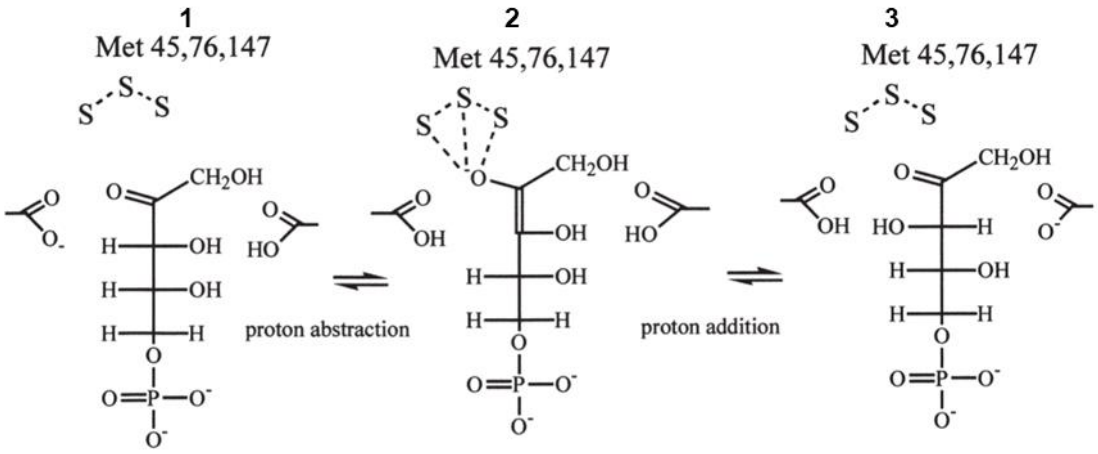

Figure 8. D-ribulose-5-phosphate 3-epimerase (RPEase) epimerization by abstraction/protons addition. The epimerized stereocenter in a position of a keto group has led to the catalytic mechanism in which deprotonation (**1**) and reprotonation (**3**) take place via an ene-diolate intermediate (**2**). The keto group is situated on the C2 carbon, and the stereocentre at C3 is inverted. Source: Allard et al. (2001).

c) Epimerization by elimination/nucleotides readdiction.

The enzyme UDP-N-acetylglucosamine 2-epimerase might be necessary for bacteria since it catalyzes the reversible interconversion of UDP-N-acetylglucosamine (UDP-GlcNAc) and UDP-N-acetylmannosamine (UDP-ManNAc). This mechanism occurs by the elimination and readdiction of UDP from the molecule (Figure 9) (Sala et al., 1996).

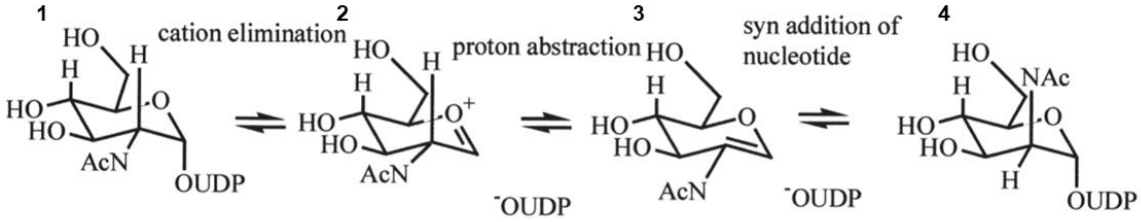

Figure 9. UDP-N-acetylglucosamine 2-epimerase: epimerization by nucleotide elimination and re-addition. **1.** The first step enters with the initial elimination of UDP from UDP-GlcNAc generates the intermediate 2-acetamidoglucal. **2.** The elimination of UDP was triggered by a cationic elimination. **3.** Readdition of UDP with protonation of the C2 atom at the opposite face. **4**. The syn addition of UDP gives the product UDP-ManNAc. Source: Allard et al. (2001).

d) Epimerization by carbon-carbon ligation cleavage.

The enzyme L-ribulose-5-phosphate 4-epimerase interconverts L-ribulose 5-phosphate and D-xylulose 5-phosphate by inverting the configuration at the C4 stereocenter and without the incorporation of solvent-derived oxygen and hydrogen (Figure 10) (Salo et al., 1972). This enzyme enhances bacteria to use arabinose as the energy source, connecting the arabinose pathway to the pentose phosphate pathway (Johnson and Tanner, 1998).

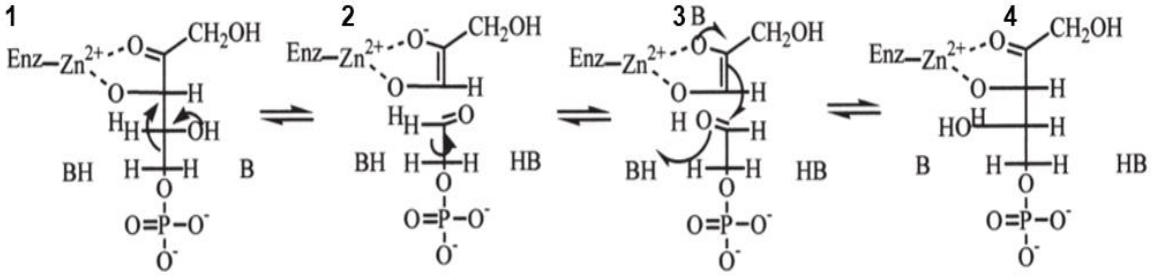

Figure 10. Epimerization by carbon-carbon bond cleavage as carried out by L-ribulose-5-phosphate 4-epimerase. B represents the base, and HB the protonated base. **1.** The first step starts with an abstraction of the proton from the C4 hydroxyl group, followed by the C3–C4 bond cleavage. **2.** Dihydroxyacetone endiolate is generated **3.** Glycolaldehyde is generated. **4**. The C–C glycolaldehyde bond must be rotated by 180° to allow the inversion of stereochemistry at C4 after the regeneration of the C3–C4 bond. Source: Allard et al. (2001).

e) Epimerization by ring-opening epimerization or mutarotation.

The foremost example of this reaction is the galactose mutarotase, a ubiquitous enzyme that converts the β anomer to the α anomer (inversion of chirality at C1) of galactose (Figure 11) (Hucho and Wallenfels, 1971). Galactose mutarotase enzymes have been reported in bacteria (Thoden et al., 2003), plants (Martyn bailey et al., 1966), fungi (Martyn bailey et al., 1966), and mammals (Timson and Ã, 2003), including humans (hsGalM) (Thoden and Holden, 2005). It has been suggested that galactose mutarotase be included in a superclass of enzymes (Thoden et al., 2003). In the first step of the Leloir pathway, these enzymes actuate on galactose metabolism, converting β-D- galactose to α-D-galactose, playing an auxiliary role on carbohydrate metabolism (Holden et al., 2003). Presumably, *X. citri* XAC4296 protein, which contains the aldose 1-epimerase domain, might perform the epimerization by ring-opening or mutarotation (Thoden et al., 2003).

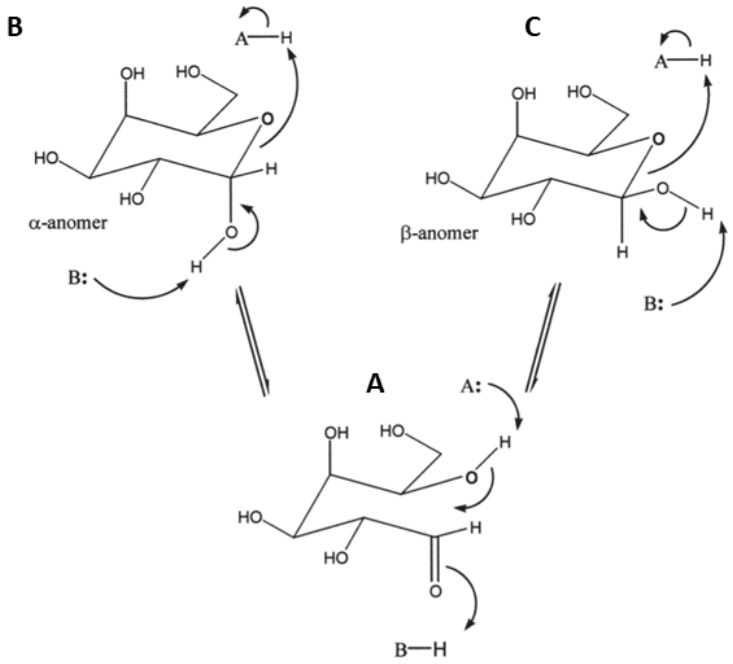

Figure 11. Galactose mutarotase epimerization by mutarotation. The galactose mutarotase linear form (**A**) has a keto group at C1, which suggests the interconversion between the α (**B**) and β (**C**) forms is quite rapid. Source: Allard et al. (2001).

2.6. Epimerases as multifunctional enzymes of the bacterial metabolism

In cellular metabolism, sugar is converted into a few simple carbohydrates (monosaccharides): glucose, fructose, and galactose (Thoden et al., 2003). Carbohydrates are central to many essential metabolic pathways, which involve: Glycolysis, Gluconeogenesis, Glycogenolysis, Glycogenesis, Pentose phosphate pathway, and more specifically in the Fructose metabolism and Galactose metabolism. In this context, isomerases classified as epimerases play a central role, contributing to sugar interconversions (Allard et al., 2001) (Figure 5).

For instance, the isomerases from the EM pathway, like the phosphoglucose isomerase/phosphoglucoisomerase (PGI) is a cytoplasmic protein that interconverts aldehyde-D-glucose 6-phosphate into keto-D-fructose 6-phosphate (Figure 5) (Rose, 1975). Moreover, the triose-phosphate isomerase (TPI) is an enzyme that catalyzes the reversible interconversion of dihydroxyacetone phosphate into D-glyceraldehyde 3-phosphate (Albery and Knowles, 1976). Finally, the ribose-5-phosphate isomerase interconverts ribulose-phosphate 3-epimerase into ribulose-5-phosphate in the Calvin cycle and Penthouse phosphate pathway (Nowitzki et al., 1995).

An example of epimerases in the cell metabolism is present in the Leloir pathway (LP), which is an exclusive mechanism to convert galactose to glucose without external galactose (Figure 12) (Frey, 1996). This pathway uses as an initial substrate D-galactose, which is metabolized to glucose-1-phosphate by four enzymes: aldose-1-epimerase or galactose mutarotase (*galM*), galactokinase (*galK*), galactose-1-phosphateuridylyl transferase (*galT*), and UDPgalactose-4-epimerase (*galE*) (Holden et al., 2003). This metabolic pathway is used as an energy and carbon source during the anabolic pathway of carbohydrate metabolism. For instance, it is used to synthesize cell wall compounds and exopolysaccharides, where the galactosides are required as building blocks (Frey, 1996).

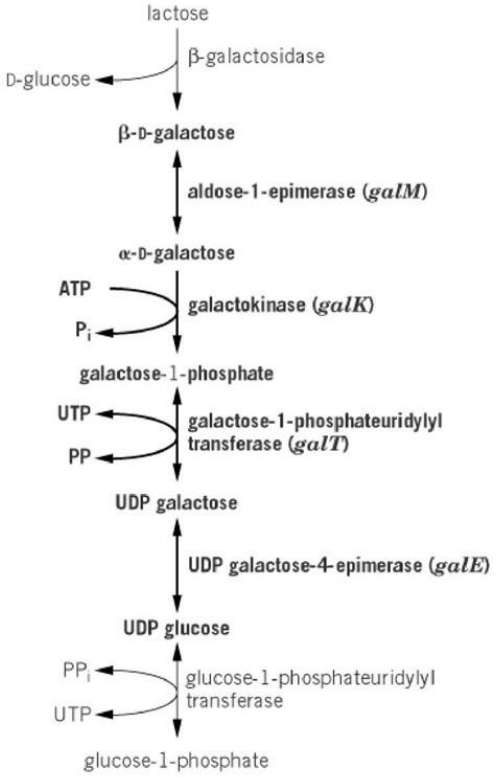

Figure 12. The Leloir pathway of D-galactose metabolism in *Streptococcus thermophilus*. Starting from the upper side of the panel, the lactose is converted in β-D-galactose by the β-galactosidase; β-D-galactose can mutarotate spontaneously to the α-anomer (α-D-galactose) at a slow rate, the enzyme aldose-1-epimerase (*galM*) converts the β-d-galactose into α-d-galactose before phosphorylation (5); the galactokinase (*galK*) converts the α-D-galactose in galactose-1-phosphate; the galactose-1-phosphateuridylyl transferase (*galT*) converts galactose-1-phosphate in UDP galactose; the UDPgalactose-4-epimerase (*galE*) converts the UDP galactose in UDP glucose. Aldose-1-epimerase links the enzymes of lactose and galactose metabolism into a common pathway. Source: adapted from Sørensen et al., 2016.

Another example of epimerase from the LP is the *galM* (aldose 1-epimerase) (STH8232_RS07000) from *Streptococcus thermophilus,* which converts D-glucose into L-glucose (Poolman et al., 1990). This enzyme is part of the *gal* operon, and it was characterized by several microorganisms, including *E. coli* (Bouffard et al., 1994). The Aldose 1-epimerase is also active on D-glucose, L-arabinose, D-xylose, D-galactose, maltose and lactose pathways. In addition, this enzyme is involved in the hexose pathway metabolism, which is also part of the carbohydrate metabolism (Poolman et al., 1990). Noteworthy that the aldose 1-epimerase domain is also present in the *X. citri* XAC4296 protein.

In *Saccharomyces cerevisiae,* the GAL10 (*galE*, YBR019C) gene contains a mutarotase related domain (galactose mutarotase) and an additional UDP-galactose-

4-epimerase domain, which confers this protein twice as many amino acids residues (699 aa) as the bacterial or the human protein (LGALS10) (Majumdar et al., 2004). The UDP-galactose 4-epimerase catalyzes the conversion between UDP-galactose and UDP-glucose in the galactose metabolic pathway (for eukaryotes and prokaryotes) (Wilson and Hogness, 1969). In addition, enzymatic assays showed that *gal10* has an additional aldose 1-epimerase activity. Therefore, it is considered a bifunctional enzyme (Majumdar et al., 2004; Scott and Timson, 2007). On the other hand, *galE* is also related as a virulence factor in many bacterial pathogens such as *Erwinia amylovora* (Metzger et al., 1994), *Pasteurella multocida* (Fernández de henestrosa et al., 1997), *Vibrio cholera* (Nesper et al., 2001), *Porphyromonas gingivalis* (Nakao et al., 2006), *Aeromonas hydrophila* (Agarwal et al., 2007). In *X. campestris pv. campestris*, *galE* is also necessary for bacterial full virulence (Li et al., 2014), suggesting that the epimerase *galE* might act beyond the glycolytic pathways.

Interestingly, in addition to the lytic transglycosylase domain, the XAC4296 protein from *X. citri* also bears an epimerase domain presumably related to a mutarotase activity, supporting its role as a bifunctional enzyme. Recently, several bifunctional proteins were characterized as acting in two or more roles in plants, animals, yeast, and prokaryotes, the so-called Multidomain and Multifunctional Enzymes (MFEs) (Vogel et al., 2004; Cheng et al., 2012). MFEs may coordinate the crosstalk of dissimilar biological processes, such as metabolism, regulatory pathways, virulence factors, and virulence (Gancedo and Flores, 2008). Indeed, the study of MFEs is important for the understanding of living systems (more details of MFEs are shown in the next topics).

2.7. Metabolism, cell shape, and chromosome segregation

Bacteria respond swiftly to nutrient availability and changes in their environment, adjusting their shape and size (Wang and Levin, 2009). In conditions of unrestricted nutrient availability, bacteria capitalize on the available resources by increasing cell size and reproducing more often (Wang and Levin, 2009). During restrict nutrient conditions, bacteria balance growth, and cell size, showing a remarkable homogeneity across a population, suggesting that the cell growth and division cycles are regulated and not random (Sperber and Herman, 2017).

Many efforts were made to understand the relationship between bacterial metabolism and cell growth. For instance, the relation between metabolism and cellular elongation has been shown using ManA (mannose-6-phosphate isomerase) protein as a model (Elbaz and Ben-yehuda, 2010). ManA is responsible for phosphoglucose isomerase activity catalyzing glucose-6-phosphate to fructose-6-phosphate isomerization (Hansen et al., 2004). Therefore, ManA is directly involved in carbon metabolism and impacting cell shape (Elbaz and Ben-yehuda, 2010). For instance, in *Bacillus subtilis,* ManA is needed for the cell to keep its rod shape and be viable in the Luria-Bertani (LB) medium. However, ManA is not required for bacterial growth in the minimal medium containing glucose as a sole carbon source (Elbaz and Ben-yehuda, 2010). Studies performed on *B. subtilis* revealed that *ΔmanA* mutant shows rounded cells and does not grow after changing from a minimum medium to an LB medium, also showing atypical nucleoid morphologies (Figure 13) (Elbaz and Ben-yehuda, 2010). Two hypotheses were proposed to explain this observation. The first postulates that *ΔmanA* mutant offers reduced galactose levels and GalNAc (N-acetylglucosamine, a component derived from teichoic acid), so the *ΔmanA* phenotype may be due to issues in the synthesis of teichoic acid (Yeom et al., 2009). Moreover, UDP-GalNAc (uridine-diphosphate-N-acetylgalactosamine) is a substrate for teichoic acid synthesis, generated by UDP-GlcNAc epimerization suggesting that *ΔmanA* mutant might also be hindered in its ability to synthesize UDP-GlcNAc (Young and Arias, 1967).

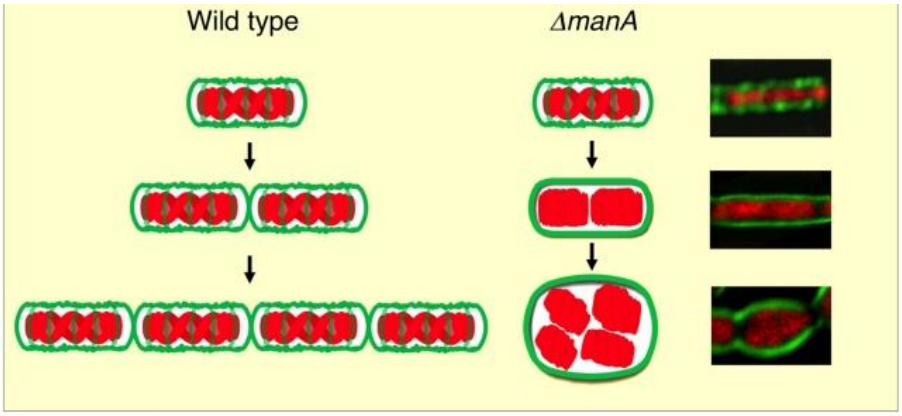

Figure 13. Model linking cell wall integrity and chromosome morphology in wild-type cells of *Bacillus subtilis* and *ΔmanA*. Cell wall (green) and chromosome (red) in wild type and *ΔmanA* cells. In wild-type cells, the nucleoid organization and segregation are coordinated with cell wall synthesis and elongation. In the absence of ManA, the normal extension of the cell wall is blocked, as indicated by the disappearance of

helical sidewall staining. The nucleoid is detached from cell wall components and the synchronization is lost between cell growth and DNA replication and segregation, resulting in the formation of polyploid cells. Source: Elbaz; Ben-Yehuda, 2010 (2010).

A first explanation for the round cell and altered chromosomal structure phenotype obtained from *ΔmanA* mutant can be made by observing the *Escherichia coli* phenotype when pyrimidine precursors are limited (Zaritsky et al., 2006). Indeed, DNA and peptidoglycan (PG) synthesis might share a precursor, UTP (Uridine triphosphate), to generate UDP-GlcNAc and the nucleosides dCTP (deoxycytidine triphosphate), and dTTP (deoxythymidine triphosphate), suggesting that cellular growth is susceptible to UTP disturbances (Zaritsky, 2015). This observation possibly explains the correlation observed between cell growth and DNA replication during a stationary state (Zaritsky, 2015). A second possibility that might explain the observed results is that in glucose deficient LB growth conditions, ManA contributes significantly to converting fructose-6-phosphate to glucose-6-phosphate to feed PG teichoic acid paths and DNA synthesis (Elbaz and Ben-yehuda, 2010).

Taken together, these findings indicate that *manA* can perform more than one function simultaneously in the cell. Therefore, ManA probably regulates some aspects of cell envelope biogenesis, although its diffuse location does not explain how this mechanism would occur (Elbaz and Ben-yehuda, 2010).

Studies on genetic interactions between carbon/nitrogen metabolism and cell division are abundant, and several examples were demonstrated more deeply in recent revision papers (Monahan et al., 2014; Monahan and Harry, 2016). It was observed that the loss or inactivation of central metabolism-related genes (e.g., *pgm* - Phosphoglycerate mutase, *pgcA*- Phosphoglucomutase, *ugtP* - Diacylglycerol glucosyltransferase, *opgH*- Glucans biosynthesis glucosyltransferase H, and *pykA*- Pyruvate kinase) might result in a more active FtsZ protein activity (Filamenting temperature-sensitive mutant Z) that is directly related to bacterial cell division, and thus, making cells multiply more frequently (Debarbieux et al., 1997; Hill et al., 2013). For instance, in *B. subtilis*, the *pykA* deletion, which catalyzes PEP (Phosphoenolpyruvate) conversion to pyruvate, activates an *ftsZ* temperature-sensitive allele, possibly suggesting that heightened levels of PEP (gluconeogenesis) are correlated to observed defects in cell division (Monahan et al., 2014). Also, *pykA* deletion alters *ftsz* normal regulation, resulting in ~40% of cells with multiple or

subpolar rings (Monahan et al., 2014). Although a direct relation between PykA and *ftsZ* was not demonstrated, the following experiment showed that PdhA (an enzyme that feeds pyruvate on tricarboxylic acid cycle – TCA) super expression promotes *ftsZ* additional polar ring formation on mutant *ΔpykA* (Monahan et al., 2014). However, when exogenous pyruvate was added, *ΔpykA* phenotype was restored, *suggesting* that *pdhA* relies on pyruvate resulting from *pykA* indirect action and not from pykA itself to assembly *ftsZ* ring (Monahan et al., 2014).

Moreover, the loss of *gdhZ* (glutamate dehydrogenase), *kidO* (NADH-binding oxidoreductase), and *pycK* genes may inhibit cell division (Beaufay et al., 2015). The *gdhZ* is the enzyme responsible for converting glutamate and NAD+ in α-ketoglutarate, ammonia, and NADH in this microorganism. *gdhZ* was identified in an interaction assay with *ftsZ*, and *gdhZ* deletion results in abnormal cell division, resulting in a mix of cell populations showing short, standard, and filamentous phenotypes (Beaufay et al., 2015). Indeed, *gdhZ* physically interacts *in vivo* with FtsZ, stimulating FtsZ GTPase activity in a glutamate-independent manner (Beaufay et al., 2015). Therefore, *gdhZ* enzymatic activity is required for *ftsZ in vivo* activity since *gdhZ* mutant will not stimulate *in vitro* GTPase activity, suggesting that *gdhZ* might be necessary to stimulate GTP hydrolysis (Beaufay et al., 2015).

The bifunctional regulator KidO is another protein that promotes the disassembly of *ftsZ* (Beaufay et al., 2015). *kidO* is believed to play a role in conjunction with *gdhZ* to regulate *ftsZ* disassembly during the cell cycle and under nitrogen limiting conditions. *kidO* deletion resulting phenotypes are not so pronounced as those associated with *gdhZ* deletion; however, the proteins suffer a similar cell cycle regulation and co-localize with FtsZ rings (Radhakrishnan et al., 2010; Beaufay et al., 2015). Therefore, *kidO* inhibits lateral filament grouping of *ftsZ* in an NADH-dependent manner *in vitro*, while also is proposed to work in cooperation with *gdhZ*, using NADH produced from *gdhZ* enzyme activity to inhibit this process (Beaufay et al., 2015).

Taken together, these observations strongly suggest that enzymes related to the central metabolism, such as the epimerases that present a role on the EM and/or ED pathways, may indirectly impact the bacterial cell shape and chromosome segregation.

2.8. The role of Lytic transglycosylases in cell shape by interacting with Peptidoglycan Metabolism

In addition to the epimerase domain, which may be related to the bacterial central metabolism, showing indirect impacts on the cell shape and chromosome segregation, the XAC4296 also contains a lytic transglycosylase domain. In Gram-negative and Gram-positive microorganisms, the bacterial cell wall is the major stress-bearing and shape-maintaining element, and its integrity is of critical importance to cell viability (Denome et al., 1999). Furthermore, the bacterial cell wall needs to endure expansion, contraction, and remodeling processes to occur proper division and shape and size adjustments. The structure of the cell wall consists of the cross-linked polymer Peptidoglycan (PG). This polymer consists of long glycan chains with alternating 1,4-linked N-acetylglucosamine (GlcNAc) and N-acetylmuramic acid (MurNAc) subunits. The chemistry of the glycan chains varies only slightly between different bacteria, mostly on stem peptides linked to the carboxyl group of MurNAc (Vollmer and Bertsche, 2008).

PG synthesis can be divided into three different stages (Van Heijenoort, 1998), the first step starts in the cytoplasm from precursors UDP-N-acetylmuramyl-pentapeptide (UDP-MurNAc-pentapeptide) and UDP-N-acetylglucosamine (UDP-GlcNAc). In the second step, UDP-N-acetylmuramyl-pentapeptide is carried to the membrane, where lipid intermediates are synthetized: UDP-N-acetylmuramyl-pentapeptide is transferred to the membrane acceptor, producing Lipid I ([MurNAc-(pentapeptide)-pyrophosphoryl-undecaprenol]) (Reviewed by van Heijenoort, 1998). GlcNAc from UDP-GlcNAc is then added to lipid I, giving rise to Lipid II [GlcNAc-(1,4)-MurNAc-(pentapeptide)-pyrophosphoril-undecaprenol]. The third and last step is performed on the outside of the membrane through PBPs (Penicillin-Binding Proteins) action, which catalyzes transglycosylation and transpeptidation reactions responsible for PG glycolytic and peptidic ligations (Figure 14).

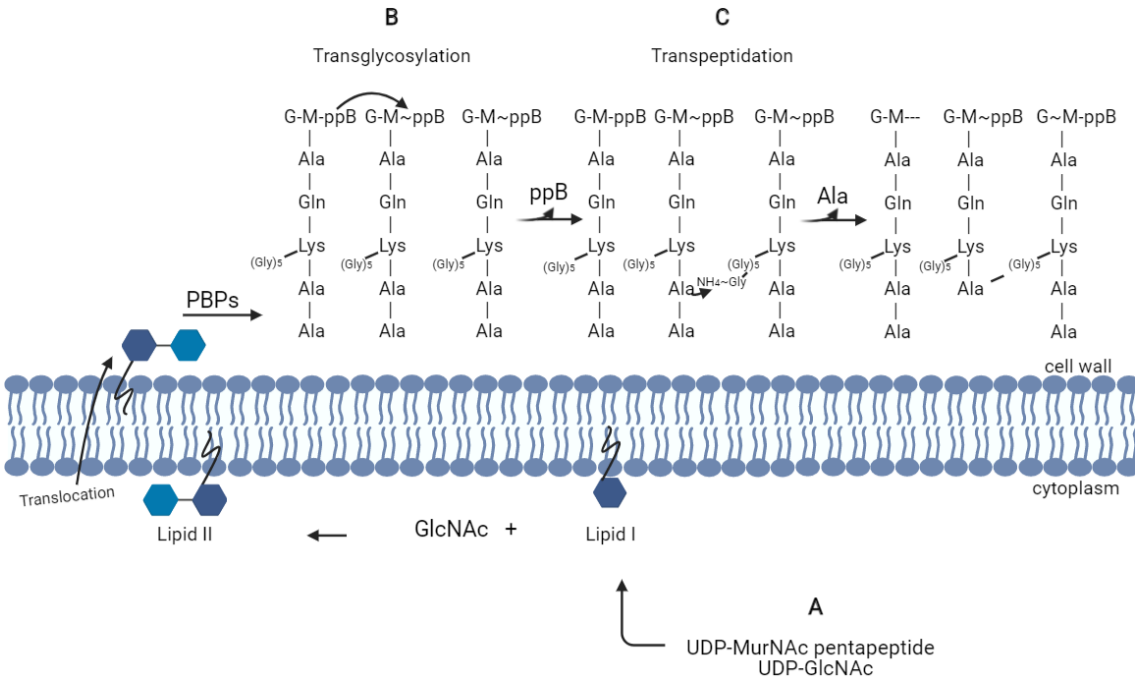

Figure 14. The maintenance and synthesis of peptidoglycan are performed in three steps. **A:** The first step includes UDP-MurNAc pentapeptide conversion from UDP-GlcNAc in the cytoplasm, followed by Lipid I and Lipid II production. In the cytoplasmic membrane's extracellular leaflet, Lipid II is polymerized, cross-linked, and processed by transglycosylase (**B**), transpeptidase (**C**), and carboxypeptidase activities by penicillin-binding proteins (PBPs). The PBPs acts by reducing the ends of the N-acetylmuramic acid (M) of the nascent lipid-linked peptidoglycan strand, which is likely transferred onto the C-4 carbon of the N-acetylglucosamine. The outer membrane is not shown. Abbreviations: GlcNAc, N-acetylglucosamine; MurNAc, N-acetylmuramic acid. Adapted from Scheffers and Pinho (2005).

Many enzymes are involved in peptidoglycan biosynthesis; for example (a) the Peptidoglycan glycosyltransferases (GTFs) polymerize the glycan chains; (b) the transpeptidases (TPases) form peptide crosslinks; (c) the PBPs, peptidoglycan hydrolases, that are present in multiple variants in all bacteria, these proteins are responsible for both the elongation of glycan strands (transglycosylation) and the formation of cross-links between the peptides (transpeptidation) of PG; (d) N-acetylmuramidases (lysozymes); (e) N-acetylglucosaminidases; (f) amidases (g) endopeptidases; (h) carboxypeptidases, and (i) the Lytic transglycosylases (LTs), that act in peptidoglycan recycling and cell-wall-antibiotics detection (Scheffers and Pinho, 2005).

LTs comprise a family of proteins showing a key role in peptidoglycan dynamics (Hoeltje et al., 1975). The LTs are organized into 6 distinct families (1, 2, 3, 4, 5, and

6) distributed across 14 subfamilies (1A, 1B, 1C, 1D, 1E, 1F, 1G, 1H, 2A, 3A, 3B, 4A, 5A, 6A), and grouped according to their domain structure and function (Dik et al., 2017) (Figure 15 and Table 1).

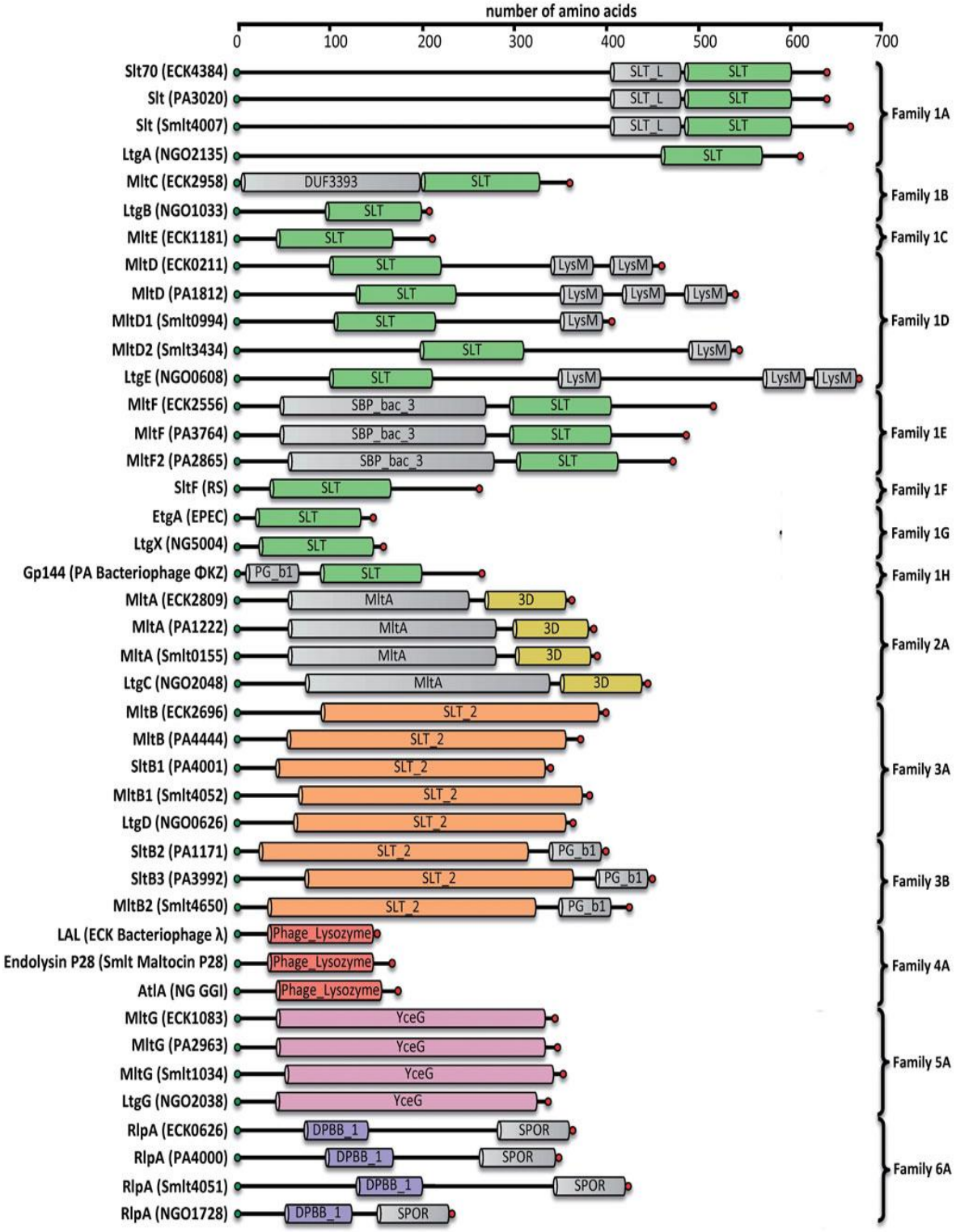

Figure 15. Lytic transglycosylase (LTs) domain architecture and family organization. Model LTs classified in *Escherichia coli* K12 (ECK4384, ECK2958, ECK1181, ECK0211, ECK2556, ECK2809, ECK2696, ECK1083, ECK0626), *Pseudomonas aeruginosa* PAO1 (PA3020, PA1812, PA 3764, PA2865, PA 1222, PA4444,

PA4001,1171, PA3992, PA2963, PA4000), *Stenotrophomonas maltophilia* KJ (Smlt4007, Smlt0994, Smlt3434, Smlt0155, Smlt4052, Smlt4650, Smlt1034, Smlt4051) and *Neisseria gonorrhoeae* FA1090 (NGO2135, NGO1033, NGO0608, NGO5004, NGO2048, NGO0626, NGO2038, NGO1728) according to the presence of domains and putative function. Domains were assigned based on InterPro database: SLT (IPR008258), LysM (IPR018392), DUF3393 (IPR023664), SBP_bac_3 (IPR001638), PG_binding_1 (IPR002477), MltA (IPR034654), 3D (IPR034654), SLT_2 (IPR031304), Phage_lysozyme (IPR023347), YceG (IPR003770), DPBB_1 (IPR007112), SPOR (IPR007730). Source: Dik et al. (2017).

Table 1. List of domains found in Lytic Transglycosylase (LTs) (2018). Domain information was obtained on InterPro databases. Source: Dik et al., 2017; Oliveira et al., 2018.

Domain	**Function (InterproScan) (FINN *et al.*, 2017)**
SLT (IPR008258)	Related to proteins encoded by bacteriophages for 2, 3, and 4 secretion systems. This domain presents cleavage activity of the β-1,4 glycosidic ligation between acid residues N-acetylmuramic acid and N-acetylglucosamine, and the formation of muropeptides containing a 1,6 anhydro ligation in the muramic acid residue.
LysM (IPR018392)	Related to peptidoglycan binding and plant-pathogen interactions.
DUF3393 (IPR023664)	Unknown domain presenting potential function related to murein degradation during the recycling of muropeptides and cell elongation and/or cell division.
SBP_bac_3 (IPR001638)	Involved in the active transport of solutes across the cytoplasmic membrane.
PG_binding_1 (IPR002477)	Related to peptidoglycan binding.
MltA (IPR034654)	Helps binding to peptidoglycan.
3D (IPR034654)	Composed of three conserved residues of aspartic acid, presumably related to peptidase activity.
SLT_2 (IPR031304)	Related to SLT domain.
Phage_lysozyme (IPR023347)	Related to breaking down the peptidoglycan, hydrolyzing the 1,4-beta ligation between N-acetylglucosamine and N-acetylmuramic acid in heteropolymers.
YceG (IPR003770)	Related to the end of peptidoglycan polymerization by endolytic breaking of nascent chains.
DPBB_1 (IPR007112)	Related to outer membrane proteins and specificity for peptidoglycan.
SPOR (IPR007730)	Related to cell division, morphogenesis, and sporulation processes.

The LTs show catalytic activity related to peptidoglycan polysaccharide fragmentation on glycosidic ligation between amino acid residues NAG-NAM, resulting in muropeptides formation containing 1,6-anhydrous ligation on muramic acid residue (1,6-anhydromuramic) (Höltje, 1998). These muropeptides are transported to the cytoplasm through AmpG transmembrane protein, degraded, and their subproducts are used on the Lipids Biosynthesis II pathway or induce the lactamase production (Jacobs et al., 1994; Heidrich et al., 2002). Products from the Lipids Biosynthesis II pathway are transported from cytoplasm to periplasm, where they will be reincorporated on PG metabolism (Barreteau et al., 2008; Bouhss et al., 2008; Scheffers and Tol, 2015; Leclercq et al., 2017) (Figure 16).

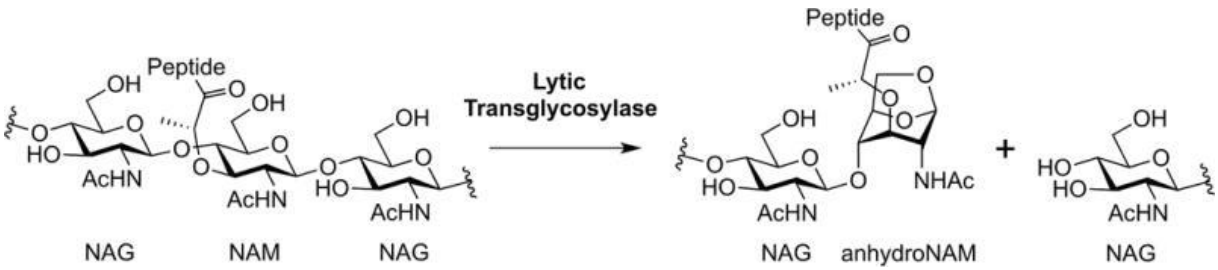

Figure 16. Chemical reaction performed by Lytic transglycosylase (LTs). This reaction is defined as the breaking down of polysaccharides in the glycosidic ligation between acid residues NAG-NAM, which goes through an oxocarbenium, which intercepts glucosamine 6-hydroxyl group, resulting in the formation of muropeptides containing a 1,6 anhydrous ligation in the muramic acid residue. Source: Dik et al., 2017.

LTs can make space on the PG sacculus, allowing several metabolic processes to occur in that space (Scheurwater et al., 2008). For instance, the LT may expand the sacculus and, consequently, cell growth by creating PG precursors sites (Höltje, 1998; Scheurwater et al., 2008). Together with amidases, they split the septum allowing separation during cell division (Heidrich et al., 2002). LTs are also involved in endospore germination in Gram-positive cells, facilitating the insertion of macro complexes that extend through the PG sacculus, such as T3SS, T4SS, flagella, and pili on Gram-negative cells (reviewed in Koraimann, 2003).

These proteins are autolytic due to their ability to cause complete cellular lysis if their activity proceeds uncontrolled (Scheurwater and Clarke, 2008). In general, LTs are ubiquitous on PG-producing microorganisms (Blackburn and Clarke, 2001). Still, each species shows a different repertoire, with some species showing duplicated content, suggesting that LTs might have functional redundancy (Scheurwater and

Clarke, 2008; Dik et al., 2017). It was demonstrated in *E. coli* that individual deletion in each one of the six LTs present on this bacterium genome, and even in all of them at the same time, compromised septum cleavage during cell division, resulting in cell chains and an increase in permeability of the outer membrane (Heidrich et al., 2002). However, no lethal effect was observed with individual LTs in *E. coli*, adding to the hypothesis of functional redundancy among LTs and to other proteins (Heidrich et al., 2002). Additionally, it has been suggested that some LT functions are essential for the bacterium when facing different physiological conditions, indicating that it is not possible to knock out all LTs (Scheurwater and Clarke, 2008).

LTs are also related to pathogenicity and virulence processes. For example, the LT EtgA (1G Family) from enteropathogenic *Escherichia coli* is required for efficient T3SS function (García-gómez et al., 2011). The *Pseudomonas syringae*, LTs HrpH (1D Family), HopP1 (4A Family), and HopAJ1 (3B Family) can facilitate the translocation of effector proteins by the T3SS (Oh et al., 2007). In *X. axonopodis* pv. *glycines,* HpaH (1G Family) contributes for virulence and Hyper sensibility Response (HR) (Noël et al., 2002). In *X. oryzae* pv. *oryzicola,* Hpa2 (1G Family) is related to virulence and responsible for translocating effectors by the T3SS, interacting with the *hrpF* translocon (Li et al., 2011). In *X. campestris* pv. *vesicatoria*, HpaH (1G Family) can promote T3SS effector protein transport and interacts with T3SS structural proteins HrpB1 and HrpB2 and the pilus protein HrpE (Hausner et al., 2017). In *X. campestris* pv. *campestris*, the membrane-bound lytic transglycosylase (XC_0706) (3A Family) is important for cell division, and the Hpa2 (1G Family) affects T3SS effector translocation (Wang et al., 2019).

The *X. citri* LT content and diversity were already unraveled (Oliveira et al., 2018). *X. citri* encodes a total of 17 LTs: 12 belonging to families 1A, 1B, 1C, 1D (two copies), 1F (three copies), 1G (2 copies), 3A, 3B (two copies), 5A, 6A, and one which is non-categorized and not showing a common LT domain (Table 2). It was also demonstrated that the *mltB2*.1 and *mltB2*.2 (3B Family) LTs were laterally acquired, and using site-directed deletion mutagenesis, they were functionally characterized (Oliveira et al., 2018). These *mltB* genes (*mltB2*.1 and *mltB2*.2) are directly related to *X. citri* virulence and affect CC progression, indicating that the acquisition by lateral transfer leads to evolutive advantages for the bacterium (Oliveira et al., 2018).

Table 2. Lytic Transglycosylase (LTs) and biosynthetic peptidoglycan transglycosylase are found in *Xanthomonas citri* (*X. citri*). The search for LT genes was performed on the GenBank database at NCBI using the BLAST tool (Altschul et al., 1997), and consensus analysis was performed using ClustalX (Larkin et al., 2007) and InterProScan (Finn et al., 2017) tools using the classification proposed by Dik et al. (2017). LT XAC4296 (XAC_RS21660) is an exclusive protein in *Xanthomonadaceae*, it shows the domains SLT_2 and PG_binding1 from the 3B LT family and an additional epimerase domain. Proteins VirB1 (XAC_RS13315 and XAC_RS22400) and Hpa2 (XAC_RS02185) were found after a new BLAST search. Adapted from Oliveira et al., 2018.

Locus Tag	Gene name	InterproScan/PFAM and Uniprot	LT classification	Presumed acting role
XAC_RS18005	*slt*	Lytic_TGlycosylase_superhlx_U (IPR008939), SLT_1 (IPR008258; PF01464) and Q8PGQ5	1A	cell-wall recycling / peptido-glycan monomer production
XAC_RS12500	*yjbJ/mltC*	SLT_1 (IPR008258; PF01464) and Q8PJS2	1B	peptidoglycan degradation
XAC_RS11470	*mltE*	SLT_1 (IPR008258; PF01464) and Q8PKB9	1C	Insertion of the type 6 secretion system (T6SS)
XAC_RS13860	*mltD2*	SLT_1 (IPR008258; PF01464); LysM (IPR018392; PF01476) and A0A0U5FH84; A0A0U5FC25	1D	Acting primarily toward rearrangement of the peptidoglycan layer
XAC_RS05550	*mltD1*			
XAC_RS13315	*sltF*	SLT_1 (IPR008258; PF01464) and Q8PJB8	1F	Insertion of the type 4 secretion system (T4SS)
XAC_RS02185	*hpaH/etgA*	SLT_1 (IPR008258; PF01464) and A0A0U5GFN3	1G	Insertion of the T3SS and T4SS
XAC_RS03435	*mltB*	SLT_2 (IPR031304; PF13406) and Q8PPM4	3A	cell-wall recycling and potential virulence (cell-wall resistance)
XAC_RS16355	*mltB2*	SLT_2 (IPR031304; PF13406); Pb_binding_1 (IPR002477; PF01471) andQ8PHM6; Q8PRL3	3B	Rearrangement of the peptidoglycan layer for insertion of the secretion system
XAC_RS22275	*mltB2*			
XAC_RS05780	*mltG*	YceG (IPR003770; PF02618) and Q8PNE1	5A	regulates peptidoglycan strand length
XAC_RS03440	*rlpA*	RlpA-like_sf (IPR036908); SPOR (IPR007730; PF05036)	6A	cell division or morphogenesis
XAC_RS21660	*n/a*	SLT_2 (IPR031304; PF13406); PB_binding_1 (IPR002477; PF01471); Gal_mutarotase_sf_dom (IPR011013; PF13802) and A0A1T1SC85	3B (?)	carbohydrate metabolic process / peptidoglycan binding function
XAC_RS15470	*mtgA*	Pep_trsgly (IPR011812), PBP_transglycosylase (IPR036950), Transgly (PF00912) and Q8PI51	unclassified	peptidoglycan biosynthesis

XAC_RS13315*	*virB1*	SLT_1 (IPR008258; PF01464)	1F	Insertion of the type 4 secretion system (T4SS)
XAC_RS22400*	*virB1*	SLT_1 (IPR008258; PF01464)	1F	Insertion of the type 4 secretion system (T4SS)
XAC_RS02185*	*hpa2*	SLT_1 (IPR008258; PF01464)	1G	Insertion of the T3SS and T4SS

Interestingly, this work also identified a non-categorized LT named XAC4296 (GenBank locus_tag: XAC_RS21660) which is exclusively found in the *X. citri* and *X. albilineans* (Figure S1). Similar to MltB2.1 and MltB2.2 proteins, XAC4296 presents the domain signature of the 3B family (SLT_2 and PB_binding_1) but also exhibits an additional aldose-1-epimerase (IPR011013) domain related to carbohydrate metabolism (Oliveira et al., 2018) (Figure 17). Therefore, XAC4296 shows a multidomain architecture resembling canonical multidomain and Multifunctional Enzymes (MFEs).

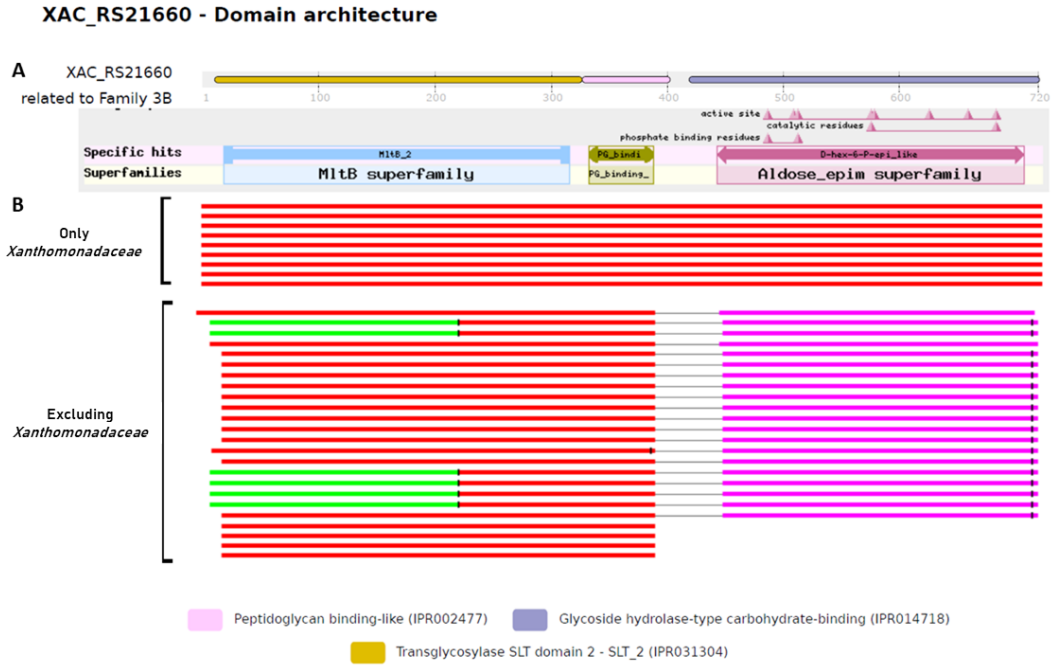

Figure 17. XAC4296 (XAC_RS21660) domain architecture in *Xanthomonadaceae* and non-*Xanthomonadaceae*. **A.** XAC4296 presents the domain signature of the 3B transglycosylase family (SLT_2 and PB_binding_1) and an additional aldose-1-epimerase (EP - IPR011013) domain related to carbohydrate metabolism. **B.** Search for XAC4296 in *Xanthomonadaceae* shows the exclusive XAC4296 domain architecture to the genus, and in non-*Xanthomonadaceae*, the transglycosylase and EP domains appear as two separated genes. Source: Oliveira et al., 2018.

Orthologs for the LT and epimerase domains of XAC4296 exist as two separated genes in other non-Xanthomonas microorganisms (Oliveira et al., 2018). In other words, the XAC4296 appears to be originated from a previous gene fusion event from the separated and independent 3B LT gene and epimerase gene (Figure 17). Moreover, no signal of mobile genetic elements was found surrounding XAC4296, indicating that its origin is not related to recombination events generated by

transposable elements (Oliveira et al., 2018). Therefore, the evolutionary origins of this gene fusion event are still unknown.

2.9. Multidomain and multifunctional enzymes (MFEs)

Proteins are biopolymers, commonly formed by distinct segments of amino acid chains linked by peptide bonds and showing extraordinary diversity. Many proteins are composed of independent segments named as domains, that confer specific structure and function (Xu and Nussinov, 1998). Therefore, the protein domain is a region of the protein's polypeptide chain structurally independent from the rest of the protein, forming a compact folded three-dimensional structure (Xu and Nussinov, 1998). A polypeptide chain may have a single domain or several other domains that may be recombined in new arrangements to provide new functions or even to create new functionally distinct proteins (Xu and Nussinov, 1998). For instance, the LTs corresponds to a family of multidomain proteins, where each domain is related to a specific and complementary function (Figure 15).

The multidomain proteins have likely emerged from selective pressure during evolution and may have arisen by distinct genetic mechanisms (Vogel et al., 2004) (Figure 18). Duplication is one of the primary sources for creating new genes and new superfamilies through domains rearrangement (Vogel et al., 2004). Another mechanism for generating new domain combinations is gene fusion, gene fission, and “domain shuffling” (Pasek et al., 2006).

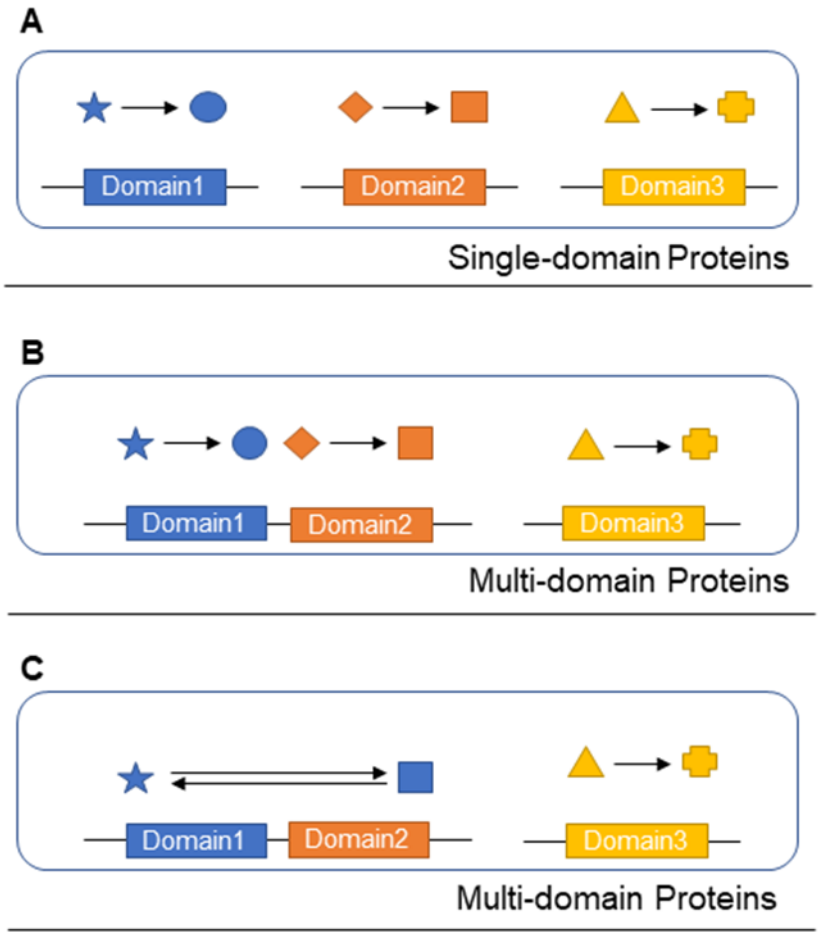

Figure 18. Schematic representation of proteins in bacteria. **A**. Single domain proteins (blue, orange, and yellow) perform a single function, each domain catalyzes one reaction. **B**. multidomain protein (blue and orange), each domain catalyzes one reaction, and the single-domain protein (yellow) performs a single function. **C**. Multidomain protein (blue and orange) performs multiple functions, now, the domains might be catalyzing two steps, single-domain protein (yellow) performs a single function. Adapt from Vogel et al., 2004.

The function of proteins with multiple domains is determined by domain structure, composition, and, in most cases, interactions between their domains and with other proteins (Janin and Wodak, 1983). To understand the functional relationship in multidomain proteins it is necessary to understand the domain function separately (Janin and Wodak, 1983). Often, domains might have a specific function, or contribute to the function of a multidomain protein in cooperation with other domains. Therefore, to understand the multidomain function, it is essential to know their three-dimensional structure and consider each domain's interactions (Vogel et al., 2004).

Some proteins that might act as chemical catalysts are known as enzymes that work by accelerating chemical reactions, converting substrates into different molecules known as products. These enzymes that couple two or more reactions, might have one or more domains, and are called Multifunctional Enzymes (MFEs). Each MFEs domain has an independent function or contributes to the new function in cooperation with other domains in the same polypeptide chain (Cheng et al., 2012). Enzymes that catalyze consecutive steps in the metabolic pathway might be combined into one specific protein (Zientz et al., 2004), suggesting that these MFEs emerged to support broader substrates, but higher specificity (Schmidt et al., 2003).

The MFEs are classified into three classes according to the mechanism of promiscuity (Hult and Berglund, 2007). First, different reaction conditions might change the enzyme catalytic function, for example, various solvents, extreme temperature, altered pH. Second, some enzymes might have broad substrate specificity. Third, the catalytic promiscuous enzymes might use a single-active site to catalyze different reactions (Cheng et al., 2012).

Many studies were performed to understand the molecular details and roles within the multidomain combinations (Han et al., 2007). For instance, the c-di-GMP binding protein (FimX, GenBank locus_tag: PA4959) from *Pseudomonas aeruginosa* is a multidomain protein, composed of four domains: (a) the putative response regulator (CheY-like) domain; (b) the PAS-PAC domain, commonly involved in environmental sensing; (c) the DUF1 domain (or GGDEF), and (d) the DUF2 domain (or EAL), involved in cyclic di-GMP metabolism. *In silico* investigation of FimX suggests these domains might be performing the same function. Mutant FimX strains gene showed strongly reduced levels of extracellular pili, impaired twitching motility, as reported for the CheY-like domain, and mutant strains are insensible to environmental signal, as reported for the PAS-PAC domain. However, the FimX mutant has a phosphotransfer activity involved in the cyclic di-GMP metabolism, as reported for DUF1 and DUF2 domains (Huang et al., 2003).

The multidomain protein phosphoribosylamine-glycine ligase (GARS) is a ubiquitous protein from purine biosynthesis (Antle et al., 1996). GARS protein is related to catalysis of the second step in purine biosynthesis in all organisms: in bacteria is encoded by the *purD* gene, in yeast is encoded by the ADE5/7 gene, and in eukaryotes is encoded by the GARS gene, each protein has different substrate specificity. Interestingly, GARs from humans is a trifunctional enzyme (Daubner et al., 1985). In

all (micro)-organisms this protein is formed by four domains: GARS-N, GARS-A, GARS-B, and GARS-C, however, in bacteria, the *purD* is a monofunctional enzyme, ADE5/7 and GARS are bifunctional or trifunctional enzymes (Banerjee et al., 2012).

2.10. Gene fusion and new multidomain proteins

Gene fusion is a type of recombination that generally results in a new gene formed when two independent genes are juxtaposed or concatenated. This mechanism provides new proteins with different domain architecture, such as MFEs and multidomain proteins (Pasek et al., 2006). Therefore, this event is central to the evolution of genome architecture (Snel et al., 2000).

Gene fusion may occur by duplication, sequence divergence, and recombination events, such as translocation and inversion (Enright and Ouzounis, 2001; Pasek et al., 2006). In contrast, in gene fission, the genes are split and can be produced by either recombinational events or single base events, such as frameshift or nonsense mutations (Pasek et al., 2006). These events may create an accidental fusion of DNA sequences associated with different genes, or break one gene into several parts (Kummerfeld and Teichmann, 2005), or generate pseudogenes (by gene fission frequently) (Darby et al., 2007). In addition, gene fusion may be created from double-stranded DNA breakages followed by a DNA repair error (Mitelman et al., 2007).

Gene fusion events may occur in non-coding sequence regions or at a coding sequence, leading to misregulation of the expression of a gene, but the affected gene might still be controlled by the cis-regulatory sequence of another one (Durrens et al., 2008). In coding sequences, gene fusion might generate the assembly of a new gene, from already existing ones. These new proteins show new functions by adding peptide modules, generating multi-domain proteins or MFEs (Yanai et al., 2001; Pasek et al., 2006).

Multidomain proteins and MFEs might be generated by two combinations: gene fusion by terminal indels (C-terminal or N-terminal), which involves an intermediate step in which components coexist as juxtaposed and yet distinct genes (Pasek et al., 2006). Direct fusion, a rare event where gene fission might occur, which is based on the maintenance of the terminal region of one gene and the initial regulatory regions

of another, involving the gain of these regulatory signals (Kummerfeld and Teichmann, 2005) (Figure 19).

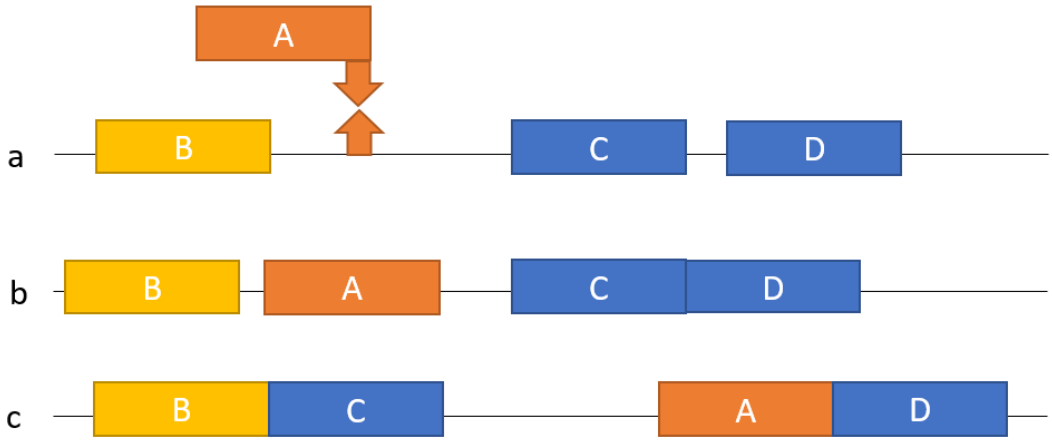

Figure 19. Schematic representation of gene fusion mechanism. a) gene insertion/deletion (yellow and orange blocks) in a genome stretch. b) maintenance of new gene insertion in the genome stretch (orange block) and gene fission between the two next genes in the genome stretch (blue blocks). c) exchange of domain is the substitution of one domain for another. Adapt from Parsek et al., 2006.

Frequently, gene fusions involve consecutive genes that encode proteins performing successive steps in the metabolic pathway, contributing to multiple domain bacterial proteins evolution (Pasek et al., 2006).

The purine biosynthesis is one of the major examples of gene fusion in Bacteria, Archaea, and Eukarya domains. Purines are a heterocyclic aromatic organic compound consisting of two rings. It plays a role in basal metabolism, contributing to cell signaling and encoding the bases of the genetic code of all living organisms (Chua and Fraser, 2020). For example, in Bacteria, the conversion of XMP (5'-xanthylic acid) to GMP (5'-guanylic acid) is only performed by the bifunctional GMP synthetase protein; in contrast, in Archaea, the interconversion of XMP to GMP is performed by two different enzymes with different ATP pyrophosphatase activities for XMP adenylation and glutamine amidotransferase to add an amine group to create GMP (Oliver et al., 2013).

3. MAIN AND SPECIFIC OBJECTIVES

This work aims to characterize XAC4296, a protein exclusively found in the *Xanthomonas* genus, using *in silico* analysis and functional assays, such as site-direct mutagenesis, pathogenicity assays, and fluorescence microscopy to determine the chromosome segregation and subcellular localization. Beyond the protein characterization, this work also focuses on determining XAC4296 role on *X. citri* virulence and pathogenicity and generating new insights into the *Xanthomonas* multidomain protein evolutionary advantage.

The specific objectives are:

- *In silico* investigation for XAC4296 through 3D protein modeling, genomic context, and phylogenetic analyses;
- Site-directed mutagenesis for mutant construction and complemented strain construction to investigate the role of XAC4296 in *X. citri*;
- *Ex-planta* and *in planta* assays (infiltration and spray method) to investigate the role of XAC4296 and Δ4296 in *X. citri* pathogenicity and virulence;
- Morphological characterization of the mutant Δ4296 to investigate the role of XAC4296 in *X. citri* cell morphology and division;
- Investigation of chromosome segregation to evaluate the relation between Δ4296 and XAC4296 with chromosome segregation;
- Sucrose and glutamic acid measurements to evaluate XAC4296 influence in X. citri metabolism;
- Subcellular localization using fusion strategy with mCherry reporter protein to determine the subcellular localization of XAC4296 *in vivo.*

4. MATERIALS AND METHODS

4.1. *In silico* analysis

Global comparisons using sequenced *Xanthomonadaceae* genomes deposited in the public National Center for Biotechnology Information (NCBI) repository were made using TBlastN (Altschul et al., 1997). For XAC4296 homolog detection we used as tBlastN parameters a query coverage and identity >90% and >60%, respectively, and including all three characteristics domains (Table S2 show a complete list of genomes carrying XAC4296 homolog).

Molecular modeling was performed with the Robetta webserver (Kim et al., 2004). Alignments were plotted with ESPript 3 (Gouet et al., 2003). The 3D models were drawn with the chimera tool (Pettersen et al., 2004). Molecular modeling was performed with the Robetta webserver (Kim et al., 2004).

The Chimera Tool was used to generate the three-dimensional structures and interactive visualization of the XAC4296 protein (Pettersen et al., 2004). The three-dimensional structures of the PDB (Protein Data Bank) used as a mold to model the first and second modules were respectively, 5AO8 and 2HTA. These proteins were selected according to the ranking established by the alignment performed by software MAFFT 7,309 (Katoh and Standley, 2013). The stereochemical quality of the generated models was evaluated by analyzing Ramachandran's plot, carried out by Chimera Tool. The three-dimensional models were analyzed in two modules, the first considering 420 amino acids with the SLT_2 and PG_Binding1 domains, similar to the Lytic Transglycosilases; the second module considering 309 amino acids with the EP_1 domain, similar to epimerases.

The XAC4296 homolog sequences were aligned with MAFFT 7.309 (Katoh and Standley, 2013), and their best-fit evolutionary models were predicted with ProTest 3.2.4. A maximum-likelihood tree was reconstructed with RaxML 8.2.9 using a bootstrap value of 1000. The final tree was visualized in FigTree 1.4.4 (http://tree.bio.ed.ac.uk/software/figtree) and edited with Inkscape 0.92.4 (http://www.inkscape.org). The Integrated Microbial Genomes & Microbiomes(IMG/M) system (Markowitz et al., 2012) was used for comparative analyses.

4.2. Strains and growth conditions

Bacterial strains and plasmid strains used in this study are shown in Table 3. The *Xanthomonas citri* (*X. citri*) strains were grown in nutrient broth (NB: 0.5% peptone, 0.3% beef extract), nutrient agar (NA: 0.5% peptone, 0.3% beef extract, 0.15% agar) supplemented with L-arabinose (0.05% w/v) and sucrose (5% w/v) when required, XVM2 (20 mM NaCl, 10 mM $(NH_4)_2SO_4$, 5 mM $MgSO_4$, 1 mM $CaCl_2$, 0.16 mM KH_2PO_4, 0.32 mM K_2HPO_4, 0.01 mM $FeSO_4$, 10 mM fructose, 10 mM sucrose, 0.03% casaminoacids, pH 6.7) at 29ºC. *Escherichia coli* strains were cultivated in Luria-Bertani medium (LB: 1% tryptone, 0.5% yeast extract, 0.10 % NaCl, 0.15% agar; pH 7) and SOB media (SAMBROOK et al., 1989) at 37°C. Antibiotics were used as needed at the following concentrations: kanamycin (Kn), 30 µg/ml; carbenicillin (Carb), 50 µg/ml; streptomycin (Str), 50 µg/ml; gentamycin (Gen), 10 µg/ml; ampicillin (Amp), 100 µg/ml.

Table 3. List of strains and plasmids used in this study.

Bacterial strains and plasmids	Relevant features	Reference
Xanthomonas citri; X. citri	*Xanthomonas citri subsp. citri,* wild type strain, citrus pathogen	(Da Silva et al., 2002)
X. citri-p	*X. citri* harboring pMAJII, Ap^r, Neo^r/Km^r	This work
Δ4296	*X. citri* Δ4296 deletion mutant of *X. citri*	This work
Δ4296c	Complemented strain. Δ4296 harboring pMAJIIc-4296; Amp^r, Kan^r	This work
E. coli DH10B	Δ (*mcrA*, *mcrBC*, *mrr*, A1 and hsdRMS), pir+, *lacZ* for screening	Invitrogen
pNPTS138	Suicide vector, LacZ, Km^r	(Bueno et al., 2021)
pMAJIIc	mCherry expression vector; Ap^r; Neo^r/Km^r; araC-p*ara*; amy106-912; integrative vector in *X. citri*	(Pena et al., 2020)
pNPTS138-Δ4296	Suicide vector, LacZ, Km^r	This work
pMAJIIc-4296	Recombinant vector, protein subcellular localization in *X. citri*	This work
X. citri-p	*X. citri* harboring pMAJII-4296	This work

	recombinant vector, protein subcellular localization

4.3. RNA extraction and cDNA synthesis from XAC4296

X. citri total RNA was extracted using RNeasy protect bacteria Mini kit (*Qiagen*) according to the manufacturer. The first strand of complementary DNA was synthesized from 1µg of total RNA using a qScript® cDNA SuperMix (*Qiagen*). Before cDNA synthesis, RNA samples were treated with DNaseI. The DNA and RNA quantification was performed using Qubit HS (High Sensitivity) (*Thermo Fisher*). Primers F4296 (F) and pMAJIIc (R) were used for PCR reaction using the cDNA as template (Table S3). PCR products were checked by agarose gel electrophoresis and DNA sequencing.

4.4. Mutant construction

Mutant of gene XAC4296 was generated using homologous suicide plasmid (pNPTS138) integration through site-directed mutagenesis by PCR overlap extension approach (Lee et al., 2004). To construct the deletion mutant of XAC4296 ORF, we used *X. citri* genomic DNA as a template and primers described in Table S2. The first PCRs amplifications were made separately using pairs of primers A(F)-B(R) and C(F)-d(R) to generate templates with self-complementary tails. The second PCR was performed using pair of primers A(F)-D(R) and the product A-B and C-D as a template. According to the manufacturer's instructions, the final PCR products, and pNPTS138 suicide vector were double digested with *Nhe*I/*Hind*III enzymes (*New England BioLabs inc*®). According to the manufacturer's instructions, ligation between vector and fragments was performed with T4 DNA Ligase (*New England BioLabs inc*®). The recombinant vector pNPTS138-Δ4296 was transformed into chemically competent *E. coli* DH10B (Sambrook et al., 1989), and transformant colonies were selected using antibiotics and Lac-Z promoter. The constructions were checked by gel electrophoresis and sequencing on a 3730xI DNA analyzer (*Thermo Fisher Scientific*) using primers XACF-XAC-Seq. Finally, the pNPTS138-Δ4296 construction was used for *X. citri* electroporation (Amaral et al., 2005), and colonies were selected by kanamycin

resistance and sucrose susceptibility (Kaniga et al., 1991). Mutant Δ4296 was confirmed by sequencing.

4.5. Cloning XAC4296 at pMAJIIc

X. citri 4296 ORF was PCR amplified using primers pMAJIIc (F)-pMAJIIc (R) (Supplementary Table S) from *X. citri* genomic DNA. The PCR product and the integrative vector pMAJIIc were double digested with *NheI/XhoI* enzymes (*New England BioLabs inc*®) and ligated with T4 DNA Ligase (*New England BioLabs inc*®), according to manufacturer's instructions. The recombinant vector pMAJIIc-4296 was transformed into chemically competent *E. coli* DH10B (Sambrook et al., 1989). Colonies were selected using kanamycin resistance. The selected colonies were transformed in *X. citri* and mutant strain Δ4296 using electroporation (Amaral et al., 2005) and colonies were selected using kanamycin resistance. The recombinant plasmid DNA (pMAJIIc-XAC4296) was purified using Promega Wizard® Plus SV Minipreps DNA Purification System according to the manufacturer's instructions and the inserted XAC4296 DNA sequence was confirmed by sequencing. The recombinant plasmid was used to transform both mutant strain 4296 and *X. citri* wild type strain by electroporation. Colonies were selected by kanamycin resistance and the integrative vector version was identified; they were further selected on NA plates supplemented with 0.2% soluble starch followed by iodine vapor crystals exposure. We obtained the complemented strain Δ4296-pMAJIIc-4296 (named Δ4296c) and recombinant strain *X. citri*-p used for protein subcellular localization. The constructions were checked by gel electrophoresis and DNA sequencing.

4.6. Pathogenicity assay

We used two methods for pathogenicity assays: spray and infiltration. In the spray method. *X. citri* WT and mutant Δ4296 were cultivated in NB medium for 16 hours to O.D. 600nm ~0.8 and diluted in fresh NB medium to O.D. 600nm of 0.3. Cells were collected by centrifugation and resuspended in autoclaved tap water to an O.D. 600 nm of 0.3, equivalent to 10^8 CFU/mL. Three different "Pêra Rio" sweet orange (*Citrus sinensis* L. Osbeck) plants were sprayed with each bacterial suspension until all leaves were fully coated, then covered with a clear plastic bag for 24 h (Li and Wang,

2011). All leaves were quantified, and leaves presenting citrus canker (CC) symptoms were photographed 25 days after inoculation (DAI).

For pathogenicity assays by infiltration method, strains of *X. citri* and mutant Δ4296 were cultivated in NB medium for 16 hours to O.D. 600nm ~0.8 and diluted in fresh NB medium to O.D. 600nm of 0.3. Cells were collected by centrifugation and resuspended in autoclaved tap water to an O.D. 600 nm of 0.3, equivalent to 10^8 CFU/mL. This inoculum was diluted 100-fold (10^6 CFU/mL) and infiltrated on the underside of three young leaves (technical replicates) in three different plants (biological replicates) of “Pera Rio” orange (*C. sinensis* L. Osbeck) using hypodermic syringes (Laia et al., 2009). Symptoms were observed for 25 days, and photos were taken at 4, 8, 12, 15 and 25 days after inoculation (DAI).

Inoculated plants were kept in a high-efficiency particulate air (HEPA) filtered plant laboratory with controlled environmental conditions (28–30 °C, 55% humidity, 12 hours light cycle).

4.7. *Ex vivo* growth curves

X. citri and Δ4296 mutant were cultivated in NB medium for 16 hours and diluted in fresh NB medium to O.D. 600 nm of ~0.1. When was necessary, cells were resuspended in different conditions: NB with antibiotic, NB with sucrose, NB with glutamic acid. Cell cultures were distributed on 96 well plates and were incubated in a Synergy H1 microplate reader (BioTek®, Winooski, VT, USA) under constant agitation at 29 °C, and automated O.D. readings were taken every 30 min. Growth curves were generated using Graphpad Prism 6 software, based on three technical and three biological replicates (Lacerda et al., 2017).

4.8. *In planta* growth curves

X. citri and Δ4296 mutant were cultivated in NB medium for 16 hours until O.D. 600nm got around 0.8 and diluted in fresh NB medium to O.D. 600nm of 0.3. Cells were collected by centrifugation and resuspended in falcon tubes containing 50 mL of autoclaved tap water to an O.D. 600 nm of 0.3, equivalent to 10^8 CFU/mL. This inoculum was diluted 100-fold (10^6 CFU/mL) and infiltrated on the underside of fifteen young leaves in four different plants (biological replicates) of “Pera Rio” orange (*C.*

sinensis L. Osbeck) using hypodermic syringes. The strains were exuded from leaves at days 0, 1, 3, 6, and 10 DAI, and the number of cells per leave was achieved using the microculture strategy (Laia et al., 2009).

4.9. Microscopy

X. citri WT, Δ4296 mutant, and Δ4296c strains were cultivated in NB media until O.D. 600nm got around 0.3 ABS at 29 ºC. We performed analysis in different conditions: with ampicillin (20 µg/mL), sucrose 2% (w/v) and glutamic acid 2% (wv). For morphological analysis, strains were collected by centrifugation, and pellet cells were resuspended in 0.85% NaCl. For chromosome investigation, we used 4',6-diamidino-2-phenylindole DAPI coloration at a final concentration of 0.01%. Cultures were treated with propidium iodide (IP) for cell viability investigations at a 0.001 mg/mL final concentration Drops of 10µL of cell culture were placed on microscope slides coverslip (Martins et al., 2010). We performed the assays three times and quantified cells individually (n=800). Microscopy slides were immediately visualized using an Olympus BX61 microscope equipped with a monochromatic camera OrcaFlash 2.8 (Hamamatsu, Japan). The software CellSens Version 11 (Olympus) was used for data collection and analysis.

4.10. Fluorescence microscopy

Protein subcellular localization was performed using *X. citri* WT strain (as negative control) and *X. citri* -pMAJIIc..4296. The strain was cultivated in NB medium until O.D. 600nm got to ~0.2 ABS at 29ºC when the medium was supplemented with arabinose 0.05% and incubated from 6 to 24 hours. The culture was collected at different times, and drops of 10µL of cell culture were placed on microscope slides coverslip (Martins et al., 2010). Following treatments, cells were immediately visualized using an an Olympus BX61 microscope equipped with a monochromatic camera OrcaFlash 2.8 (Hamamatsu, Japan). Image analysis was performed using the software ImageJ (http://rsb.info.nih.gov/ij/).

4.11. Statistics

The data was tested by Welch's ANOVA test (p= 0.05) using GraphPad Prism 8.0.1. Graphics were generated using Microsoft Office Excel for Windows.

5. RESULTS

5.1. *In silico* analyzes of XAC4296

We analyzed the XAC4296 gene (2,163 bp) using different *in silico* approaches, corroborating that the XAC4296 gene and their homologs present in other *Xanthomonas* species is not associated with common mobile genetic elements, such as prophages, insertion sequences, transposons, integrons, and genomic islands. Therefore, we hypothesize that the XAC4296 gene is likely originated from a previous gene fusion event (Figure 20A and B).

Molecular modeling performed with the Robetta software provided both *ab initio* and comparative modeling for protein tridimensional (3D) structure. However, the Robetta approach could not generate a unique 3D structure containing both LT and epimerase domains present in XAC4296, and thus, representing the entire protein. Therefore, for the understanding of the XAC4296 structure, both domains were modeled separately. While the LT located on the N-terminus of XAC4296, containing the SLT_2 and PG_Binding1 domains, was modeled based on a sequence of 408 amino acids (Figure 20B), the XAC4296 C-terminus, having the epimerase bearing the aldose-1-epimerase domain, was modeled based on 312 amino acids sequence (Figure 20B). The confidence value for both models was 0.86 and 0.81, respectively, supporting a reasonable quality of both 3D structure predictions.

The first module resembles a classic 3B LT showing the 3D structure of the SLT_2 and PG_Binding1 domains (Figure 20 B and C) sustained by the amino acid alignment (Figure 21). The alignment between orthologs sequences reveals higher identity (70-90%) to the SltB3 (5NAZ) protein from *P. aeruginosa*, *Slt35* (5AO8), MltB (1LTM), and Slt35 (1D0K) from *E. coli* (Van Asselt; Dijkstra, 1999; Lee et al., 2016) and SltB1 (4ANR) and SltB1 (5O8) from *P. aeruginosa* (Figure 22). In contrast, the 3D structure of the XAC4296 second module shows the aldose-1-epimerase domain (Figure 20B), supported by the amino acid alignment (Figure 22). Alignments among ortholog proteins showed high similarity, ranging from 80 to 99%. The proteins that showed the highest similarity (~87%) were 2HTA from *Salmonella typhimurium*, 2JOV from *Clostridium Perfringens*, 2CIQ, and 2CIR from *Saccharomyces cerevisiae* S288C and 3K25 from *Synechocystis* sp.

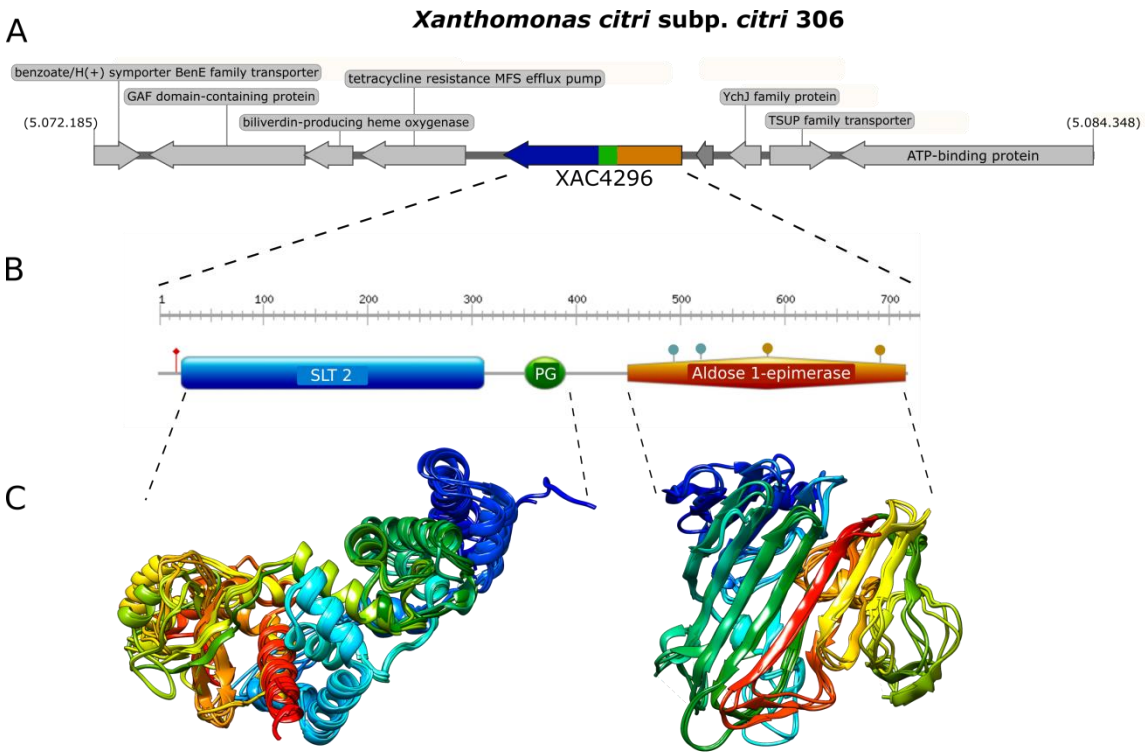

Figure 20. Genome context, protein domain, and structure of XAC4296. A: Genome context of XAC4296 from *Xanthomonas citri* (*X. citri*) genome. B: Protein domain and structure of XAC4296. XAC4296 has 720 aa with the LT domain associated with 3B family: Transglycosylase SLT domain (SLT_2) (PF01464.) and Peptidoglycan binding (PG_binding_1) (PF01471) domains, and the Aldose 1-epimerase (PF01263) domain, related to carbohydrate metabolism. C: Molecular modeling cartoon representation of XAC4296 domains.

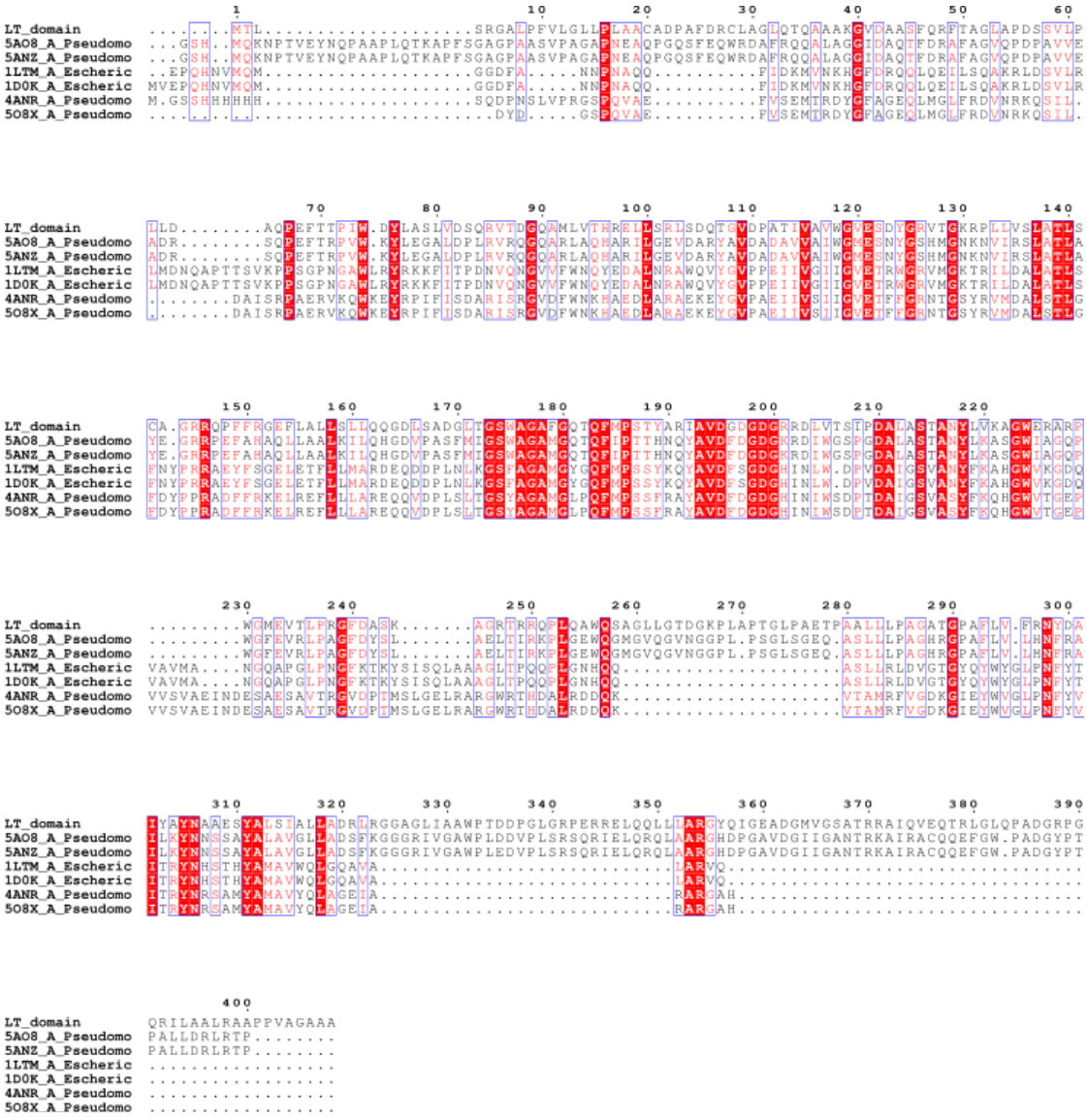

Figure 21. Alignment between the first XAC4296 module formed by SLT_2 and PG_binding1. Alignment was performed using the 3D models at Protein Data Bank (PDB). 5AO8 and 5ANZ: SltB3 of *Pseudomonas aeruginosa*; 1LTM: the soluble lytic transglycosylase Slt35 from *Escherichia coli*; 1D0K: the SLT35, 4ANR and 5O8X: the SltB1 from *Pseudomonas aeruginosa*.

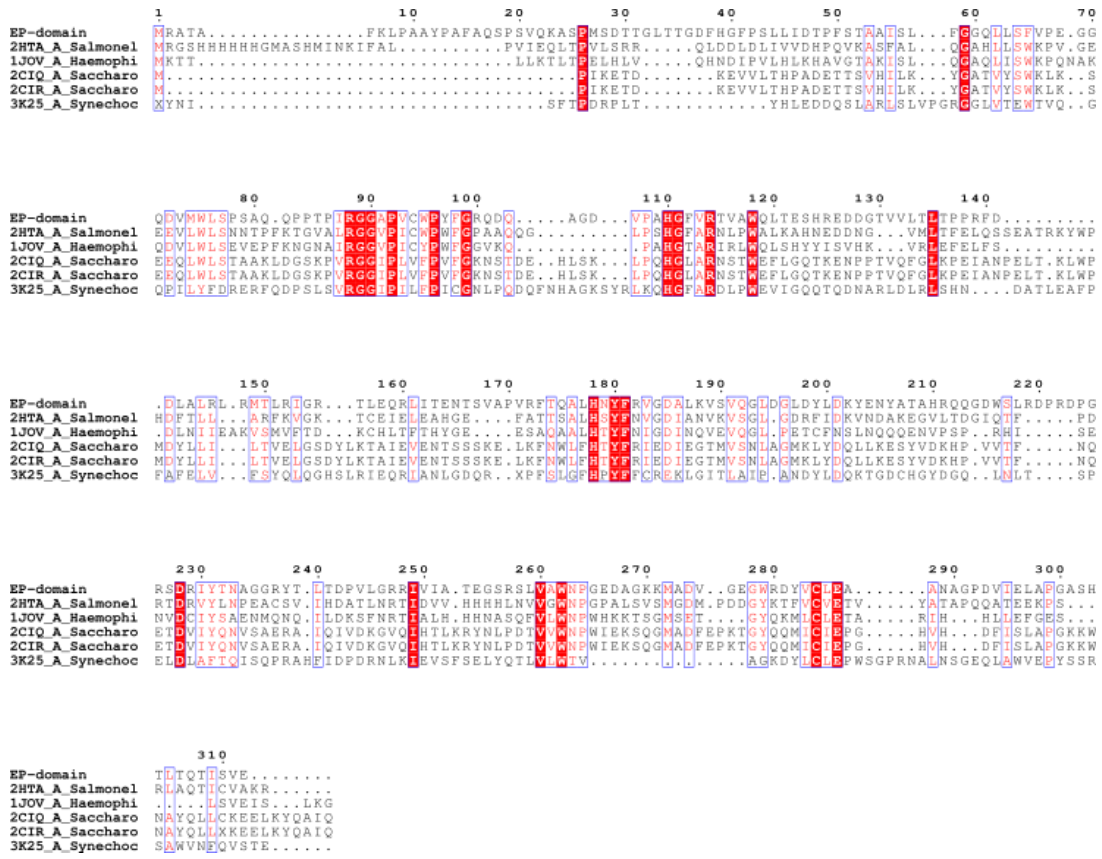

Figure 22. Alignment between the second XAC4296 module formed by Aldose 1-epimerase domain. 2HTA: the mutarotase YeaD from *Salmonella typhimurium*; 1JOV: the HI1317 from *Haemophilus influenzae*; 2CIQ and 2CIR: the ymr099c from *Saccharomyces cerevisiae* S288C; 3K25: the Slr1438 from *Synechocystis* sp. PCC 6803.

The 3D structure of the first module of XAC4296 (LT domains) was further evaluated using SltB3 (5AO8) from *P. aeruginosa* as a model (Figure 23A). The structures alignments reveal 37,40% identity and RMSD= 0.923 Å (Root Mean Square Deviation). The 3B LT family of proteins shows α-helix, and the core domain forms a large and deep groove, where the peptidoglycan substrate is supposed to bind (Figure 23B) (Lee et al., 2016). That is the location of the active-site residue Glu-139 (but SltB3 Glu-141) (Figure 23B, red area), related to the protonation event to promote the breakdown of glycosidic bond, and subsequent generation of the transient oxocarbenium species that entraps the C-6 hydroxyl in generating the 1,6-anhydromuramyl moiety as the product. (Figure 23B) (Lee et al., 2016).

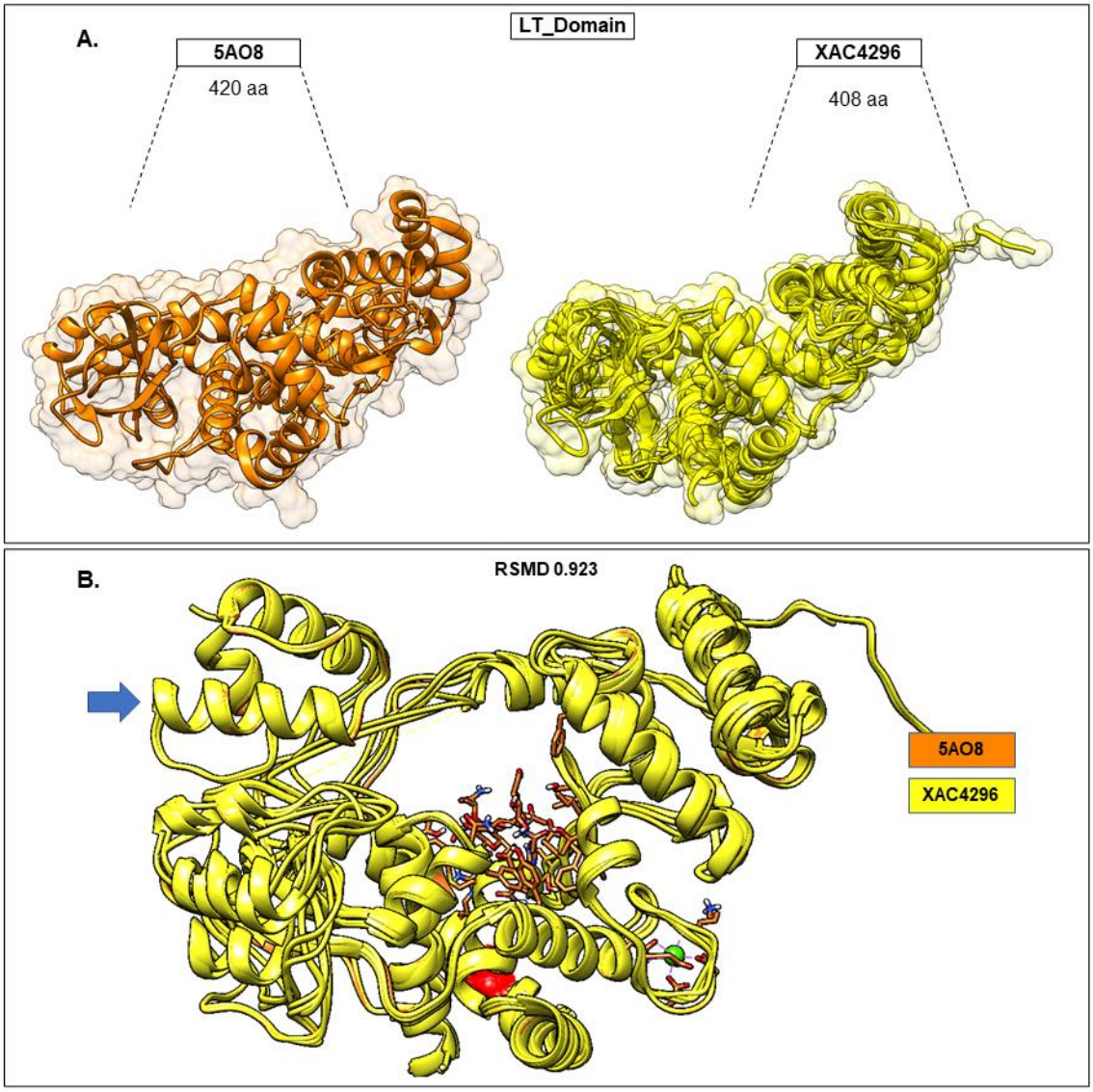

Figure 23. 3D structure of the first module of XAC4296 from *Xanthomonas citri* (*X. citri*) (containing the LT domains PG_Binding1 and SLT_2), was performed using SltB3 from *Pseudomonas aeruginosa,* in complex with NAG-NAM-pentapeptide (5AO8) as a model (Figure 23A). Ligand NAG-NAM is depicted as capped sticks and colored in light blue for C atoms, red for O atoms, and white for N atoms. The Blue arrow indicates *α-helix* in the secondary structure of the protein. A red amino acid in the structure indicates the catalytic site acid Glu-139. The model was created using the Chimera software version 1.15 (Pettersen et a., 2004).

XAC4296 EP domain showed high sequence identity to other well-characterized mutarotases. XAC4296 second module (EP domain) was performed using YeaD (2HTA) from *Salmonella typhimurium* as a model (Figure 24A). Structures alignment reveal 31,93% of identity and a RMSD of 0.725 Å. The 3D second module shows regions adopting β-sandwich folds similar to GalMs and 2HTA (Figure 24A and B, black arrow). The catalytic and substrate-positioning residues of YeaD protein corresponds

to the His-95, His-164, Asp-208, and Glu-267 amino acids (Chittori et al., 2007), while in XAC4296 it is located on the Asp-204 and Glu-267 amino acids(Figure 24B, red and green aa).

Taken together, these findings support that XAC4296 has two completely independent domains, that might preserve the transglycosylase and epimerase activities separately.

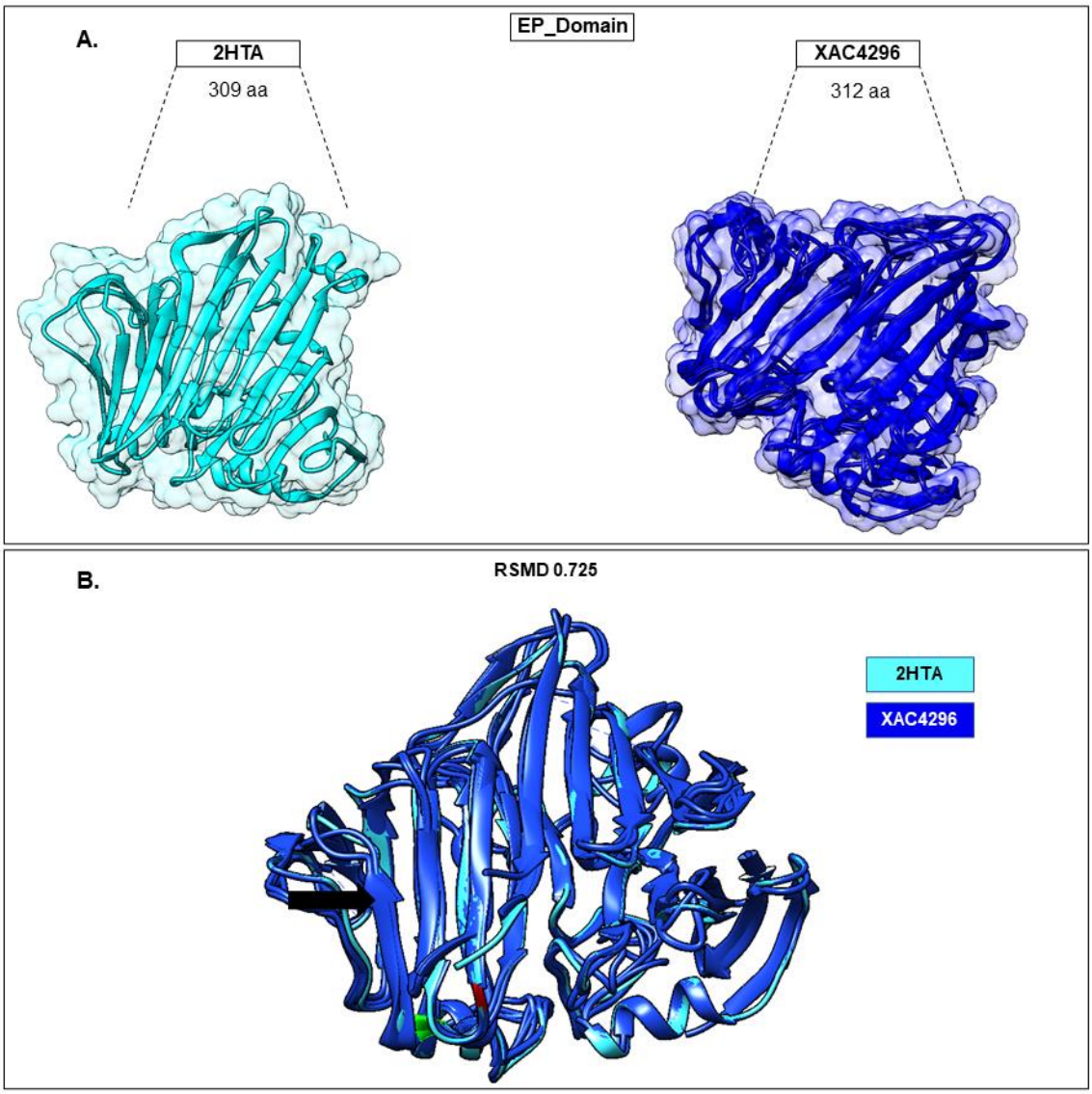

Figure 24. 3D Structure of a putative mutarotase (XAC4296 second module) from *Xanthomonas citri* (*X. citri*), with YeaD from *Salmonella typhimurium* as a model. Catalytic and substrate-positioning residues: Asp-204 and Glu-264 (green and red amino acid, respectively). The black arrow indicates the β-sheet among the protein. The model was created using software Chimera version 1.15 (Pettersen et a., 2004).

Comparative analyses support that XAC4296 homologs are exclusively found in many different species of *Xanthomonas*, *Pseudoxanthomonas*, and *Stenotrophomonas*, accounting for up to 308 complete sequenced genomes available in the GenBank database (Figure 25 and Table S2). The maximum-likelihood phylogenetic tree constructed using the full-length protein sequences of XAC4296 homologs shows similarity with two species of *Pseudoxanthomonas* genus, 36 species of *Stenotrophomonas* genus, and 270 species of *Xanthomonas* genus that were assigned in 19 clades (Figure 25 A).

Moreover, considering these three genera, the XAC4296 homologs are generally located in a conserved genomic context (Figure 26) and are not associated with common mobile genetic elements, such as prophages, Insertion Sequences, Transposons, Integrons, and Genomic Islands. Therefore, strongly supporting that the XAC4296 origin is not associated to common lateral gene transfer mechanisms. It is noteworthy to mention that the XAC4296 homolog is not present in the *X. albilineans* and in the phylogenetically closely-related *Xylella* genus (Figure 25 A). *Xylella* carries an independent epimerase gene (i.e.i.e., WP_010894718.1) and a least 4 LTs genes, all located at distant genomic loci. Conversely, in addition to an aldose 1-epimerase domain containing gene (i.e. XALC_0947 and XaFJ1_GM000925), the *X. albilineans* species (e.g. GPE PC73 and Xa-FJ1 strains), also carries the two modules (LT and Epimerase) as separated and overlapping genes (21 nt of overlapping), each gene showing the domains modules in different frames and resembling a degenerated XAC4296 homolog (Figure S2). Moreover, the other *Xanthomonas* species, *Pseudoxanthomonas* and *Stenotrophomonas* carry their own set of LTs (varying in number and diversity of families); however, the aldose-1-epimerase domain is exclusive for each XAC4296 homolog, and thus, do not exist as an alone or duplicated feature, much the same as D-hexose-6-phosphate mutarotase gene in these genomes, as observed in *Xylella* and *X. albilineans*.

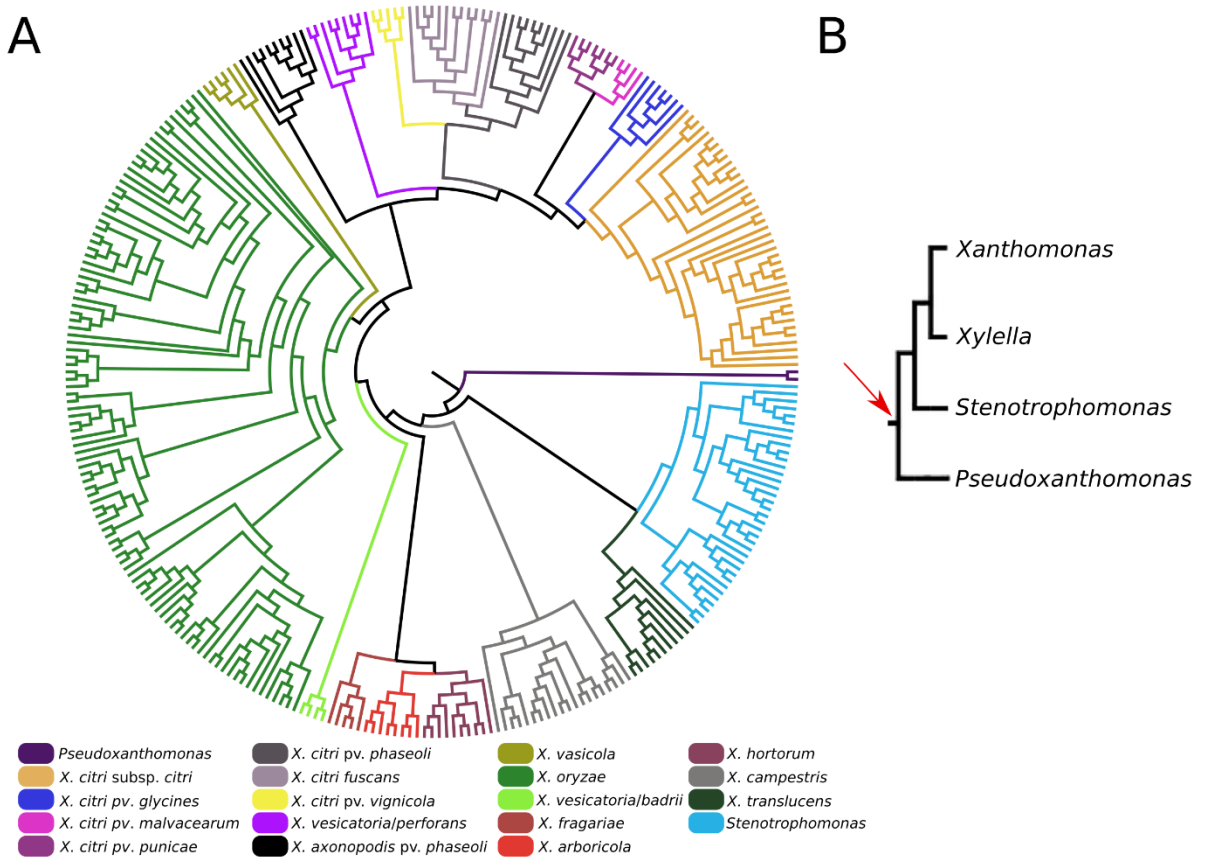

Figure 25. Maximum-likelihood phylogenetic tree of XAC4296 homologs across *Xanthomonadaceae* family supports the XAC4296 potential origin before *Xanthomonas*, *Xylella*, *Pseudoxanthomonas*, and *Stenotrophomonas* differentiation. The closely-related *Xylella* genus lost the XAC4296 homolog. **B.** Phylogenetic construction of the *Xanthomonadaceae* family phylogroup formed by *Xanthomonas*, *Xylella*, *Pseudoxanthomonas*, and *Stenotrophomonas* (based on (Bansal et al., 2021). The red arrow indicates the potential gene fusion event that originated the XAC4296 ancestor.

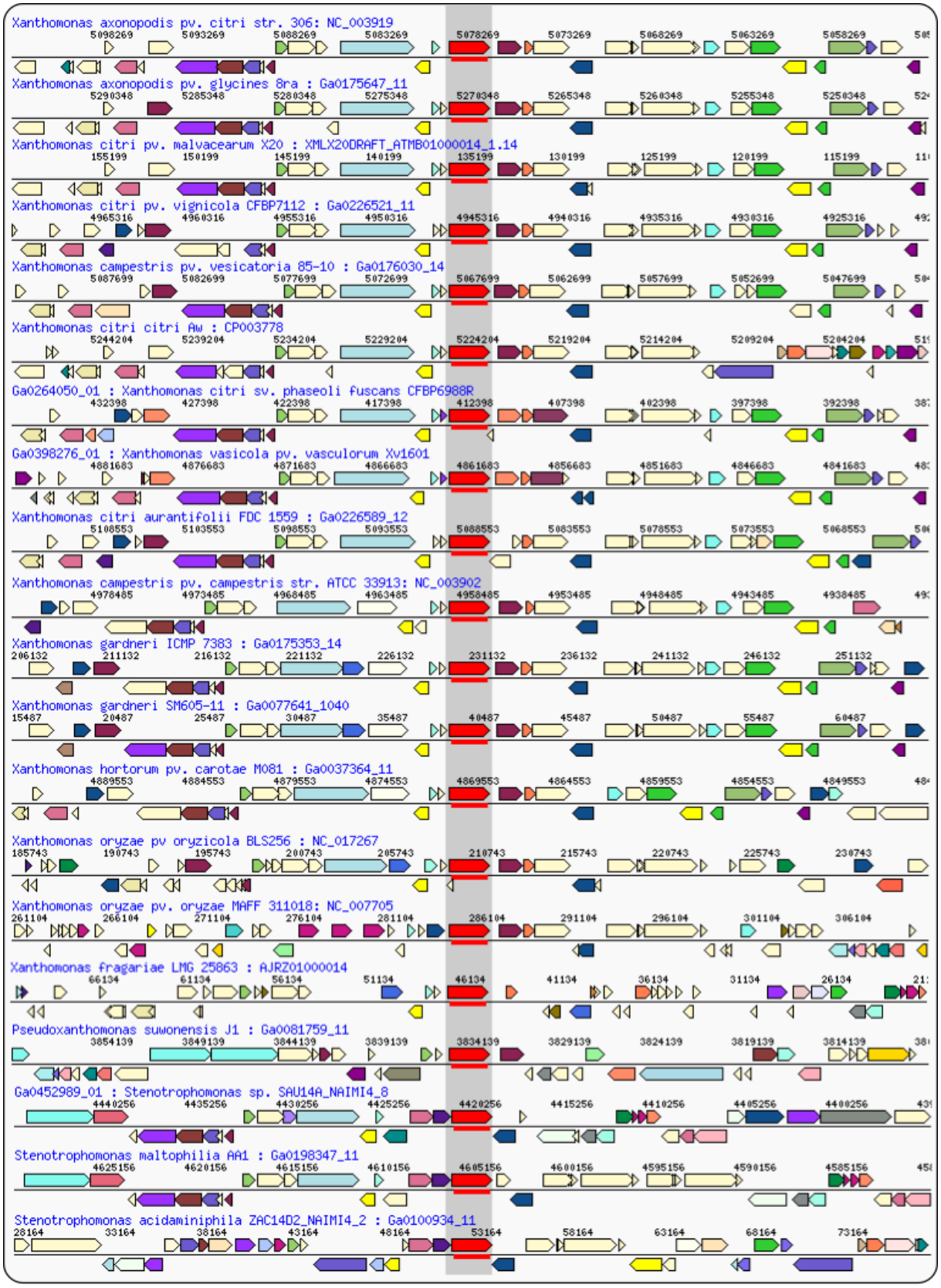

Figure 26. Genetic organization of XAC4296 across *Xanthomonas, Pseudoxanthomonas,* and *Stenotrophomonas* spp. The central gray rectangle represents the XAC4296 position in each Xanthomonadales genome.

5.2. *X. citri* expresses XAC4296 gene in *Citrus sinensis* L. Osbeck

As observed in our previous results, XAC4296 and their homologs present in *Xanthomonas*, *Pseudoxanthomonas*, and *Stenotrophomonas* were originated at the last common ancestor of these lineages. However, so far there is no evidence of the functionality of this gene and its role during plant-pathogen interactions. To confirm XAC4296 expression during plant-pathogen interaction, *Citrus sinensis* L. Osbeck (considered a moderately resistant host, Figure 3) was inoculated with WT *X. citri*, and the pathogen was exuded five days later. The synthesis of double-stranded cDNA from total RNA was performed and used as a template for PCR reaction. The fragment with approximately 2,200 pb was obtained, suggesting that XAC4296 is expressed during plant-pathogen interaction (Figure 27).

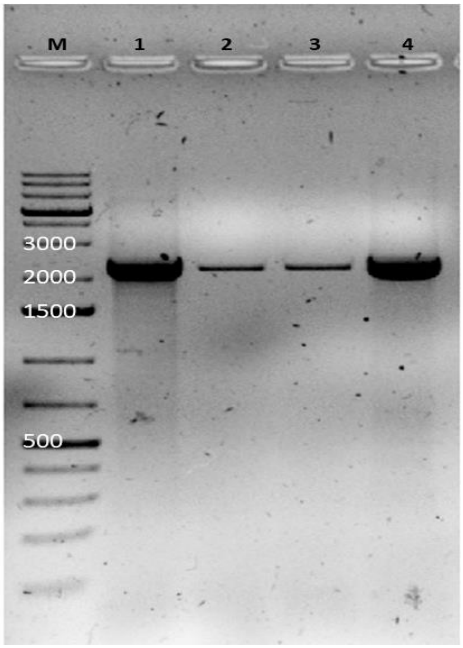

Figure 27. 1% agarose gel showing amplification of XAC4296 gene in *X. citri.* (M) 1Kb Fermentas DNA Ladder marker. (1) PCR product of genomic DNA (~2400 bp) used as a positive control (non-infecting condition). (2,3,4) PCR product of *X. citri* cDNA obtained from total RNA of 5 days infected *Citrus sinensis* L. Osbeck with *X. citri* expressing *in vitro*.

5.3. Pathogenicity assay supports the relation between XAC4296 and citrus canker progression

We further investigated the role of XAC4296 on *X. citri* virulence and pathogenicity. The XAC4296 gene was deleted by site-directed mutagenesis to generate mutant Δ4296, and the integrative plasmid pMAJIIc (Pena et al., 2020) was employed to construct the complemented strain Δ4296c. Young leaves of the moderately susceptible cultivar “Pêra Rio” sweet Orange (*Citrus sinensis* L. Osbeck) were spray inoculated with the WT *X. citri* and Δ4296 mutant strains and symptoms were evaluated up to 25 days post inoculation (dpi) (Figure 28, Table 4).

At the last time-point (25 dpi), the WT *X. citri* strain presented the highest number and size of canker lesions compared with the Δ4296 mutant (Figure 28). We also performed inoculation by infiltration in three citrus variets with different susceptibility to *X. citri*: the most susceptible cultivar “Galego” acid lime (*Citrus latifolia* Tan), a moderately susceptible cultivar “Pera Rio” sweet orange (*Citrus sinensis* L. Osbeck), and the least susceptible orange variety “Ponkan” (*Citrus reticulata*). All cultivars showed a very similar result, but the mutant Δ4296 presented water soaking, hyperplasia, and necrosis like wild type strain *X. citri* and the complemented strain (Δ4296c) (Figure 29).

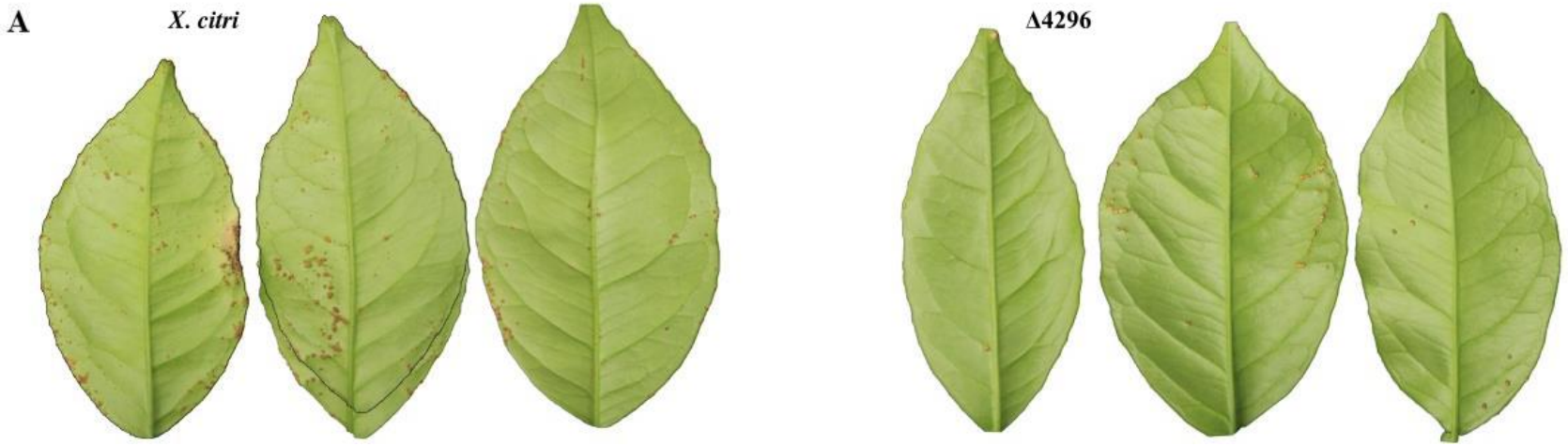

Figure 28. Pathogenicity test by spray method. Citrus canker disease progression in "Pera Rio" sweet orange leaves sprayed with 10^8 CFU/mL bacterial suspension of *X. citri* and mutant Δ4296. Representative leaves of each treatment with the highest disease severity 25 days post inoculation are presented.

Table 4. Quantification of citrus canker lesions in “Pera Rio” sweet orange leaves (*Citrus sinensis* L. Osbeck) inoculated by the spray method. The number of lesions were counted in the abaxial surface of the leaves.

Strain	Number of leaves without CC lesions	Total CC lesions	Average of CC lesions per leaf
X. citri	46	884[a]	46,52%[a]
Δ4296	41	395[b]	19,42%[b]

Different letters mean significant differences according to the Tukey test, p= 0.05, n=65.

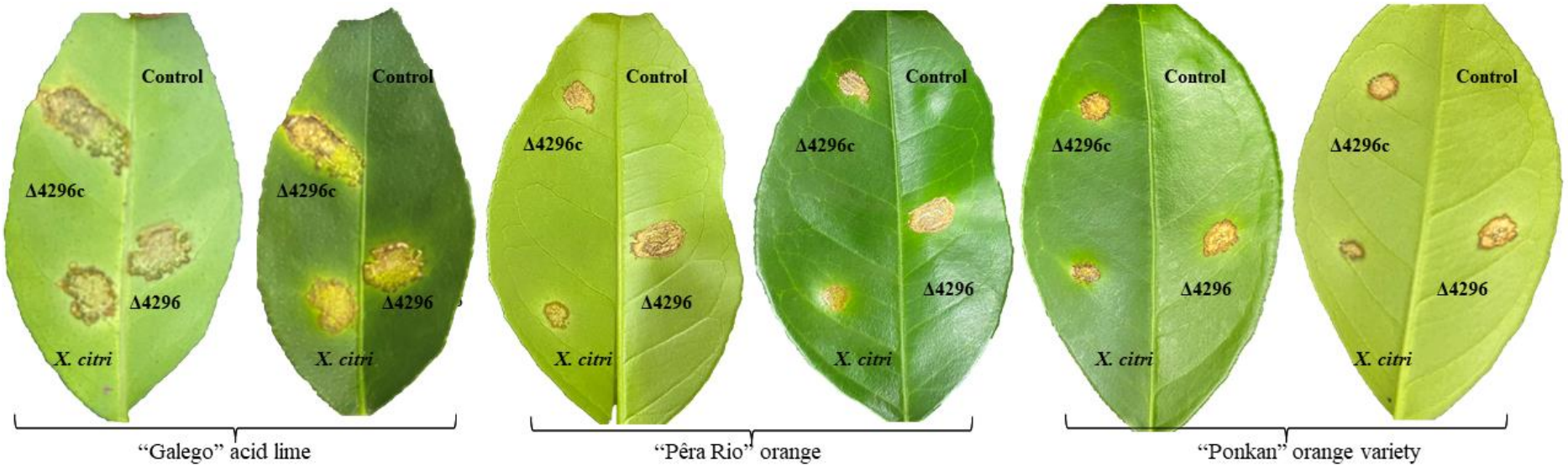

Figure 29. Pathogenicity test by infiltration method. Citrus canker disease progression in leaves of different citrus varieties infiltrated with 10^6 CFU/mL bacterial suspension of *X. citri*, Δ4296, Δ4296c and autoclaved tap water as negative control after 25 days post of inoculation. On each leaf, *X. citri* and Δ4296c were infiltrated on the left-hand central vein, while mutant the Δ4296 and negative control were infiltrated on the right-hand side.

These results indicate that the effects of XAC4296 mutation are statistically significant different for the spray method, presenting a decrease in approximately 42% of lesions compared to the WT *X. citri* (Table 4). The infiltration method did not show any difference in CC lesions compared to the WT *X. citri*, whereas the spray method showed fewer and smaller canker lesions when inoculated with the mutant.

The effects of XAC4296 mutation on canker formation may be related with bacterial epiphytic colonization but an indirect effect on *X. citri* pathogenicity and virulence. Various analyses on different aspects of bacterial cell growth and microscopical analysis were performed to address these possibilities.

5.4. *Ex planta* bacterial growth indicates XAC4296 is not an essential gene

We performed *ex vivo* growth curves for *X. citri* wild type, Δ4296, Δ4296c, and *X. citri* -p using NB and XVM2 defined medium to investigate cell viability (Figure 31A and B, respectively). All strains developed similar growth patterns over time (Figure 31). This is mainly observed on an NB-rich medium (Figure 30A). Δ4296 mutant produced slightly more than wild-type *X. citri* on XVM2 defined medium (Figure 30B). Moreover, since XAC4296 functions may be involved in basal metabolism, cell morphology may be affected during Δ4296 growth, as the higher cell mass in the XVM2 inducing liquid cultures indicates (as measured by O.D. 600). These results indicate that XAC4296 is not essential for bacterial development but may be important for cell morphology.

To investigate *planta* bacteria growth, plant discs were collected from inoculated leaves with *X. citri* wild type and Δ4296 mutant and processed for further inoculation in the NA medium for bacterial cell count. *X. citri* and Δ4296 showed similar growth development on the Lag, Log phases and cellular death (Figure 30C). These results indicate that XAC4296 is not required for virulence in *X. citri* but may be involved in epiphytic colonization.

Moreover, the effect of XAC4296 is unlikely to be directly linked to *ex planta* cell growth since the growth curves of the *X. citri*, and the mutant appeared nearly close, as shown in Figure 30B, therefore, we conclude that XAC4296 is a non-essential protein for *X. citri* development. However, XAC4296 may be involved in cell division

and shape due to its domains (LT and epimerase) and cell mass (as measured by O.D. 600). To evaluate the role of XAC4296 in cell morphology, we further performed microscopical analysis.

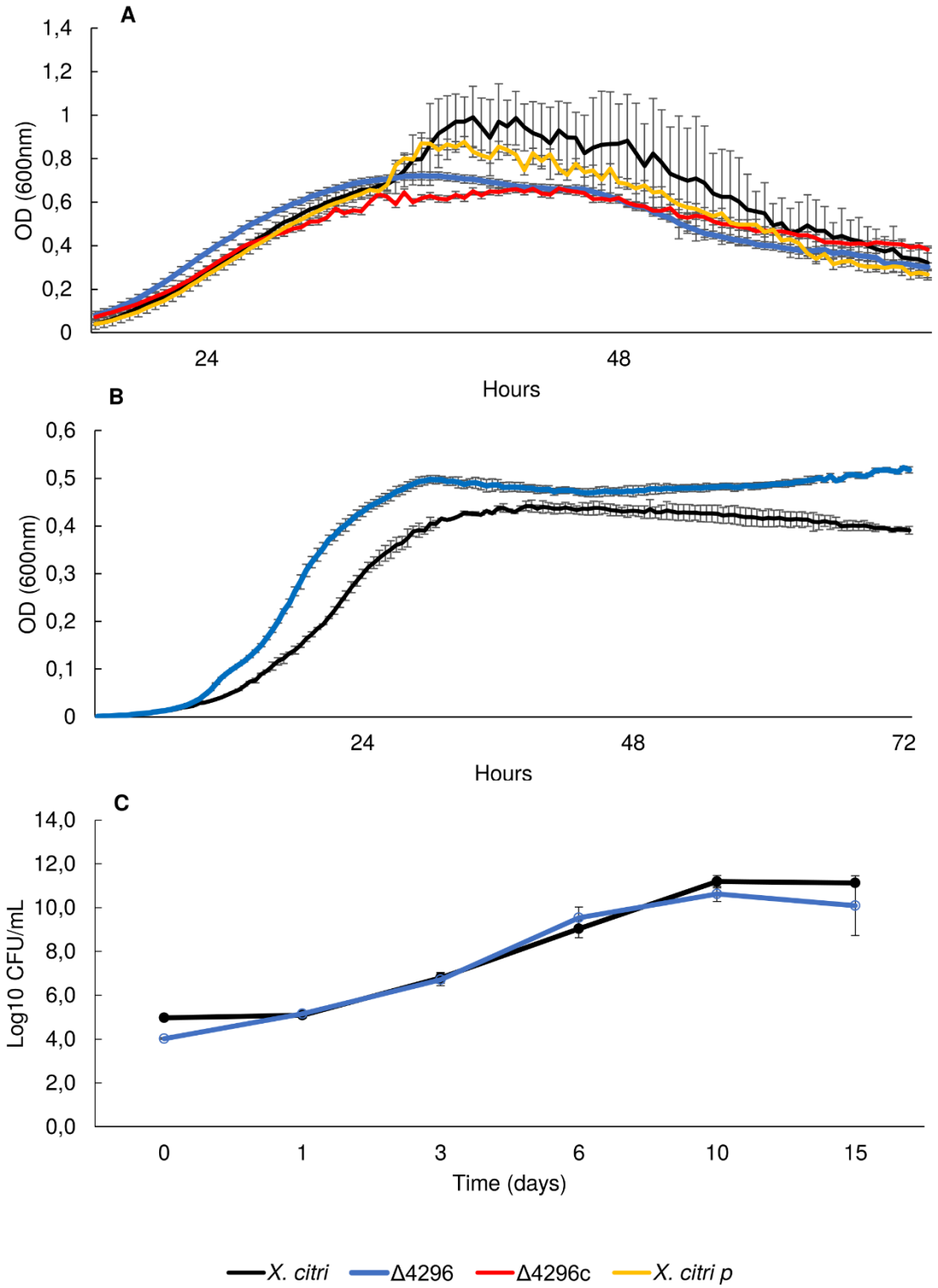

Figure 30. Comparison of the growth curves of *ex planta* bacterial growth and *in planta* bacterial growth. **(A)** *Ex planta* bacterial growth curve performed on rich medium NB for 72 h. **(B)** *Ex planta* bacterial growth was achieved on XVM2 defined medium for 72

h. **(C)** *In planta* bacterial growth curve. Error bars indicate the standard error of three independent technical replicates.

5.5. Δ4296 cells displayed abnormal nucleoid distribution, chains, and short filaments

We used phase-contrast microscopy to investigate the impact of the Δ4296 mutant on cell shape. Cultures of Δ4296 showed different shapes, including short filaments and chains (Table 5, Figure 31).

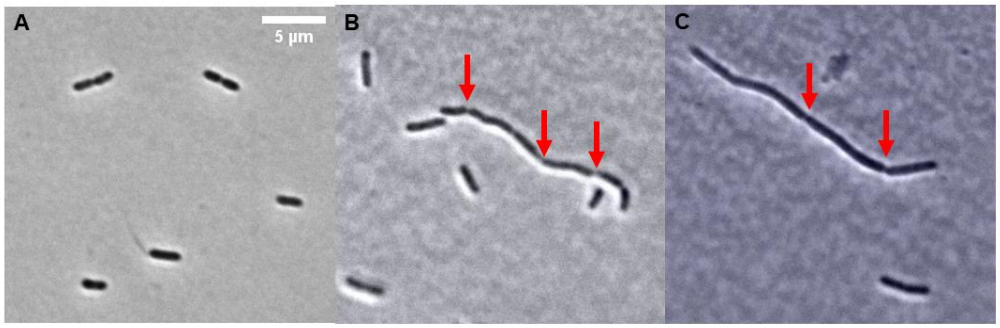

Figure 31. Phase-contrast images showing the morphology of *Xanthomonas citri* (*X. citri*) (A) and Δ4296 (B, C) strains grown to exponential phase in NB medium. Red arrows indicate sept constriction in short filaments (magnification of 100X) — scale=5 µm.

To evaluate the cell morphology quantitatively, 800 individual cells of wild-type *X. citri*, Δ4296 mutant, and Δ4296c (complemented strain) were analyzed. Different Δ4296 phenotypes were observed compared to wild-type *X. citri*. The reverted phenotype is also observed in the complemented strain Δ4296c (Table 5, Figure 32). For instance, approximately 35% of the cells exhibited short filaments (Table 4 Figure 32).

Short filaments and chains are classified according to cell morphology: elongated cells showing asymmetric cell envelope constriction at the onset of bacterial cytokinesis are called filamented cells; each filamented cell was counted. While chains, the cells create daughter cells by budding which in turn create more by budding, but without concluded division cycle and showing septum constriction; each chain was

counted. The chromosome investigation was realized in the filamented cells and chains, each phenotype had one chromosome per cell.

Table 5. Comparison of cell morphology aspects *Xanthomonas citri* (*X. citri*), mutant Δ4296, and Δ4296c strains in rich medium (NB).

	Short filaments %	**Chain %**	**Nucleoid %**
X. citri	0.50[a]	0[a]	0[a]
Δ4296	30.625[b]	15.75[b]	37.125[b]
Δ4296c	0.25[a]	0[a]	0.5[a]

Total n= 800 cells measured. Data correspond to the average cell morphology— different letters mean significant difference according to Welch's ANOVA test, p =0.05.

Moreover, 4',6-diamidino-2-phenylindole (DAPI) dying was employed to investigate bacterial chromosome organization. In wild-type *X. citri* and Δ4296c, we observed a similar pattern for chromosome organization, cell shape, and cell division (Figure 32A-C). However, theΔ4296 showed a continuous mass chromosome into elongated cells and nucleoid accumulation (Figure 32, white arrows). We also observed septum constriction (Figure 32, red arrows), indicating competent cell division even in the absence of the XAC4296 gene. Together, these findings suggest that the first cell error probably occurs mostly during chromosome segregation and only subsequently during cell division, as a result of the poor chromosome segregation and not from the cell division process itself.

These results demonstrate that the length of chromosome distribution in the Δ4296 mutant strain was a lot broader than that of the wild type and the Δ4296c complemented strain (Figure 32).

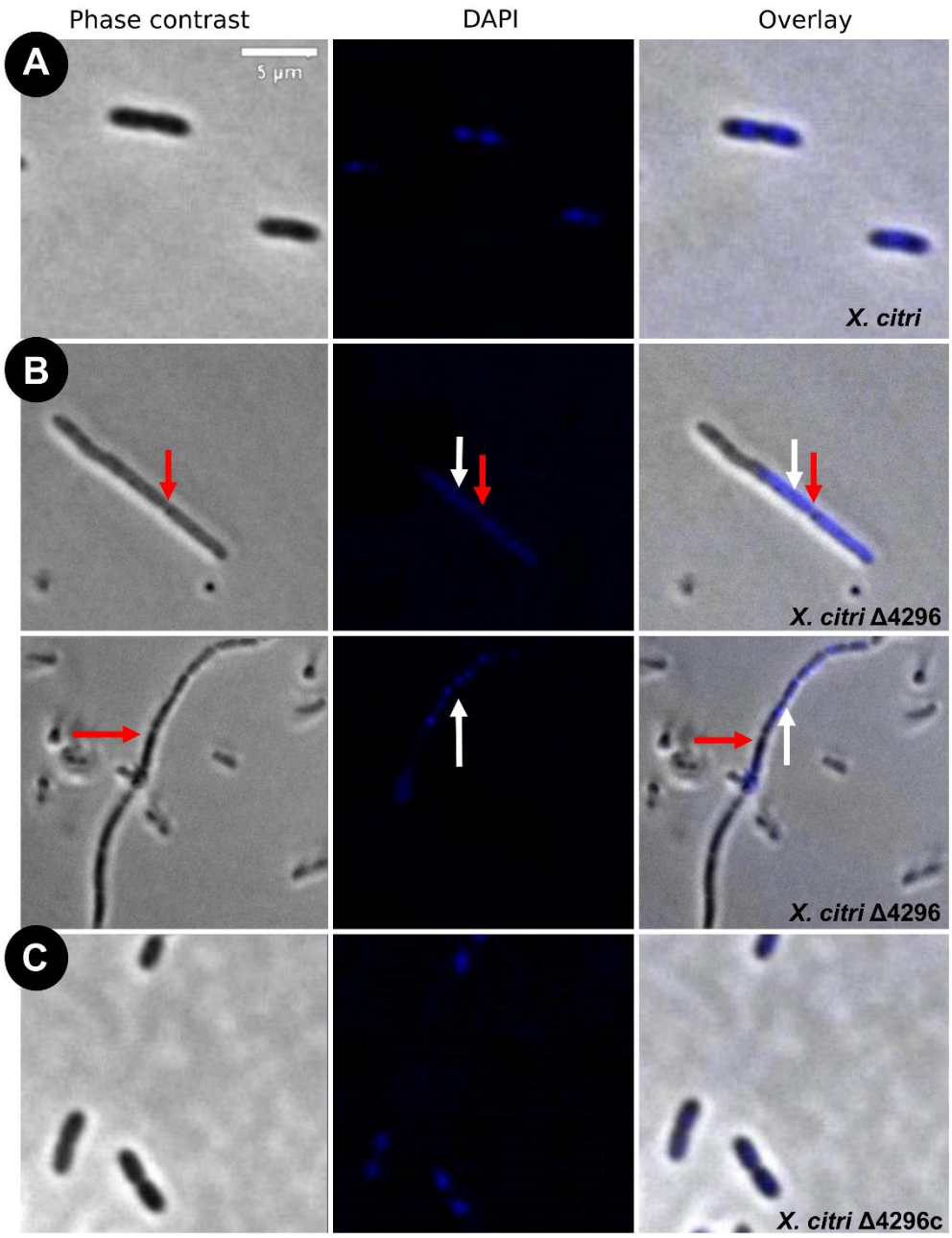

Figure 32. Morphological analysis and chromosomal segregation of *Xanthomonas citri* (*X. citri*), Δ4296, and Δ4296c strains. The figure shows microscopy phase contrast, DAPI, and overlay of the two filters, respectively, for A: *X. citri* WT; B: Δ4296 and C: Δ4296c (magnification of 100X). White arrows indicate nucleoid distribution; red arrows indicate septum constriction (magnification of 100X), -scale=5 µm.

5.6. XAC4296 is required for proper cell wall synthesis in *Xanthomonas*

We observed the wild-type *X. citri* and Δ4296 cells growth in the presence of ampicillin (Figure 33) and subsequently visualized by fluorescence microscopy (Figure 34).

In the presence of ampicillin, no morphological defect was detected in the *X. citri* cells, in contrast, all Δ4296 cells suffered morphological defects, not only in their cell shape but also in their nucleoid morphologies (Figure 34 and Table 6).

The Δ4296 mutant showed a significant delay in growth development in the presence of ampicillin, unlike the wild-type *X. citri* strain (Figure 33), which generally grows well in the presence of ampicillin. Many *Xanthomonas* spp. are naturally resistant to ampicillin (Weng et al., 2004) (XAC3163/XAC_RS16030), however, since XAC4296 first module is homologous to the LTs 3B family, which functions may be related to cell wall dynamics (Dik et al., 2017), in the absence of XAC4296, antibiotic sensitivity is pronounced. Therefore, this result is compatible with the LT role in cell wall reconstruction when cells were cultivated in the presence of the β-lactam antibiotic.

This observation raised the idea that XAC4296 is required for cell wall synthesis and dynamics, which is compatible with the presence of the LT domain. To evaluate the hypothesis that XAC4296 is indeed related to cell wall synthesis and dynamics, we challenged the mutant cells using ampicillin antibiotic to interfere with cell wall construction (Delcour, 2009) and compared the resultant phenotypes with that of wild type cells (Figure 34, Table 6). In culture media with ampicillin, Δ4296 cells display morphological defects (Figure 34), which are reminiscent of the phenotypes exhibited by cell wall mutants (Chastanet and Carballido-lopez, 2012), as suggested by literature.

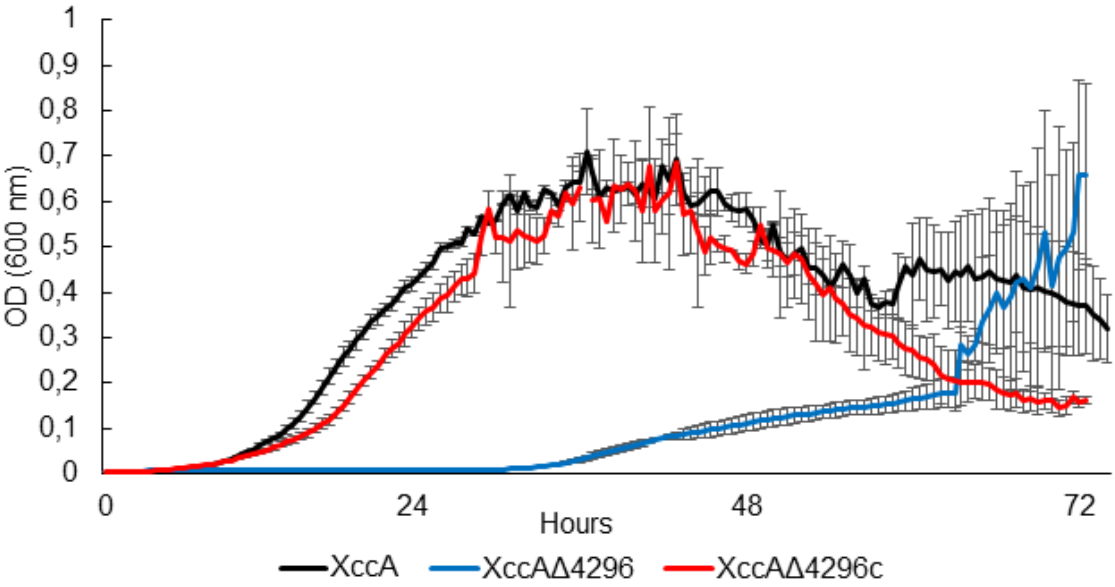

Figure 33. *Ex planta* bacterial growth curves performed on rich medium and ampicillin 20µg/mL for *Xanthomonas citri* (*X. citri*), Δ4296, and Δ4296c. Δ4296 growth is affected in the presence of ampicillin. Error bars indicate the standard error of three independent biological and technical replicates.

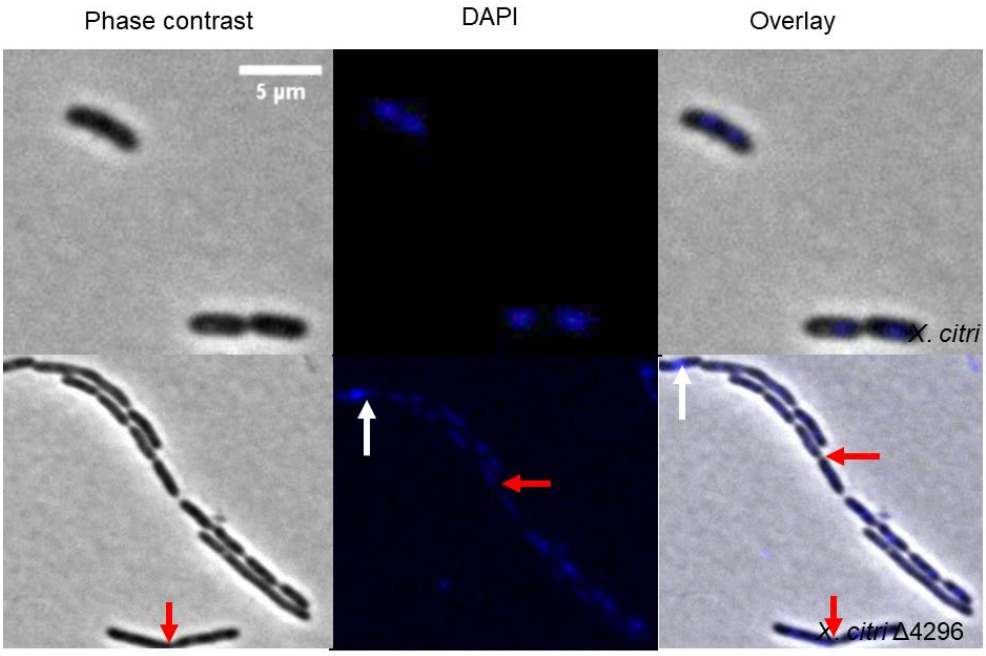

Figure 34. Morphological analysis of *Xanthomonas citri* (*X. citri*) and Δ4296 strains on NB supplemented with ampicillin 20µg/mL. The figure shows the phase contrast, DAPI, and overlay of the two filters, respectively, for A: *Xanthomonas citri* (*X. citri*); B: Δ4296 (magnification of 100X). White arrows indicate the chromosome distribution, and red arrows indicate septum constriction (magnification of 100X). Scale=5µm.

Table 6. Comparison of cell morphology aspects for *Xanthomonas citri* (*X. citri*), mutant Δ4296, and Δ4296c strains in rich medium (NB) with ampicillin 20µg/mL.

	Short filaments (%)	**Chain (%)**	**Nucleoid (%)**
X. citri	0^a	0.25^a	0^a
Δ4296	100^b	50^b	100^b
Δ4296c	0^a	0^a	0^a

Total n= 800 cells measured. Data correspond to the average cell morphology— different letters mean significant difference according to Welch's ANOVA test, p =0.05.

For *X. citri* (Figure 34A), we did not observe any chromosomal mass spanning through the cell. In contrast, cultures of Δ4296 mutant showed a continuous distribution of chromosomal mass spanning through the elongated cells and also cell chain formation (Figure 34, white arrows). These results strongly indicate that XAC4296 mutation also affects chromosome segregation and, subsequently, cell division.

Finally, to investigate Δ4296 cell viability in the presence of ampicillin, a live-dead cells assay was performed (Figure 35). The live-dead assay showed no significant difference between mutant and wild type strain in NB medium with ampicillin, revealing 10% dead cells for *X. citri* wild type strain and 12% dead cells for Δ4296 mutant (Table 7). Since XAC4296 has a possible transglycosylase domain and might be related to cell wall biosynthesis, the propidium iodide (IP) was used as a DNA intercalant for dead cells, because it does not permeate intact cell membranes, which could show potential cell death increase caused by the lack of XAC4296 transglycosylase activity. DAPI coloration was used as DNA intercalant for dead cells (Boulos et al., 1999). These results demonstrate that XAC4296 is not linked to membrane disruption, since cell mortality did not show a statistically significant increase for the mutant. The same phenomenon can be seen in Figure 33, where the mutant struggles to multiply until almost 72 hours, but eventually reaches an exponential phase. This is another indication that cell death on the mutant did not increase compared to wild *X. citri*.

Table 7. Live-dead quantification for *Xanthomonas citri* (*X. citri*), mutant Δ4296, and Δ4296c strains in rich medium with ampicillin 20µg/mL.

	Live cells	Dead cells	%
X. citri	300	30	10[a]
Δ4296	300	37	12.3[a]

Total n= 300 cells measured. Data correspond to the average cell death — same letters meaning no significant difference according to *Tukey test*- 0.05.

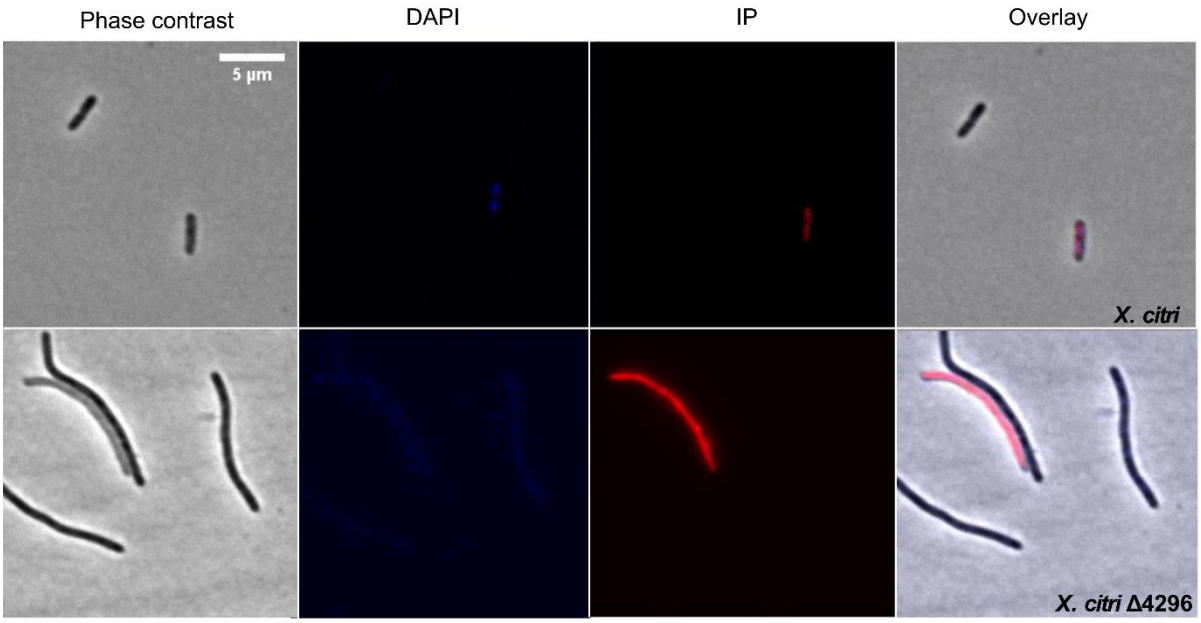

Figure 35. Live-dead assay for *Xanthomonas citri* (*X. citri*) and mutant Δ4296 strains. The figure shows the phase contrast, DAPI, Propidium iodide (IP), and overlay of the two filters, respectively (magnification of 100X). Scale=5µm.

5.7. Δ4296 phenotype can be suppressed with nutrient supplementation

As mentioned above, Δ4296 cells display morphological defects and the mutation itself affects chromosomal segregation. Since XAC4296 has two modules, the LT (related to cell wall biosynthesis) and a second module related to an epimerase domain (involved in the production of complex carbohydrate polymers that are used in bacterial cell walls and carbohydrate metabolism), our results strongly suggest that XAC4296 protein might have an indirect relation with basal metabolisms, despite its

still unknown function. To investigate this relationship, macromolecular metabolical compounds were utilized as a supplement in the cultures.

5.7.1. Sucrose

.In order to investigate this possible relation, cells were examined individually to quantify their phenotypes and nucleoid organization in the wild-type *X. citri* and Δ4296 mutant strains in the presence of sucrose and sucrose with ampicillin.

Growth curves of wild-type *X. citri* and Δ4296 mutant appeared nearly identical when cells were grown in the presence of sucrose (Figure 36A and B), differently from those cultivated in ampicillin (Figures 33 and 34). Subsequently, cells were visualized by fluorescence microscopy, and fewer morphological nor nucleoid organization defects were detected (Figure 37). Cells showed full phenotypic and chromosomal reversion as the wild type phenotype in both conditions (Figure 37A and B) (Table 8). These results indicate that XAC4296 might contribute indirectly to basal metabolism and that sucrose plays a crucial role in restoring the chromosomal segregation and cell division as the wild-type strain.

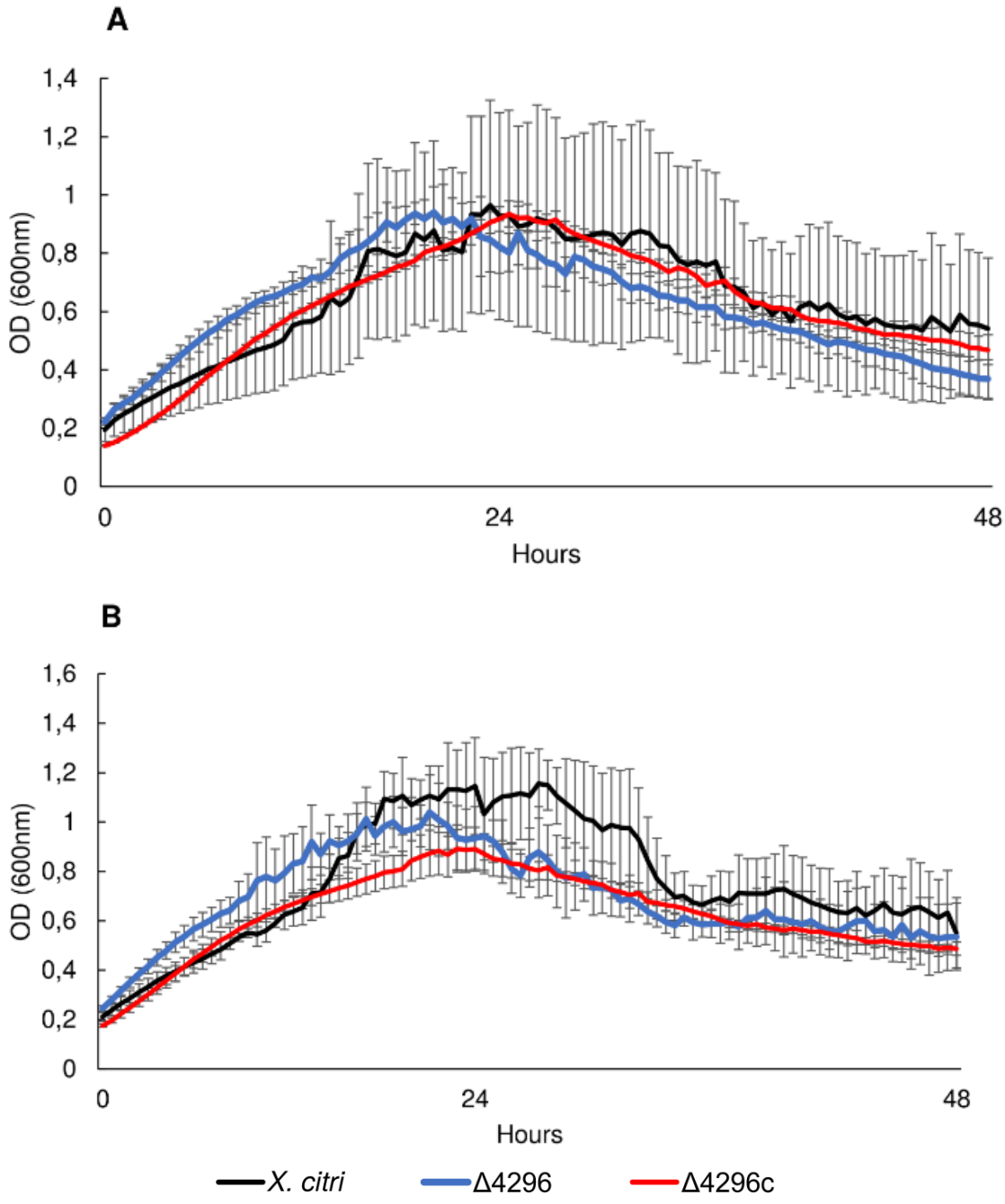

Figure 36. *Ex planta* growth curve for *Xanthomonas citri* (*X. citri*), Δ4296 mutant, and Δ4296c in different conditions. A: NB medium supplemented with sucrose 0.1%; B: NB medium supplemented with sucrose 0.1% (w/v) and ampicillin 20µg/mL. Error bars indicate the standard error of three independent biological and technical replicates

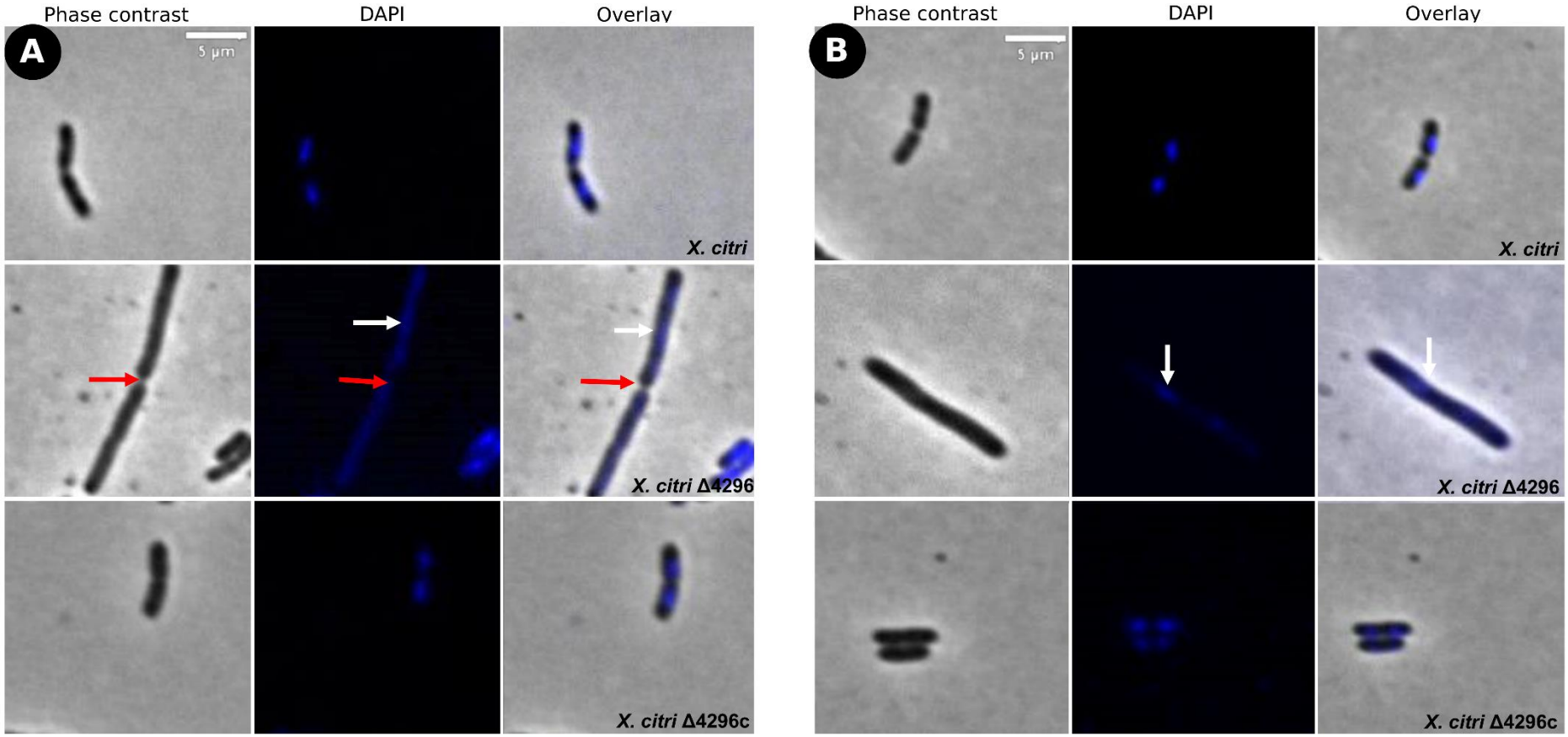

Figure 37. Short filaments and chain phenotype show full reversion in the presence of sucrose as carbon source **(A)** Morphological analysis of *X. citri*, Δ4296, and Δ4296c strains on NB supplemented with sucrose 0.1% (w/v). **(B)** NB supplemented with sucrose 0.1% (w/v) and ampicillin 20 µg/mL. The figure shows the phase contrast, DAPI, and overlay of the two filters, respectively, for *X. citri*; Δ4296 and Δ4296c. White arrows indicate the chromosome distribution, and red arrows indicate septum constriction (magnification of 100X), scale=5 µm.

Table 8. Comparison of cell morphology aspects for *Xanthomonas citri* (*X. citri*) mutant Δ4296, and Δ4296c strains in rich medium (NB) with sucrose and ampicillin 20µg/mL.

		Short filaments(%)	Chain (%)	Nucleoid (%)
NB medium sucrose 0.1%	*X. citri*	1 [a]	0.38 [a]	0 [a]
	Δ4296	1.75 [a]	0.75 [a]	0.5 [a]
	Δ4296c	0.25 [a]	0.38 [a]	0 [a]
NB medium sucrose 0.1% ampicillin 20µg/mL	*X. citri*	0.13 [a]	1.25 [a]	0.5 [a]
	Δ4296	2.25 [a]	188 [a]	1 [a]
	Δ4296c	0.25 [a]	0.13 [a]	0 [a]

Total n= 800 cells measured. Data correspond to the average cell morphology— different letters mean significant difference according to Welch's ANOVA test, p =0.05.

5.7.2. Glutamic acid

Glutamic acid is another metabolical compound that might be linked to XAC4296 activity and basal metabolism. To investigate the possible XAC4296 role in basal metabolism, we added glutamic acid in cultures with NB medium in the presence of ampicillin and performed morphological and chromosome investigation of Δ4296 and *X. citri* strains.

In a much similar manner, when sucrose was added, the addition of glutamic acid on NB with ampicillin enhanced Δ4296 growth to the point where it matches that of the wild type *X. citri* (Figures 38 A and B).

Subsequently, the same cells were cultivated on NB with ampicillin and glutamic acid and examined in the microscope. Cells no longer presented short filaments, nucleoid, and chains formation (Figure 39A and B, Table 9). Addition of glutamic acid on the media prevented all the chromosomal and cell division errors we observed when the mutant Δ4296 was cultivated on NB with added ampicillin (Figure 39A and B).

These results reforces our hypothesis that XAC4296 contributes indirectly to basal metabolism and that glutamic acid also plays a crucial role in chromosomal and phenotype reversion of the wild-type condition.

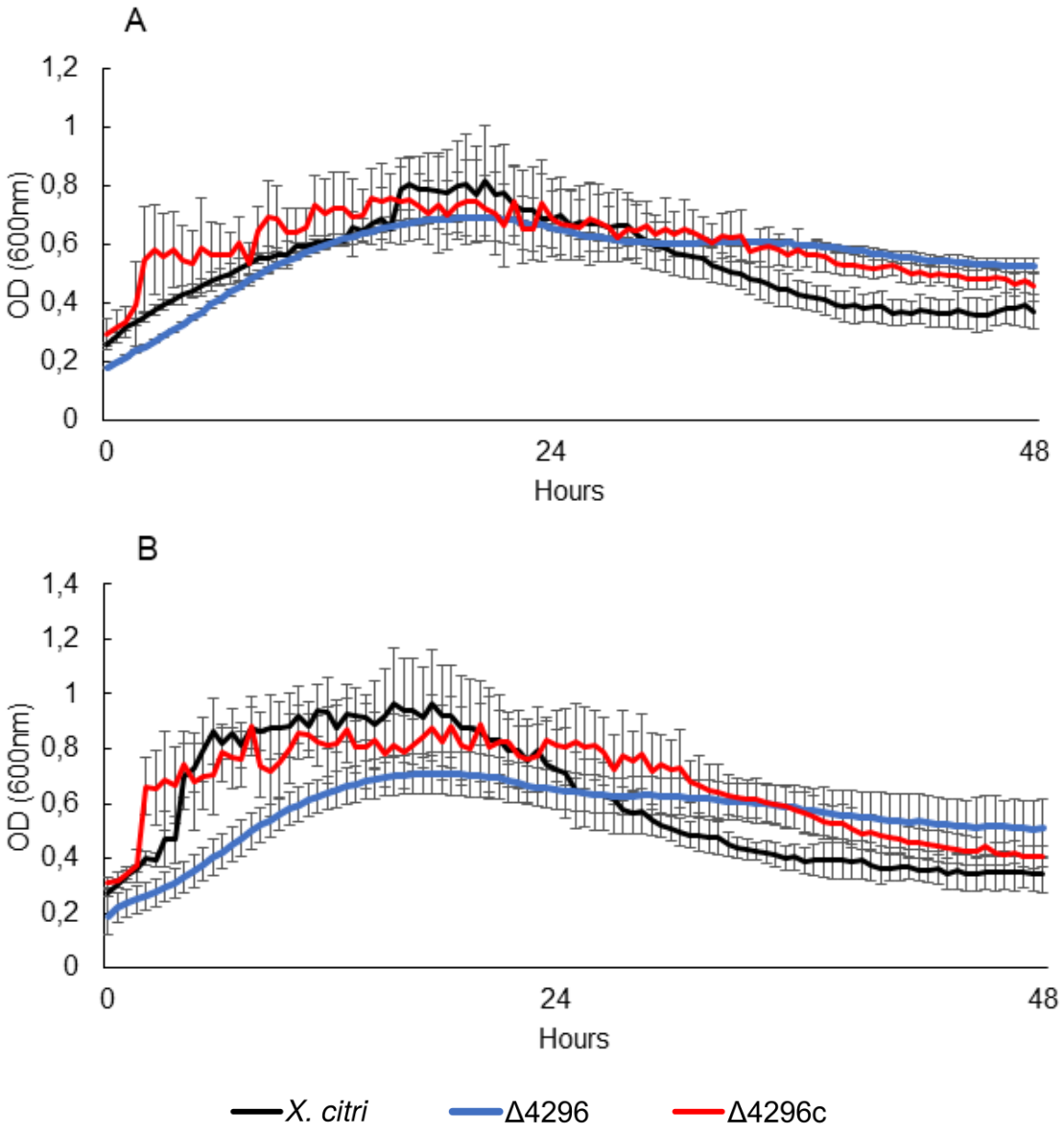

Figure 38. *Ex planta* growth curve for *Xanthomonas citri* (*X. citri*), Δ4296 mutant, and Δ4296c in different conditions. A: NB medium supplemented with glutamic acid 2% (w/v); B: NB medium supplemented with glutamic acid 0.1% (w/v) and ampicillin 20µg/mL. Error bars indicate the standard error of three independent biological and technical replicates.

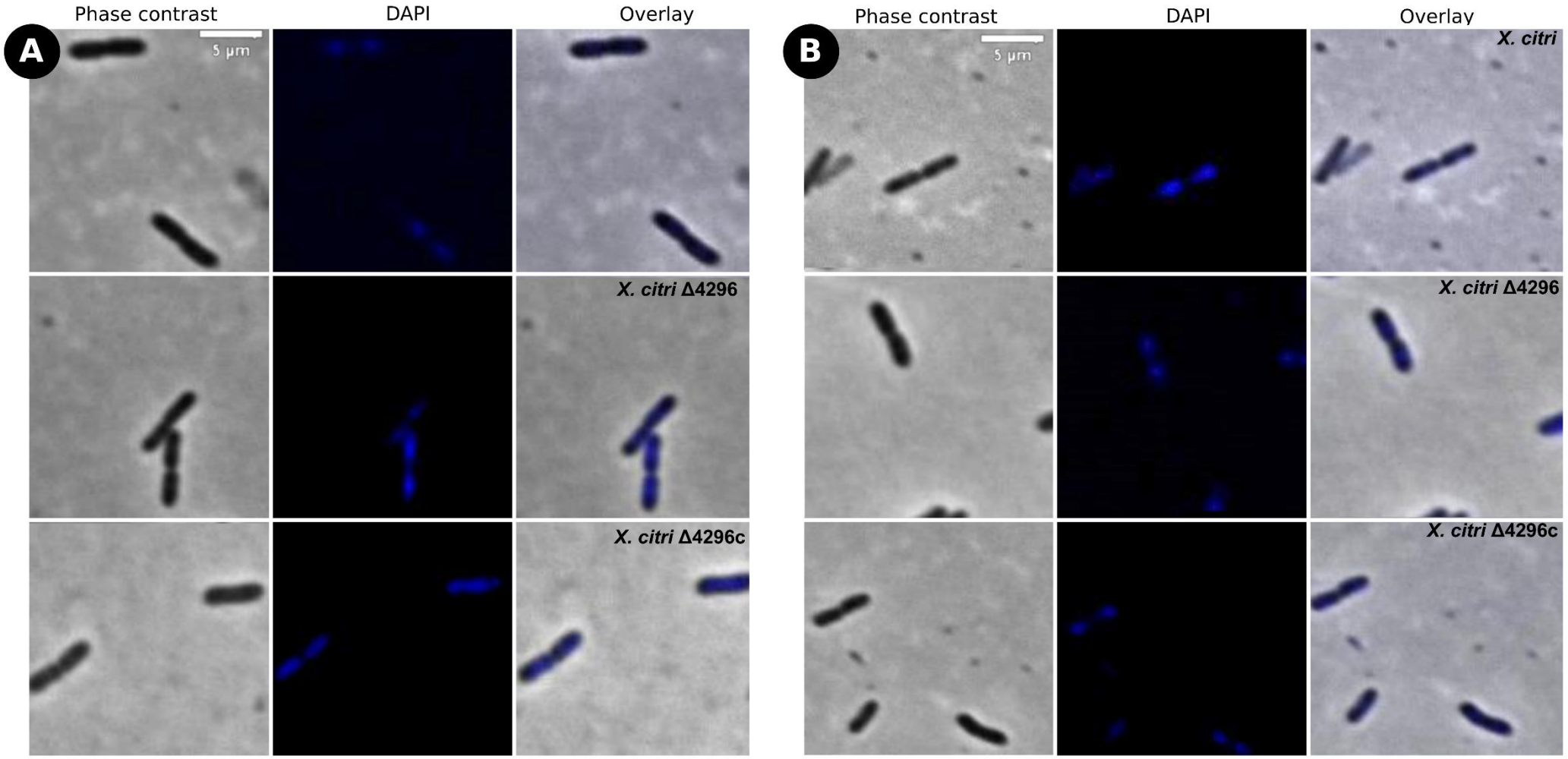

Figure 39. Short filaments, chain phenotype, and nucleoid organization show full reversion of the wild-type phenotype in the presence of glutamate as carbon source (A) Morphological analysis of *X. citri*, Δ4296, and Δ4296c strains on NB supplemented with glutamic acid 0.1% (w/v). (B) NB supplemented with glutamic acid 0.1% (w/v) and ampicillin 20 µg/mL. The figure shows the phase contrast, DAPI, and overlay of the two filters, respectively, for *X. citri*, Δ4296 and Δ4296c (magnification of 100X). Scale=5µm.

Table 9. Comparison of cell morphology aspects for *Xanthomonas citri* (*X. citri*), mutant Δ4296, and Δ4296c strains inrich medium (NB) with glutamic acid or ampicillin 20µg/mL.

		Short filaments (%)	Chain (%)	Nucleoid (%)
NB medium glutamic acid 0,1%	*X. citri*	0[a]	0 [a]	0 [a]
	Δ4296	0 [a]	0 [a]	0 [a]
	Δ4296c	0 [a]	0 [a]	0 [a]
NB medium glutamic acid 0,1% ampicillin 20µg/mL	*X. citri*	0.13 [a]	0 [a]	0 [a]
	Δ4296	0 [a]	1 [a]	0 [a]
	Δ4296c	0 [a]	0 [a]	0 [a]

Total n= 800 cells measured. Data correspond to the average cell morphology. Different letters mean significant difference according to Welch's ANOVA test, p =0.05.

5.8. XAC4296 is a cytoplasmic protein

The subcellular localization of XAC4296 was assessed using mCherry fluorescence emission by constructing *X. citri* -pMAJIIc-4296 vectors. Using the native XAC4296 promoter it was possible to observe the natural protein expression profile. Since mCherry reporter protein is optimized to fluoresce on cell periplasm and cytoplasm, these traits make it a good vector choice to investigate XAC4296 protein position in the cell (Figure S1). *X. citri* was used as a negative control to perform the localization assay. The results shown in Figure 40 supports the fact that XAC4296 is spread across the whole-cell cytoplasm but not concentrating at any specific cell position.

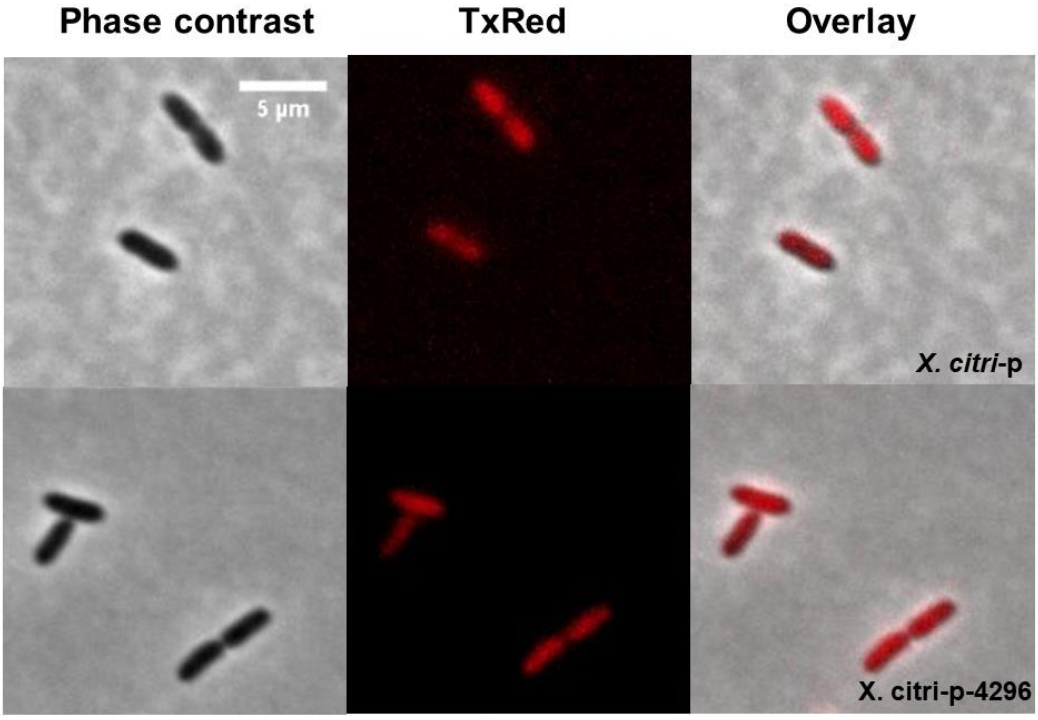

Figure 40. Subcellular localization of XAC4296 fused with mCherry in *X. citri*-p-4296 strain. *X. citri*-p was used as a negative control. The figure shows phase contrast (A1), TxRed (A2), and overlay of the two filters (A3), respectively (100X magnification). Scale=5µm.

6. DISCUSSION

In this work, we investigate the role of the XAC4296 in *Xanthomonas citri* metabolism and virulence using *in silico* and molecular approaches. The XAC4296 protein contains two distinct modules: the first containing the SLT_2 (IPR031304) and PG_Binding1 (IPR002477) domains, homologs to LTs 3B Family. The second module contains the aldose-1-epimerase domain (IPR015443), classified as an epimerase superfamily. Proteins belonging to the LTs (Lytic Murein Transglycosylases) family cleave the polysaccharide of the peptidoglycan at the NAM-NAG glycosidic bond by intramolecular cyclization of the N-acetylmuramyl moiety to yield a 1,6-anhydro-N-acetyl-β-D-muramyl (1,6-anhydroMurNAc) product during the peptidoglycan biosynthesis (Dik et al., 2017). On the other hand, epimerases are usually involved in metabolic pathways such as inversion of D-alanine and D-glutamate for bacterial cell wall metabolism (Sala et al., 1996); biosynthesis of a variety of cell surface polysaccharides; biosynthesis of LPS and capsular sugar precursors (McNeil et al., 1990); and complex biosynthetic pathways, such as Glycolysis, Entner-Doudoroff, Leloir and others that present several chemical steps (Nowitzki et al., 1995; Teige et al., 1995). Epimerases are also involved in the oxidation, acetylation, dehydration, and carbohydrate reduction (reviewed by Allard et al., 2001). Our molecular modeling results also support that the LT and epimerase modules can act independently and may synergistically function as a canonical MFE, thus, performing multiple physiologically biochemical or biophysical functions simultaneously in the cell.

Previous studies revealed that the XAC4296 modules exist as separate and independent genes in other γ-proteobacteria (Oliveira et al., 2018). Our results indicate that XAC4296 homolog is widespread in different *Xanthomonas* species and exists in other members from the *Xanthomonadaceae* family*, such as Stenotrophomonas and Pseudoxanthomonas.* It is worth mentioning that the *Xanthomonas, Stenotrophomonas, Xylella and Pseudoxanthomonas* genus from the *Xanthomonadaceae* family are closely related and form a phylogroup (Bansal et al., 2021). Therefore, our results support that the XAC4296 origin may be related with a previous gene fusion origin before or during this phylogroup differentiation. However, *Xylella* and *Xanthomonas albilineans* does not have the XAC4296 homolog. For

instance, *Xylella* carries an independent D-hexose-6-phosphate mutarotase gene containing the aldose-1-epimerase domain and their LT gene repertoire in distinct genomic loci, whereas the *X. albilineans* shows both protein modules, the LT and epimerase, homologs to XAC4296, as separated but overlapping genes, in addition to a independent D-hexose-6-phosphate mutarotase gene. It is known that the *Xylella* genus has undergone drastic genome reduction since diverging from the *Xanthomonas* genus (Pieretti et al., 2009; Firrao et al., 2021), and that *X. albilineans* has experienced significant genomic erosion, having unique genomic features in comparison to other *Xanthomonas* species (Pieretti et al., 2015). Therefore, the most parsimonious hypothesis to explain this absence of XAC4296 homologs in *Xylella* and *X. albilineans* is that while *Xylella* lost their XAC4296 homolog during the genome reduction process, but maintaining their epimerase gene alone, and their own LTs repertoire, the *X. albilineans* genome is accumulating mutation and nucleotide deletion that led to the formation of two separated genes, and thus, suggesting for a current process of gene decay. Both hypotheses are based on the current knowledge that the genome reduction or erosion process is currently shaping *Xylella* and *X. albilineans* to adapt both pathogen to a restricted host range.

This work further evaluated XAC4296 role in *X. citri* fitness, virulence, and pathogenicity. Our results indicate that the XAC4296 gene is not essential for *X. citri* survival or *in planta* CC development but it play a role in bacterial fitness. Our findings also support XAC4296 direct relationship with *X. citri* pathogenicity, particularly CC progression. However, this result is not surprising since previous studies revealed thet role of the LT domain from the 3B family plays a role (or is involved) in *X. citri* pathogenicity and fitness (Oliveira et al., 2018).

To explore the involvement of the XAC4296 LT domain with the peptidoglycan metabolism, the cell morphology was examined under the microscope using DAPI-staining. *X. citri* lacking XAC4296 formed chains related to late cell division errors. In these cells, the early division is normal, forming constriction but does not progress until complete closure of the septum and cell separation. This is not an unexpected result since many studies based on LTs mutants (from different families) reported similar phenotypes (Lommatzsch et al., 1997; Heidrich et al., 2002; Cloud and Dillard, 2004; Jorgenson et al., 2015). Indeed, cell-wall biosynthesis stays in a homeostatic balance between construction and demolition (Johnson et al., 2014). In the absence of the

activity of the LT domain provided by XAC4296, the peptidoglycan maintenance is perturbed, leading to these morphological defects observed in *X. citri*. This finding supports the hypothesis that XAC4296 function is related to the 1,6-anhydroMurNAc-containing muropeptides production, the hallmark of LT catalysis (Dik et al., 2017). These muropeptides may be transported from the periplasm to the cytoplasm through the transmembrane protein AmpG (Jacobs et al., 1994). Next, these muropeptides are degraded in the cytoplasm, and their components are used for Lipid II biosynthesis that is assembled in the cytoplasm and, again, delivered to the periplasm for *de novo* synthesis of the peptidoglycan (Barreteau et al., 2008; Bouhss et al., 2008; Vollmer and Bertsche, 2008; Butler et al., 2013; Sieger et al., 2013; Mohammadi et al., 2014; Sham et al., 2014; Meeske et al., 2015; Scheffers and Tol, 2015; Kuk et al., 2017; Leclercq et al., 2017). Therefore, our results support the XAC4296 LT role, acting in the peptidoglycan synthesis and dynamics, consequently influencing cell shape as previously described for this class of enzymes (Dik et al., 2017) (Figures 41-43).

In this work, we observed that the short filaments phenotype intensified when ampicillin was added to the Δ4296 mutant culture, impacting cell growth. Ampicillin is a β-lactam antibiotic that blocks the activity of penicillin-binding proteins (Delcour, 2009). Although *X. citri* appears to express β-lactamase constitutively (XAC_RS19350/ XAC3833) (Weng et al., 2004), in the Δ4296 strain, the absence of XAC4296 protein seems to hinder their ability to reconstruct cell wall, making the bacteria susceptible to this antibiotic. Indeed, the bacterial exposure to β-lactams leads to disturbs in peptidoglycan recycling and accumulates MurNAc-peptides in the cytoplasm (Jacobs and Fre, 1997). In addition, during LT catalysis, the product 1,6-anhydroMurNAc-containing muropeptides are transported from the periplasm to the cytoplasm (Jacobs et al., 1994). These muropeptides are transported through the transmembrane protein AmpG (Jacobs et al., 1994). The muropeptides may be metabolized further through multiple routes to yield UDP-MurNAc-pentapeptide, a precursor of peptidoglycan biosynthesis (Uehara and Park, 2008; Gisin et al., 2013) or may bind to AmpR and converts it into an activator of *ampC* transcription. (Dietz et al., 1997; Jacobs and Fre, 1997). Here, we hypothesize that the observed behavior of Δ4296 may be explained due to bacterial decreasing of the pool of muropeptides in the periplasm, consequently in the cytoplasm, leading to peptidoglycan synthesis imbalance and interrupting *ampC* transcription, and consequently, increasing β-lactams susceptibility (Figure 43).

Therefore, our results strongly support that XAC4296 protein may also contribute to β-lactam antibiotic resistance in *X. citri*.

However, the morphological defects observed in the XAC4296 mutant (with or without the addition of ampicillin) can be directly related to the epimerase domain, since our results also indicate that the late cell division errors observed in the chain and short filaments phenotypes can be wholly restored with sucrose and glutamate supplementation. One possible way to interpret these results is that the XAC4296 epimerase domain may contribute to many reactions in carbohydrate metabolism, such as the D-hexose-6-phosphate mutarotase. Its absence leads to an imbalance of metabolic precursors related to anabolism pathways, indirectly affecting bacterial cell division and chromosome segregation in *X. citri*. In the absence of XAC4296, glutamate and sucrose supplement may probably provide substrate for alpha-glucose-6-phosphate production for the central carbon source metabolism, and together with the activity of the other LTs from the 3B family present in the *X. citri* genome and their known functional redundancy mechanism (Dik et al., 2017; Oliveira et al., 2018) restored the bacterial metabolism and, consequently, the cell cycle. In addition, the glucose-6 phosphate is the primary metabolic substrate present for the glycolysis, phosphogluconate, and Entner–Doudoroff pathways. Nonetheless, the glutamate and sucrose supplement may provide a comprehensive carbon source to the bacteria, facilitating energy metabolism and bacterial adaptation and survival to a stressful condition, free living, and wide host ranges. However, further studies like protein purification and *in vitro* tests to check XAC4296 enzymatic activity are still needed to determine its role thoroughly.

Finally, previous studies raised the possibility of combining an LT inhibitor with β-lactam antibiotics as an alternative for future antibiotic development (Williams et al., 2017). For example, the possible interaction between the LT Slt35 (3B family) and Bulgecin A (Van Asselt et al., 1999), a potent LTs inhibitor, which restores the efficiency of β-lactam antibiotics against resistant bacteria (Williams et al., 2017). Taken together, our results strongly support these previous studies, suggesting for the future development of 3B LT and epimerase inhibitors as potential new tools, not only for the control of the disease caused by *Xanthomonas* and other phytopathogens but also for antimicrobial resistance in general.

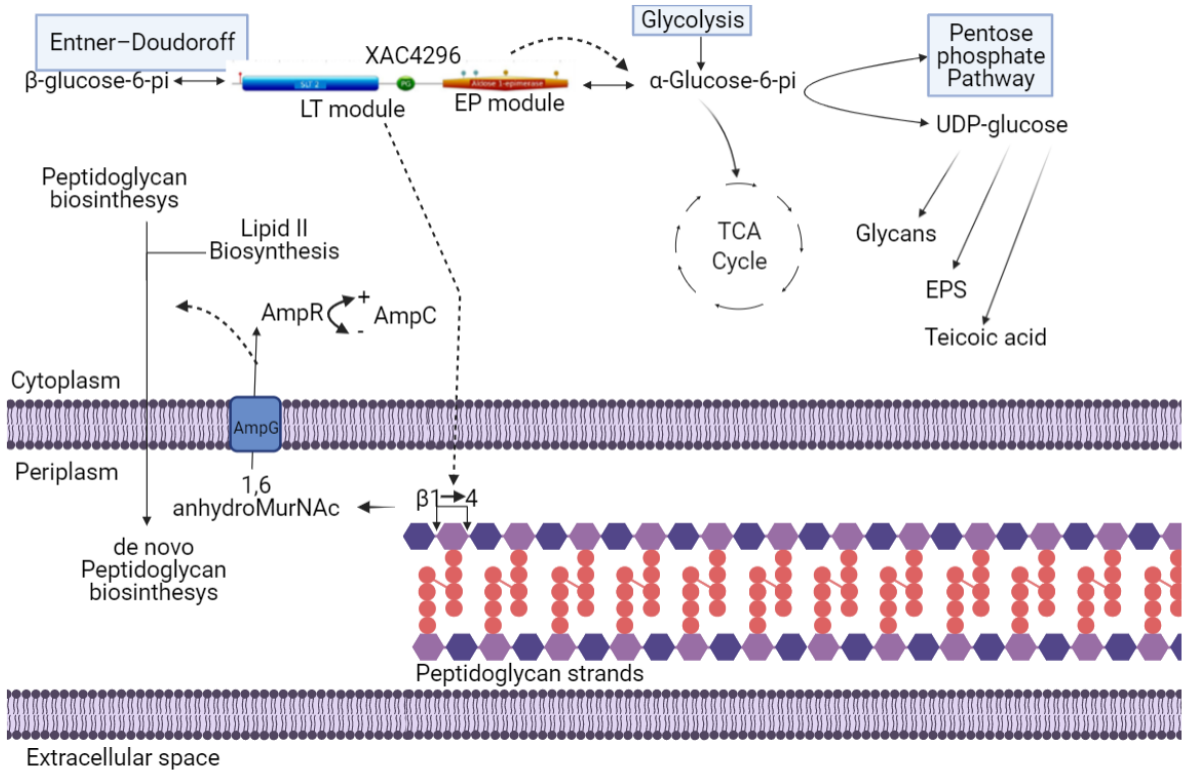

Figure 41. Possible role of the multidomain XAC4296 protein. XAC4296 might act as an epimerase in the cytoplasm, connecting the glycolysis and Entner–Doudoroff pathway. XAC4296 also might act as a transglycosylase in the periplasm, contributing for peptidoglycan synthesis and β-lactam resistance. In both cases, XAC4296 contributes indirectly to basal metabolism, and its deletion increases cells defective phenotypes.

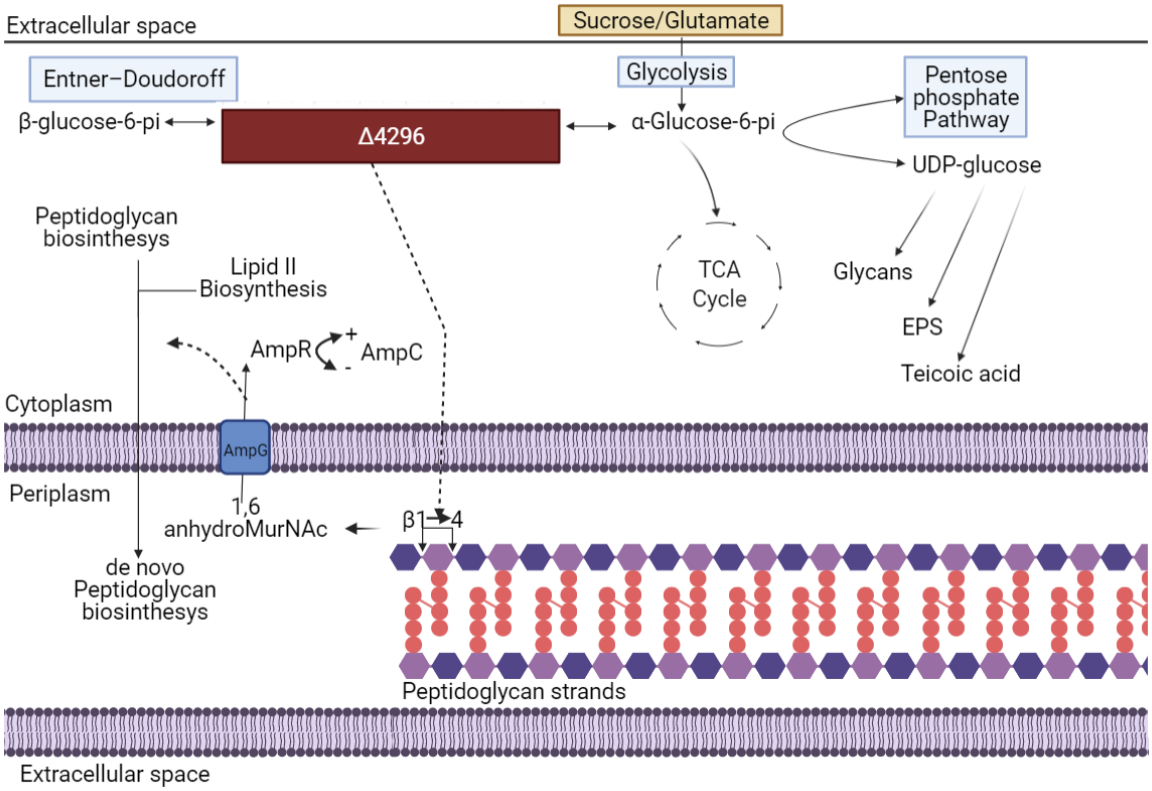

Figure 42. Possible effects of the multidomain XAC4296 deletion in *X. citri*. In the absence of the XAC4296, may occur an imbalance of metabolic precursors related to anabolism pathways, leading to late cell division and consequently chromosome segregation errors and ampicillin resistance.

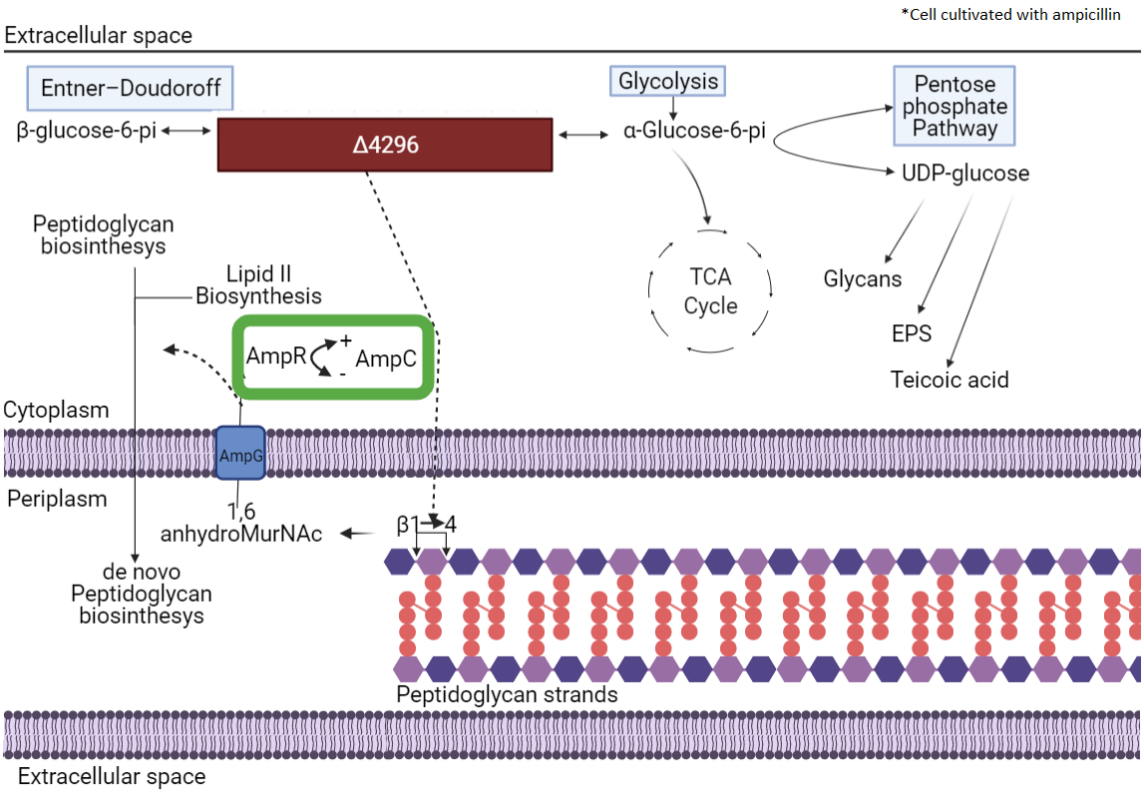

Figure 43. Possible effects of the multidomain XAC4296 depletion in cells cultivated with ampicillin. In the absence of XAC4296 may occur a bacterial decreasing of the pool of muropeptides in the periplasm, consequently in the cytoplasm, leading to peptidoglycan synthesis imbalance and interrupting ampC transcription, and consequently, increasing β-lactams susceptibility.

7. CONCLUSIONS

The XAC4296 protein seems to be related to late cell division leading to chromosome segregation errors and ampicillin resistance. Moreover, we have shown that XAC4296 mutants display a metabolism-dependent phenotype, resulting from the imbalance of metabolic precursors related to anabolism pathways, suggesting that XAC4296 also acts in central carbon metabolism. In conclusion, our results strongly indicate that XAC4296 is a multi-functional protein, playing a role as a transglycosylase as much as an epimerase, and may impacts bacterial fitness, and bringing new insights into *X. citri* and other *Xanthomonadaceae* metabolism, evolution, and antimicrobial resistance emergence.

8. REFERENCES

Agarwal S, Gopal K, Upadhyaya T, Dixit A (2007). Biochemical and functional characterization of UDP-galactose 4-epimerase from *Aeromonas hydrophila*. **Biochimica et Biophysica Acta - Proteins and Proteomics**, 1774:828–837

Aharoni A, Gaidukov L, Khersonsky O, Gould SMQ, Roodveldt C, Tawfik DS (2005). The “evolvability” of promiscuous protein functions. **Nature Genetics**, 37:73–76

Albery WJ, Knowles JR (1976). Free-Energy Profile for the Reaction Catalyzed by Triosephosphate Isomerase. **Biochemistry**, 15:5627–5631,

Alcorlo M, Martínez-caballero S, Molina R, Hermoso JA (2017). Carbohydrate recognition and lysis by bacterial peptidoglycan hydrolases. **Current Opinion in Structural Biology**, 44:87–100

Allard STM, Giraud MF, Naismith JH (2001). Epimerases: Structure, function and mechanism. **Cellular and Molecular Life Sciences**, 58:1650–1665

Altschul SF, Madden TL, Schäffer AA, Zhang J, Zhang Z, Miller W (1997). Gapped BLAST and PSI-BLAST: a new generation of protein database search programs. **Nucleic Acids Research**, 25:3389–3402

Alvarez-martinez CE, Sgro GG, Araujo GG, Paiva MRN, Matsuyama BY, Guzzo CR, Andrade MO, Farah CS (2021). Secrete or perish: The role of secretion systems in *Xanthomonas* biology. **Computational and Structural Biotechnology Journal**, 19:279–302

Amaral AM DO, Toledo CP, Baptista JC, Machado MA (2005). Transformation of *Xanthomonas axonopodis* pv. *citri* by electroporation. **Fitopatologia Brasileira**, 30:292–294

An SQ et al. (2019). Mechanistic insights into host adaptation, virulence and epidemiology of the phytopathogen *Xanthomonas*. **FEMS Microbiology Reviews**, 44:1–32

Antle VD, Liu D, McKellar BR, Caperelli CA, Hua M, Vince R (1996). Substrate specificity of glycinamide ribonucleotide synthetase from chicken liver. **Journal of Biological Chemistry**, 271:8192–8195

Banerjee D, Ghosh D, Chatterjee A, Sinha S, Nandagopal K (2012). No evidence for mutations that deregulate GARS-AIRS-GART protein levels in children with Down syndrome. **Indian Journal of Clinical Biochemistry**, 27:46–51

Bansal K, Kumar S, Kaur A, Singh A, Patil PB (2021). Deep phylo-taxono genomics reveals Xylella as a variant lineage of plant associated *Xanthomonas* and supports their taxonomic reunification along with *Stenotrophomonas* and *Pseudoxanthomonas*. **Genomics**, 113:3989–4003

Barreteau H, Kovač A, Boniface A, Sova M, Gobec S, Blanot D (2008). Cytoplasmic steps of peptidoglycan biosynthesis. **FEMS Microbiology Reviews**, 32:168–207

Beaufay F, Coppine J, Mayard A, Laloux G, De Bolle X, Hallez R (2015). A NAD -dependent glutamate dehydrogenase coordinates metabolism with cell division in *Caulobacter crescentus* . **The EMBO Journal**, 34:1786–1800

Becker A, Katzen F, Pühler A, Ielpi L (1998). Xanthan gum biosynthesis and application: A biochemical/genetic perspective. **Applied Microbiology and Biotechnology**, 50:145–152

Behlau F (2021). An overview of citrus canker in Brazil. **Tropical Plant Pathology**, 46:1–12

Behlau F, Hong JC, Jones JB, Graham JH (2013). Evidence for acquisition of copper resistance genes from different sources in citrus-associated *xanthomonads*. **Phytopathology**, 103:409–418

Bender RA (2013). Glycolysis. **Brenner's Encyclopedia of Genetics: Second Edition**, 2:346–349

Blackburn NT, Clarke AJ (2001). Identification of four families of peptidoglycan lytic transglycosylases. **Journal of Molecular Evolution**, 52:78–84

Boch J, Bonas U (2010). *Xanthomonas* AvrBs3 family-type III effectors: Discovery and function. **Annual Review of Phytopathology**, 48:419–436

Boch J, Scholze H, Schornack S, Landgraf A, Hahn S, Kay S, Lahaye T, Nickstadt A, Bonas U (2009). Breaking the code of DNA binding specificity of TAL-type III effectors. **Science**, 326:1509–1512

Bogdanove AJ, Schornack S, Lahaye T (2010). TAL effectors: Finding plant genes for disease and defense. **Current Opinion in Plant Biology**, 13:394–401

Bouhss A, Trunkfield AE, Bugg TDH, Mengin-lecreulx D (2008). The biosynthesis of peptidoglycan lipid-linked intermediates. **FEMS Microbiology Reviews**, 32:208–233

Boulos L, Prévost M, Barbeau B, Coallier J, Desjardins R (1999). LIVE/DEAD(®) BacLight(TM): Application of a new rapid staining method for direct enumeration of viable and total bacteria in drinking water. **Journal of Microbiological Methods**, 37:77–86

Bueno D et al. (2021). Riboswitch theo/mete as a transcription regulation tool for X*anthomonas citri* subsp. c*itri*. **Microorganisms**, 9:1–15

Butler EK, Davis RM, Bari V, Nicholson PA, Ruiz N (2013). Structure-Function Analysis of MurJ Reveals a Solvent-Exposed Cavity Containing Residues Essential for Peptidoglycan Biogenesis in *Escherichia coli.* **J Bacteriol. 2**0:4639-4649

Büttner D, Bonas U (2010). Regulation and secretion of *Xanthomonas* virulence factors. **FEMS Microbiology Reviews**, 34:107–133

Canteros BI, Gochez AM, Moschini RC (2017). Management of citrus canker in argentina, a success story. **Plant Pathology Journal**, 33:441–449

Carnell AJ (1999). Stereoinversions using microbial redox-reactions. **Advances in biochemical engineering/biotechnology**, 63:57–72

Casadevall A, Pirofski LA (2009). Virulence factors and their mechanisms of action: The view from a damage-response framework. **Journal of Water and Health**, 7:2–18

Chan YA, Hackett KT, Dillard JP (2012). The lytic transglycosylases of *Neisseria gonorrhoeae*. **Microbial Drug Resistance**, 18:271–279

Chastanet A, Carballido-lopez R (2012). The actin-like MreB proteins in *Bacillus subtilis*: a new turn. **Front Biosci (Schol Ed).** 4:1582-1606

Cheng XY et al. (2012). A global characterization and identification of multifunctional enzymes. **PLoS ONE**, 7:1–8

Chittori S, Simanshu DK, Savithri HS, Murthy MRN (2007). Structure of the putative mutarotase YeaD from *Salmonella typhimurium*: Structural comparison with galactose mutarotases. **Acta Crystallographica Section D: Biological Crystallography**, 63:197–205

Chua SMH, Fraser JA (2020). Surveying purine biosynthesis across the domains of life unveils promising drug targets in pathogens. **Immunology and Cell Biology**, 98:819–831

Chubukov V, Gerosa L, Kochanowski K, Sauer U (2014). Coordination of microbial metabolism. **Nature Reviews Microbiology**, 12:327–340

Cloud KA, Dillard JP (2004). Mutation of a Single Lytic Transglycosylase Causes Aberrant Septation and Inhibits Cell Separation of *Neisseria gonorrhoeae*. **J Bacteriol**. 186:7811–7814

Conway T (1992). The Entner-Doudoroff pathway : history , physiology and molecular biology. **FEMS Microbiol Reviews**, 103:1–27

Cornelis GR (2006). The type III secretion injectisome. **Nature Reviews Microbiology**, 4:811–825

Costerton JW (1995). Overview of microbial biofilms. **Journal of Industrial Microbiology**, 15:137–140

Da Silva ACR et al. (2002). Comparison of the genomes of two *Xanthomonas* pathogens with differing host specificities. **Nature**, 417:459–463

Darby AC, Cho NH, Fuxelius HH, Westberg J, Andersson SGE (2007). Intracellular pathogens go extreme: genome evolution in the *Rickettsiales*. **Trends in Genetics**, 23:511–520

Daubner SC, Stubbe JA, Benkovic SJ, Schrimsher JL, Schendel FJ, Young M, Henikoff S, Patterson D (1985). A multifunctional protein possessing glycinamide ribonucleotide synthetase, glycinamide ribonucleotide transformylase, and aminoimidazole ribonucleotide synthetase activities in de novo purine biosynthesis. **Biochemistry**, 24:7059–7062

Debarbieux L, Bohin A, Bohin JP (1997). Topological analysis of the membrane-bound glucosyltransferase, MdoH, required for osmoregulated periplasmic glucan synthesis in *Escherichia coli*. **Journal of Bacteriology**, 179:6692–6698

Delcour AH (2009). Outer membrane permeability and antibiotic resistance. **Biochimica et Biophysica Acta - Proteins and Proteomics**, 1794:808–816

Denome SA, Elf PK, Henderson TA, Nelson DE, Young KD (1999). *Escherichia coli* mutants lacking all possible combinations of eight penicillin binding proteins: Viability, characteristics, and implications for peptidoglycan synthesis. **Journal of Bacteriology**, 181:3981–3993

Dietz H, Pfeifle D, Wiedemann B (1997). The Signal Molecule for β -Lactamase Induction in *Enterobacter cloacae* Is the Anhydromuramyl-Pentapeptide. 41:2113–2120

Dik DA, Marous DR, Fisher JF, Mobashery S (2017). Lytic transglycosylases: concinnity in concision of the bacterial cell wall. **Critical Reviews in Biochemistry and Molecular Biology**, 52:503–542

Dow m. NM-A AND VRE (2000). The induction and modulation of plant defense responses by bacterial lipopolysaccharides. **Annu. Rev. Phytopathol.**, 3:241–261

Dunger G, Relling VM, Tondo ML, Barreras M, Ielpi L, Orellano EG, Ottado J (2007). Xanthan is not essential for pathogenicity in citrus canker but contributes to *Xanthomonas* epiphytic survival. **Archives of Microbiology**, 188:127–135

Durrens P, Nikolski M, Sherman D (2008). Fusion and fission of genes define a metric between fungal genomes. **PLoS Computational Biology**, 4:e1000200

Eisenberg RC, Dobrogosz WJ (1967). Gluconate metabolism in *Escherichia coli.* **Journal of bacteriology**, 93:941–949

Elbaz M, Ben-yehuda S (2010). The metabolic enzyme mana reveals a link between cell wall integrity and chromosome morphology. **PLoS Genetics**, 6:e1001119

Enright AJ, Ouzounis CA (2001). Functional associations of proteins in entire genomes by means of exhaustive detection of gene fusions. **Genome biology**, 2:1–7

Entner N, Douroff M (1952). Glucose and gluconic acid oxidation of *Pseudomonas saccharophila*. **The Journal of biological chemistry**, 196:853–862

Facincani AP, Aparecido ferro J, Pizauro JM, Pereira HA, De Macedo lemos EG, Do Prado AL, Ferro MIT (2003). Carbohydrate metabolism of *Xylella fastidiosa*: Detection of glycolytic and pentose phosphate pathway enzymes and cloning and expression of the enolase gene. **Genetics and Molecular Biology**, 26:203–211

Facincani AP, Moreira LM, Soares MR, Ferreira CB, Ferreira RM, Ferro MIT, Ferro JA, Gozzo FC, De Oliveira JCF (2014). Comparative proteomic analysis reveals

that T3SS, Tfp, and xanthan gum are key factors in initial stages of Citrus sinensis infection by *Xanthomonas citri* subsp. *citri*. **Functional and Integrative Genomics**, 14:205–217

Ference CM, Gochez AM, Behlau F, Wang N, Graham JH, Jones JB (2018). Recent advances in the understanding of *Xanthomonas citri* ssp. *citri* pathogenesis and citrus canker disease management. **Molecular Plant Pathology**, 19:1302–1318

Fernández de henestrosa AR, Badiola I, Saco M, Perez de rozas AM, Campoy S, Barbé J (1997). Importance of the *galE* gene on the virulence of *Pasteurella multocida*. **FEMS Microbiology Letters**, 154:311–316

Ferrasa A et al. (2020). CitrusKB: A comprehensive knowledge base for transcriptome and interactome of Citrus spp. infected by *Xanthomonas citri* subsp. *citri* at different infection stages. **Database**, 2020:1–11

Firrao G, Scortichini M, Pagliari L (2021). Orthology-based estimate of the contribution of horizontal gene transfer from distantly related bacteria to the intraspecific diversity and differentiation of X*ylella fastidiosa*. **Pathogens**, 10:1–17

Frey PA (1996). The Leloir pathway: a mechanistic imperative for three enzymes to change the stereochemical configuration of a single carbon in galactose. **The FASEB Journal**, 10:461–470

Gancedo C, Flores C-L (2008). Moonlighting Proteins in Yeasts. **Microbiology and Molecular Biology Reviews**, 72:197–210

García-gómez E, Espinosa N, De La mora J, Dreyfus G, González-pedrajo B (2011). The muramidase EtgA from enteropathogenic *Escherichia coli* is required for efficient type III secretion. **Microbiology**, 157:1145–1160

Gisin J, Schneider A, Nägele B, Borisova M, Mayer C (2013). A cell wall recycling shortcut that bypasses peptidoglycan de novo biosynthesis. **Nature Chemical Biology.** 9: 491–493

Gottwald TR, Graham s. j, Schubert TS (2002). Citrus canker: The Pathogen and Its Impact. **APS publications**, 3:36

Gottwald TR, Timmer LW (1995). The efficacy of windbreaks in reducing the spread of citrus canker caused by *Xanthomonas campestris* pv. *citri*. **Tropical Agriculture**, 72:194–201

Gouet P, Robert X, Courcelle and (2003). ESPript/ENDscript: Extracting and rendering sequence and 3D information from atomic structures of proteins. **Nucleic Acids Research**, 31:3320–3323

Graham JH (1992). Penetration through leaf stomata and growth of strains of *Xanthomonas campestris* in citrus cultivars varying in susceptibility to bacterial diseases. **Phytopathology,** 82:1319-1325

Han JH, Batey S, Nickson AA, Teichmann SA, Clarke J (2007). The folding and evolution of multidomain proteins. **Nature Reviews Molecular Cell Biology**, 8:319–330

Hansen T, Wendorff D, Schönheit P (2004). Bifunctional Phosphoglucose/Phosphomannose Isomerases from the *Archaea Aeropyrum* pernix and *Thermoplasma acidophilum* Constitute a Novel Enzyme Family within the Phosphoglucose Isomerase Superfamily. **Journal of Biological Chemistry**, 279:2262–2272

Hausner J, Hartmann N, Jordan M, Büttner D (2017). The predicted lytic transglycosylase HpaH from *Xanthomonas campestris* pv. *vesicatoria* associates with the type III secretion system and promotes effector protein translocation. **Infection and Immunity**, 85:1–18

He YW, Cao XQ, Poplawsky AR (2020). Chemical structure, biological roles, biosynthesis and regulation of the yellow xanthomonadin pigments in the phytopathogenic genus *Xanthomonas*. **Molecular Plant-Microbe Interactions**, 33:705–714

Heidrich C, Ursinus A, Berger J, Schwarz H, Höltje JV (2002). Effects of multiple deletions of murein hydrolases on viability, septum cleavage, and sensitivity to large toxic molecules in *Escherichia coli*. **Journal of Bacteriology**, 184:6093–6099

Hill NS, Buske PJ, Shi Y, Levin PA (2013). A Moonlighting Enzyme Links *Escherichia coli* Cell Size with Central Metabolism. **PLoS Genetics**, 9:e1003663

Hoeltje J V., Mirelman D, Sharon N, Schwarz U (1975). Novel type of murein transglycosylase in *Escherichia coli*. **Journal of Bacteriology**, 124:1067–1076

Holden HM, Rayment I, Thoden JB (2003). Structure and Function of Enzymes of the Leloir Pathway for Galactose Metabolism. **Journal of Biological Chemistry**, 278:43885–43888

Höltje JV (1995). From growth to autolysis: the murein hydrolases in *Escherichia coli*. **Archives of Microbiology**, 164:243–254

Höltje J-V (1998). Growth of the Stress-Bearing and Shape-Maintaining Murein Sacculus of *Escherichia coli* . **Microbiology and Molecular Biology Reviews**, 62:181–203

Huang B, Whitchurch CB, Mattick JS (2003). FimX, a Multidomain Protein Connecting Environmental Signals to Twitching Motility in *Pseudomonas aeruginosa*. **Journal of Bacteriology**, 185:7068–7076

Hucho F, Wallenfels K (1971). The Mechanism of Action of Mutarotase (Aldose 1-Epimerase) from *Escerichia coli*. **European Journal of Biochemistry**, 23:489–496

Hult K, Berglund P (2007). Enzyme promiscuity: mechanism and applications. **Trends in Biotechnology**, 25:231–238

Ismail M, Zhang J (2004). Harvest citrus disease control post-harvest citrus diseases and their control. **Outlooks on Pest Management; Saffron Walden**, 1:29–35

Jacobs C, Fre J (1997). Cytosolic Intermediates for Cell Wall Biosynthesis and Degradation Control Inducible β -Lactam Resistance in Gram-Negative Bacteria. 88:823–832

Jacobs C, Huang LJ, Bartowsky E, Normark S, Park JT (1994). Bacterial cell wall recycling provides cytosolic muropeptides as effectors for β-lactamase induction. **EMBO Journal**, 13:4684–4694

Jacques MA et al. (2016). Using Ecology, Physiology, and Genomics to Understand Host Specificity in *Xanthomonas*. **Annual Review of Phytopathology**, 54:163–187

Jalan N, Kumar D, Andrade MO, Yu F, Jones JB, Graham JH, White FF, Setubal JC, Wang N (2013). Comparative genomic and transcriptome analyses of pathotypes of *Xanthomonas citri* subsp. *citri* provide insights into mechanisms of bacterial virulence and host range. **BMC Genomics**, 14:551

Janin J, Wodak SJ (1983). Structural domains in proteins and their role in the dynamics of protein function. **Progress in Biophysics and Molecular Biology**, 42:21–78

Jeffery CJ (2003). Multifunctional proteins: Examples of gene sharing. **Annals of Medicine**, 35:28–35

Jenkins CH, Wallis R, Allcock N, Barnes KB, Richards MI, Auty JM, Galyov EE, Harding S V., Mukamolova G V. (2019). The lytic transglycosylase, LtgG, controls cell morphology and virulence in *Burkholderia pseudomallei*. **Scientific Reports**, 9:1–13

Jia H, Wang N (2020). Generation of homozygous canker-resistant citrus in the T0 generation using CRISPR-SpCas9p. **Plant Biotechnology Journal**, 18:1990–1992

Johnson AE, Tanner ME (1998). Epimerization via carbon-carbon bond cleavage. L-ribulose-5-phosphate 4- epimerase as a masked class II aldolase. **Biochemistry**, 37:5746–5754

Johnson JW, Fisher JF, Mobashery S (2014). Bacterial cell-wall recycling. **Ann N Y Acad Sci.** 1277:54–75

Jorgenson MA, Chen Y, Yahashiri A, Popham DL, Weiss DS (2015). The Bacterial Septal Ring Protein RlpA is a Lytic Transglycosylase that Contributes to Rod Shape and Daughter Cell Separation in *Pseudomonas aeruginosa*. **Mol Microbiol**, 93:319–335

Kaniga K, Delor I, Cornelis GR (1991). A wide-host-range suicide vector for improving reverse genetics in Gram-negative bacteria: inactivation of the blaA gene of *Yersinia enterocolitica*. **Gene**, 109:137–141

Katoh K, Standley DM (2013). MAFFT multiple sequence alignment software version 7: Improvements in performance and usability. **Molecular Biology and Evolution**, 30:772–780

Katzen F, Ferreiro DU, Oddo CG, Ielmini MV, Becker A, Pühler A, Ielpi L (1998). *Xanthomonas campestris* pv. *campestris gum* mutants: Effects on xanthan biosynthesis and plant virulence. **Journal of Bacteriology**, 180:1607–1617

Kemp BP, Horne J, Bryant A, Cooper RM (2004). *Xanthomonas axonopodis* pv. *manihotis gumD* gene is essential for EPS production and pathogenicity and enhances epiphytic survival on cassava (Manihot esculenta). **Physiological and Molecular Plant Pathology**, 64:209–218

Kim DE, Chivian D, Baker D (2004). Protein structure prediction and analysis using the Robetta server. **Nucleic Acids Research**, 32:526–531

Kopp J, Kopriva S, Süss KH, Schulz GE (1999). Structure and mechanism of the amphibolic enzyme D-ribulose-5-phosphate 3-epimerase from potato chloroplasts. **Journal of Molecular Biology**, 287:761–771

Koraimann G (2003). Lytic transglycosylases in macromolecular transport systems of Gram-negative bacteria. **Cellular and Molecular Life Sciences**, 60:2371–2388

Kuk ACY, Mashalidis EH, Lee S, Carolina N (2017). Crystal structure of the MOP flippase MurJ in an inward-facing conformation. **Nature Structural & Molecular Biology.** 24:171–176

Kummerfeld SK, Teichmann SA (2005). Relative rates of gene fusion and fission in multi-domain proteins. **Annu. Rev. Biochem**, 21:25–30

Lacerda LA, Cavalca LB, Martins PMM, Govone JS, Bacci M, Ferreira H (2017). Protein depletion using the arabinose promoter in *Xanthomonas citri* subsp. *citri*. **Plasmid**, 90:44–52

Laia ML, Moreira LM, Dezajacomo J, Brigati JB, Ferreira CB, Ferro MIT, Silva ACR, Ferro J A, Oliveira JCF (2009). New genes of *Xanthomonas citri* subsp. *citri* involved in pathogenesis and adaptation revealed by a transposon-based mutant library. **BMC microbiology**, 9:1–17

Lam H, Oh D-C, Cava, felipe, Takacs CN, Jon C, De Pedro M A., Waldor MK (2009). D-Amino Acids Govern Stationary Phase. **Science**, 325:1552–1555

Leclercq S, Derouaux A, Olatunji S, Fraipont C, Egan AJF, Vollmer W, Breukink E, Terrak M (2017). Interplay between Penicillin-binding proteins and SEDS proteins promotes bacterial cell wall synthesis. **Scientific Reports**, 7:1–13

Lee J, Lee HJ, Shin MK, Ryu WS (2004). Versatile PCR-mediated insertion or deletion mutagenesis. **BioTechniques**, 36:398–400

Lee M, Domínguez-gil T, Hesek D, Mahasenan K V., Lastochkin E, Hermoso JA, Mobashery S (2016). Turnover of Bacterial Cell Wall by SltB3, a Multidomain Lytic

Transglycosylase of *Pseudomonas aeruginosa*. **ACS Chemical Biology**, 11:1525–1531

Li C TE, Liao CT, Du SC, Hsiao YP, Lo HH, Hsiao YM (2014). Functional characterization and transcriptional analysis of *galE* gene encoding a UDP-galactose 4-epimerase in *Xanthomonas campestris* pv. *campestris*. **Microbiological Research**, 169:441–452

Li JP, Gong F, El Darwish K, Jalkanen M, Lindahl U (2001). Characterization of the D-Glucuronyl C5-epimerase Involved in the Biosynthesis of Heparin and Heparan Sulfate. **Journal of Biological Chemistry**, 276:20069–20077

Li YR et al. (2011). A novel regulatory role of HrpD6 in regulating hrp-hrc-hpa genes in X*anthomonas oryzae* pv. *oryzicola*. **Molecular Plant-Microbe Interactions**, 24:1086–1101

Lommatzsch R, Templin MF, Kraft AR, Vollmer W, Biochemie A (1997). Outer Membrane Localization of Murein Hydrolases : MltA , a Third Lipoprotein Lytic Transglycosylase in *Escherichia coli*. **J Bacteriol,**179:5465–5470

Majumdar S, Ghatak J, Mukherji S, Bhattacharjee H, Bhaduri A (2004). UDPgalactose 4-epimerase from *Saccharomyces cerevisiae*: A bifunctional enzyme with aldose 1-epimerase activity. **European Journal of Biochemistry**, 271:753–759

Malamud F, Homem RA, Conforte VP, Marcelo yaryura P, Castagnaro AP, Marano MR, Do Amaral AM, Vojnov AA (2013). Identification and characterization of biofilm formation-defective mutants of *Xanthomonas citri* subsp. *citri*. **Microbiology (United Kingdom)**, 159:1911–1919

Markowitz VM et al. (2012). IMG: The integrated microbial genomes database and comparative analysis system. **Nucleic Acids Research**, 40:115–122

Martins PMM, Lau IF, Bacci M, Belasque J, Do Amaral AM, Taboga SR, Ferreira H (2010). Subcellular localization of proteins labeled with GFP in *Xanthomonas*

citri ssp. *citri*: Targeting the division septum. **FEMS Microbiology Letters**, 310:76–83

Martyn bailey J, Fishman PH, Pentchev PG (1966). Mutarotase in higher plants: Distribution and properties. **Science**, 152:1270–1271

McDonald AG, Boyce S, Tipton KF (2015). Enzyme Classification and Nomenclature. **eLS**, 1–11

McNeil M, Daffe M, Brennan PJ (1990). Evidence for the nature of the link between the arabinogalactan and peptidoglycan of mycobacterial cell walls. **Journal of Biological Chemistry**, 265:18200–18206

Meeske AJ, Sham L, Kimsey H, Koo B, Gross CA, Bernhardt TG (2015). MurJ and a novel lipid II flippase are required for cell wall biogenesis in *Bacillus subtilis*. 112:6437–6442

Metzger M, Bellemann P, Bugert P, Geider K (1994). Genetics of galactose metabolism of *Erwinia amylovora* and its influence on polysaccharide synthesis and virulence of the fire blight pathogen. **Journal of Bacteriology**, 176:450–459

Mitelman F, Johansson B, Mertens F (2007). The impact of translocations and gene fusions on cancer causation. **Nature Reviews Cancer**, 7:233–245

Mohammadi T, Sijbrandi R, Lutters M, Verheul J, Martin NI, Blaauwen T DEN, Kruijff B DE, Breukink and (2014). Specificity of the Transport of Lipid II by FtsW in *Escherichia coli*. **Journal of Biological Chemistry**, 289:14707–14718

Monahan LG, Hajduk I V., Blaber SP, Charles IG, Harry EJ (2014). Coordinating bacterial cell division with nutrient availability: A role for glycolysis. **mBio**, 5:e00935-14

Monahan LG, Harry EJ (2016). You Are What You Eat: Metabolic Control of Bacterial Division. **Trends in Microbiology**, 24:181–189

Moore BD (2004). Bifunctional and moonlighting enzymes: Lighting the way to regulatory control. **Trends in Plant Science**, 9:221–228

Moser R, Aktas M, Fritz C, Narberhaus F (2014). Discovery of a bifunctional cardiolipin/phosphatidylethanolamine synthase in bacteria. **Molecular Microbiology**, 92:959–972

Nakao R, Senpuku H, Watanabe H (2006). Porphyromonas gingivalis *galE* is involved in lipopolysaccharide O-antigen synthesis and biofilm formation. **Infection and Immunity**, 74:6145–6153

Nesper J, Lauriano CM, Klose KE, Kapfhammer D, Kraiß A, Reidl J (2001). Characterization of Vibrio cholerae O1 El Tor *galU* and *galE* mutants: Influence on lipopolysaccharide structure, colonization, and biofilm formation. **Infection and Immunity**, 69:435–445

Noël L, Thieme F, Nennstiel D, Bonas U (2002). Two novel type III-secreted proteins of *Xanthomonas campestris* pv. *vesicatoria* are encoded within the hrp pathogenicity island. **Journal of Bacteriology**, 184:1340–1348

Nowitzki U, Wyrich R, Westhoff P, Henze K, Schnarrenberger C, Martin W (1995). Cloning of the amphibolic Calvin cycle/OPPP enzyme d-ribulose-5-phosphate 3-epimerase (EC 5.1.3.1) from spinach chloroplasts: functional and evolutionary aspects. **Plant Molecular Biology**, 29:1279–1291

Oa CD et al. (2006). Xanthan Induces Plant Susceptibility by Suppressing. **Society**, 141:178–187

Oh HS, Kvitko BH, Morello JE, Collmer A (2007). *Pseudomonas syringae* lytic transglycosylases coregulated with the type III secretion system contribute to the translocation of effector proteins into plant cells. **Journal of Bacteriology**, 189:8277–8289

Oliveira ACP, Ferreira RM, Ferro MIT, Ferro JA, Chandler M, Varani AM (2018). Transposons and pathogenicity in *Xanthomonas*: Acquisition of murein lytic

transglycosylases by Tn*Xax1* enhances *Xanthomonas citri* subsp. c*itri* 306 virulence and fitness. **PeerJ**, 2018:1–23

Oliver JC, Linger RS, Chittur S V., Davisson VJ (2013). Substrate activation and conformational dynamics of guanosine 5′-monophosphate synthetase. **Biochemistry**, 52:5225–5235

Pasek S, Risler JL, Brézellec P (2006). Gene fusion/fission is a major contributor to evolution of multi-domain bacterial proteins. **Bioinformatics**, 22:1418–1423

Patané JSL et al. (2019). Origin and diversification of *Xanthomonas citri* subsp. *citri* pathotypes revealed by inclusive phylogenomic, dating, and biogeographic analyses. **BMC Genomics**, 20:1–23

Pena MM, Teper D, Ferreira H, Wang N, Sato KU, Ferro MIT, Ferro JA (2020). mCherry fusions enable the subcellular localization of periplasmic and cytoplasmic proteins in *Xanthomonas* sp. **PLoS ONE**, 15:1–15

Pettersen EF, Goddard TD, Huang CC, Couch GS, Greenblatt DM, Meng EC, Ferrin TE (2004). UCSF Chimera - A visualization system for exploratory research and analysis. **Journal of Computational Chemistry**, 25:1605–1612

Pieretti I et al. (2009). The complete genome sequence of *Xanthomonas albilineans* provides new insights into the reductive genome evolution of the xylem-limited *Xanthomonadaceae*. **BMC Genomics**, 10:1–15

Pieretti I, Pesic A, Petras D, Royer M, Süssmuth RD, Cociancich S (2015). What makes *Xanthomonas albilineans* unique amongst xanthomonads? **Frontiers in Plant Science**, 6:1–7

Radhakrishnan SK, Pritchard S, Viollier PH (2010). Coupling Prokaryotic Cell Fate and Division Control with a Bifunctional and Oscillating Oxidoreductase Homolog. **Developmental Cell**, 18:90–101

Richard D et al. (2017). Adaptation of genetically monomorphic bacteria: evolution of copper resistance through multiple horizontal gene transfers of complex and versatile mobile genetic elements. **Mol Ecol**, 7:2131-2149

Rigano LA et al. (2007). Biofilm formation, epiphytic fitness, and canker development in *Xanthomonas axonopodis* pv. *citri*. **Molecular Plant-Microbe Interactions**, 20:1222–1230

Rodriguez-r LM, Grajales A, Arrieta-ortiz ML, Salazar C, Restrepo S, Bernal A (2012). Genomes-based phylogeny of the genus *Xanthomonas*. **BMC Microbiology**, 12:43

Romano AH, Conway T (1996). Evolution of carbohydrate metabolic pathways. **Research in Microbiology**, 147:448–455

Rose IA (1975). Mechanism of the Aldose-Ketose Isomerase Reactions. **Advances in Enzymology and Related Areas of Molecular Biology**, 43:491–517

Ryan RP, Vorhölter FJ, Potnis N, Jones JB, Van Sluys MA, Bogdanove AJ, Dow JM (2011). Pathogenomics of *Xanthomonas*: Understanding bacterium-plant interactions. **Nature Reviews Microbiology**, 9:344–355

Saijo Y, Schulze-lefert P (2008). Manipulation of the Eukaryotic Transcriptional Machinery by Bacterial Pathogens. **Cell Host and Microbe**, 4:96–99

Sala RF, Morgan PM, Tanner ME (1996). Enzymatic formation and release of a stable glycal intermediate: The mechanism of the reaction catalyzed by UDP-N-acetylglucosamine 2-epimerase. **Journal of the American Chemical Society**, 118:3033–3034

Salo WL, Fossitt DD, Bevill RD, Kirkwood S, Wood W (1972). L-ribulose 5-phosphate 4-epimerase from Aerobacter aerogenes. Kinetic isotope effect with tritiated substrate. **Journal of Biological Chemistry**, 247:3098–3100

Sambrook J, Fritsch ER, Maniatis T (1989). Molecular Cloning: A Laboratory Manual. In: **Molecular Cloning: A Laboratory Manual**. 2ª ed. [s.l.] Cold Spring Harbor, NY: Cold Spring Harbor Laboratory Press.

Savietto A, Polaquini CR, Kopacz M, Scheffers DJ, Marques BC, Regasini LO, Ferreira H (2018). Antibacterial activity of monoacetylated alkyl gallates against *Xanthomonas citri* subsp. *citri*. **Archives of Microbiology**, 200:929–937,

Schaad NW, Postnikova E, Lacy G, Sechler A, Agarkova I, Stromberg PE, Stromberg VK, Vidaver AK (2006). Emended classification of xanthomonad pathogens on citrus. **Systematic and Applied Microbiology**, 29:690–695

Schatschneider S, Huber C, Neuweger H, Watt TF, Pühler A, Eisenreich W, Wittmann C, Niehaus K, Vorhölter FJ (2014). Metabolic flux pattern of glucose utilization by *Xanthomonas campestris* pv. *campestris*: Prevalent role of the Entner-Doudoroff pathway and minor fluxes through the pentose phosphate pathway and glycolysis. **Molecular BioSystems**, 10:2663–2676

Scheffers D-J, Pinho MG (2005). Bacterial cell wall synthesis: New insights from localization studies. **Microbiology and Molecular Biology Reviews**, 69:585–607

Scheffers DJ, Tol MB (2015). LipidII: Just Another Brick in the Wall? **PLoS Pathogens**, 11:1–12

Scheurwater E, Reid CW, Clarke AJ (2008). Lytic transglycosylases: Bacterial space-making autolysins. **International Journal of Biochemistry and Cell Biology**, 40:586–591

Scheurwater EM, Burrows LL (2011). Maintaining network security: How macromolecular structures cross the peptidoglycan layer. **FEMS Microbiology Letters**, 318:1–9

Scheurwater EM, Clarke AJ (2008). The C-terminal domain of *Escherichia coli* YfhD functions as a lytic transglycosylase. **Journal of Biological Chemistry**, 283:8363–8373

Schmidt S, Sunyaev S, Bork P, Dandekar T (2003). Metabolites: A helping hand for pathway evolution? **Trends in Biochemical Sciences**, 28:336–341

Schubert TS, Sun X (2003). Bacterial Citrus Canker 1. **Journal of the Rio Grande Valley Horticultural Society**, 1996:2–7

Scott A, Timson DJ (2007). Characterization of the *Saccharomyces cerevisiae* galactose mutarotase/UDP-galactose 4-epimerase protein, Gal10p. **FEMS Yeast Research**, 7:366–371

Sham L-T, Butler EK, D ML, Kahne D, Bernhardt TG, Ruiz N (2014). Bacterial cell wall. MurJ is the flippase of lipid-linked precursors for peptidoglycan biogenesis. **Science,** 220:220–222

Sieger B, Schubert K, Donovan C, Bramkamp M (2013). The lipid II flippase RodA determines morphology and growth in *Corynebacterium glutamicum*. **Mol Microbiol,** 90:966–982

Snel B, Bork P, Huynen M (2000). Genome evolutiongene fusion versus gene fission. **Trends in Genetics**, 16:9–11

Sperber AM, Herman JK (2017). Metabolism shapes the cell. **Journal of Bacteriology**, 199:1–14

Sriram G, Martinez JA, McCabe ERB, Liao JC, Dipple KM (2005). Single-gene disorders: What role could moonlighting enzymes play? **American Journal of Human Genetics**, 76:911–924

Teige M, Kopriva S, Bauwe H, Süss KH (1995). Chloroplast pentose-5-phosphate 3-epimerase from potato: cloning, cDNA sequence, and tissue-specific enzyme accumulation. **FEBS Letters**, 377:349–352

Thoden JB, Holden HM (2005). The molecular architecture of galactose mutarotase/UDP-galactose 4-epimerase from *Saccharomyces cerevisiae*. **Journal of Biological Chemistry**, 280:21900–21907

Thoden JB, Kim J, Raushel FM, Holden HM (2003). The catalytic mechanism of galactose mutarotase. **Protein Science**, 12:1051–1059

Timson DJ, Ã RJR (2003). Identification and characterisation of human aldose 1-epimerase. **FEBS Letters**, 543:22–25

Ucci AP, Martins PMM, Lau IF, Bacci M, Belasque J, Ferreira H (2014). Asymmetric chromosome segregation in *Xanthomonas citri* ssp. *citri*. **MicrobiologyOpen**, 3:29–41

Uehara T, Park JT (2008). Growth of Escherichia coli: Significance of peptidoglycan degradation during elongation and septation. **Journal of Bacteriology**, 190:3914–3922

USDA (2021). **United States Department of Agriculture Foreign Agricultural Service - Citrus: World Markets and Trade**. Disponível em: <https://apps.fas.usda.gov/psdonline/circulars/citrus.pdf>.

Van Asselt EJ, Dijkstra AJ, Kalk KH, Takacs B, Keck W, Dijkstra BW (1999). Crystal structure of *Escherichia coli* lytic transglycosylase Slt35 reveals a lysozyme-like catalytic domain with an EF-hand. **Structure**, 7:1167–1180

Van Heijenoort J (1998). Assembly of the monomer unit of bacterial peptidoglycan. **Cellular and Molecular Life Sciences CMLS**, 54:300–304

Vauterin L, Hoste B, Kersters K, Swings J (1995). Reclassification of *Xanthomonas*. **International Journal of Systematic Bacteriology**, 45:472–489

Vogel C, Bashton M, Kerrison ND, Chothia C, Teichmann SA (2004). Structure, function and evolution of multidomain proteins. **Current Opinion in Structural Biology**, 14:208–216

Vollmer W, Bertsche U (2008). Murein (peptidoglycan) structure, architecture and biosynthesis in *Escherichia coli*. **Biochimica et Biophysica Acta - Biomembranes**, 1778:1714–1734

Voloudakis AE, Reignier TM, Cooksey DA (2005). Regulation of resistance to copper in *Xanthomonas axonopodis* pv. *vesicatoria*. **Applied and Environmental Microbiology**, 71:782–789

Wagner S, Grin I, Malmsheimer S, Singh N, Torres-vargas CE, Westerhausen S (2018). Bacterial type III secretion systems: A complex device for the delivery of bacterial effector proteins into eukaryotic host cells. **FEMS Microbiology Letters**, 365:1–13

Wang JD, Levin PA (2009). Metabolism, cell growth and the bacterial cell cycle. **Nature Reviews Microbiology**, 7:822–827

Wang L, Yang LY, Gan YL, Yang F, Liang XL, Li WL, Bo-le J (2019). Two lytic transglycosylases of Xanthomonas campestris pv. campestris associated with cell separation and type III secretion system, respectively. **FEMS Microbiology Letters**, 366: 7 fnz073

Weng SF, Lin JW, Chen CH, Chen YY, Tseng YH, Tseng YH (2004). Constitutive Expression of a Chromosomal Class A (BJM Group 2) β-Lactamase in *Xanthomonas campestris*. **Antimicrobial Agents and Chemotherapy**, 48:209–215

Williams AH, Wheeler R, Thiriau C, Haouz A, Taha MK, Boneca IG (2017). Bulgecin a: The key to a broad-spectrum inhibitor that targets lytic transglycosylases. **Antibiotics**, 6:1–14

Wilson DB, Hogness DS (1969). The enzymes of the galactose operon in *Escherichia coli.* II. The subunits of uridine diphosphogalactose 4-epimerase. **Journal of Biological Chemistry**, 244:2132–2136

Xu D, Nussinov R (1998). Favorable domain size in proteins. **Folding and Design**, 3:11–17

Yanai I, Derti A, DeLisi C (2001). Genes linked by fusion events are generally of the same functional category: A systematic analysis of 30 microbial genomes. **Proceedings of the National Academy of Sciences of the United States of America**, 98:7940–7945

Yeom SJ, Ji JH, Kim NH, Park CS, Oh DK (2009). Substrate specificity of a mannose-6-phosphate isomerase from bacillus subtilis and its application in the production of L-ribose. **Applied and Environmental Microbiology**, 75:4705–4710

Young FE, Arias L (1967). Biosynthesis of the N-acyl-galactosaminase in cell walls of *Bacillus subtilis*. **Journal of Bacteriology**, 94:1783–1784

Zaritsky A (2015). Cell-Shape Homeostasis in *Escherichia coli* Is Driven by Growth, Division, and Nucleoid Complexity. **Biophysical Journal**, 109:178–181

Zaritsky A, Woldringh CL, Einav M, Alexeeva S (2006). Use of thymine limitation and thymine starvation to study bacterial physiology and cytology. **Journal of Bacteriology**, 188:1667–1679

Zientz E, Dandekar T, Gross R (2004). Metabolic interdependence of obligate intracellular bacteria and their insect hosts. **Microbiology and Molecular Biology Reviews**, 68:745–770

9. APPENDIX

Table S1. Oligonucleotides utilized in this study.

Oligonucleotide name	Sequence (5'-3')	Restriction site	Purpose
A (R)**	GCCTTGGCCTGGGCTAGCCTG	*NheI***	Site-directed mutagenesis
B (F)*	TCTGCCCACGGAAGGTGCCCGTAGGGCG	----	Site-directed mutagenesis
C (R)*	CACCGCATGACGTCTGCCCACGGAAGGTGC	----	Site-directed mutagenesis
D (F)**	GGCAAAGCTTGGGTGCTTCTGGC	*HindIII***	Site-directed mutagenesis
S (R) *	CACGAGGCTTCGCACGCACC	----	Sequencing
pMAJIIc (F) **	ATCGCTAGCATGACGCTGTCCCGGGGC	*NheI***	Complementation/mCherry fusion
pMAJIIc (R) **	GTCACTCGAGCTCGACGCTGATGGTCTGGGT	*XhoI*	mCherry fusion
R4296	CACGAGGCTTCGCACGCACC	-	Sequencing
F4296	GGCAAAGCTTGGGTGCTTCTGGC		Sequencing

*F, Forward; R, Reverse. Oligonucleotides synthesized by SIGMA-ALDRICH BRASIL.
** Underlined regions represent added restriction sites;
B/C and R1/F2 oligonucleotides blue sequences are complementary to sequences in red of its pairing primer.

Table S2. Xanthomonadaceae used for comparative genomics. In this table, there are 2 species for the *Pseudoxanthomonas* genus, 36 species for the *Stenotrophomonas* genus, and 270 species for the *Xanthomonas* genus.

Genus	Species	Accession number
Pseudoxanthomonas	*Pseudoxanthomonas sp. isolate* SSD1	CP059266.1
	Pseudoxanthomonas suwonensis strain J1	CP011144.1
Stenotrophomonas	*Stenotrophomonas maltophilia* ZT1	CP019797.1
	Stenotrophomonas acidaminiphila strain T0-18	CP043567.1
	Stenotrophomonas acidaminiphila strain T25-65	CP043570.1
	Stenotrophomonas acidaminiphila strain ZAC14D2_NAIMI4_2	CP012900.1
	Stenotrophomonas indicatrix strain DAIF1	CP037883.1
	Stenotrophomonas maltophilia strain AA1	CP018756.1
	Stenotrophomonas maltophilia strain MER1	CP049368.1
	Stenotrophomonas maltophilia strain PEG-305	CP040437.1
	Stenotrophomonas maltophilia strain PEG-390	CP040436.1
	Stenotrophomonas maltophilia strain CPBW01	CP047310.1
	Stenotrophomonas maltophilia strain ISMMS2R	CP011306.1
	Stenotrophomonas maltophilia strain ISMMS2	CP011305.1
	Stenotrophomonas sp. MYb57	CP023271.1
	Stenotrophomonas sp. NA06056	CP054931.1
	Stenotrophomonas sp. SAU14A_NAIMI4_5	CP026003.1
	Stenotrophomonas sp. 364	CP047135.1
	Stenotrophomonas sp. CW117	CP062156.1
	Stenotrophomonas sp. ESTM1D_MKCIP4_1	CP026004.1
	Stenotrophomonas maltophilia strain U5	CP040429.1
	Stenotrophomonas nitritireducens strain 2001	CP016756.1
	Stenotrophomonas rhizophila strain DSM14405	CP007597.1
	Stenotrophomonas rhizophila strain JC1	CP050062.1
	Stenotrophomonas rhizophila strain QL-P4	CP016294.1
	Stenotrophomonas sp. 169	CP061204.1
	Stenotrophomonas sp. G4	CP031741.1
	Stenotrophomonas sp. KCTC 12332 strain YM1	CP014274.1
	Stenotrophomonas sp. LM091	CP017483.1
	Stenotrophomonas sp. SAU14A_NAIMI4_8	CP025999.1
	Stenotrophomonas sp. SXG-1	CP046588.1

	Stenotrophomonas sp. YAU14A_MKIMI4_1	CP025998.1
	Stenotrophomonas sp. YAU14D1_LEIMI4_1	CP025997.1
	Stenotrophomonas sp. ZAC14A_NAIMI4_1	CP026002.1
	Stenotrophomonas sp. ZAC14D1_NAIMI4_1	CP026001.1
	Stenotrophomonas sp. ZAC14D1_NAIMI4_6	CP026000.1
	Stenotrophomonas sp. ZAC14D2_NAIMI4_6	CP025996.1
	Stenotrophomonas sp. ZAC14D2_NAIMI4_7	CP025995.1
Xanthomonas	*Xanthomonas arboricola* pv. *juglandis* isolate 3	LR861807.1
	Xanthomonas arboricola pv. *juglandis* strain Xaj 417	CP012251.1
	Xanthomonas arboricola pv. pruni strain 15-088	CP044334.1
	Xanthomonas arboricola strain 17	CP011256.1
	Xanthomonas axonopodis Xac29-1	CP004399.1
	Xanthomonas axonopodis pv. *citri* str. 306	AE008923.1
	Xanthomonas axonopodis pv. *citrumelo* F1	CP002914.1
	Xanthomonas axonopodis pv. *commiphoreae* strain LMG26789	CP031059.1
	Xanthomonas phaseoli pv. *dieffenbachiae* LMG 695	CP014347.1
	Xanthomonas axonopodis pv. *phaseoli* strain CFBP412	CP020964.1
	Xanthomonas citri pv. *malvacearum* strain HD-1	CP046019.1
	Xanthomonas citri pv. *malvacearum* strain MS14003	CP023159.1
	Xanthomonas citri pv. *malvacearum* strain MSCT	CP017020.1
	Xanthomonas citri pv. *malvacearum* strain XcmH1005	CP013004.1
	Xanthomonas citri pv. *malvacearum* strain XcmN1003	CP013006.1
	Xanthomonas citri pv. *phaseoli* var. *fuscans* strain CFBP4885	CP020992.1
	Xanthomonas citri pv. *phaseoli* var. *fuscans* strain CFBP6165	CP020998.1
	Xanthomonas citri pv. *phaseoli* var. *fuscans* strain CFBP6166	CP021001.1
	Xanthomonas citri pv. *phaseoli* var. *fuscans* strain CFBP6167	CP021018.1
	Xanthomonas citri pv. *phaseoli* var. *fuscans* strain CFBP6975	CP021006.1
	Xanthomonas oryzae pv. *oryzae* PXO86	CP007166.1
	Xanthomonas oryzae pv. *oryzae* PXO99A	CP000967.2
	Xanthomonas oryzae pv. *oryzae* strain AUST2013	CP033196.1
	Xanthomonas oryzae pv. *oryzae* strain AXO1947	CP013666.1
	Xanthomonas oryzae pv. *oryzae* strain BAI3	CP025610.1
	Xanthomonas oryzae pv. *oryzae* strain BXO1	CP033201.1
	Xanthomonas oryzae pv. *oryzae* strain BXO512	CP033185.1 CP065228.1

	Xanthomonas oryzae pv. *oryzae* strain CFBP1948	
	Xanthomonas oryzae pv. *oryzae* strain CFBP1949	CP033184.1
	Xanthomonas oryzae pv. *oryzae* strain CFBP1951	CP033183.1
	Xanthomonas oryzae pv. *oryzae* strain Ug11	CP033170.1
	Xanthomonas oryzae pv. *oryzae* strain XF89b	CP011532.1
	Xanthomonas oryzae pv. *oryzae* strain K3a	CP050115.1
	Xanthomonas oryzae pv. *oryzae* strain K3	CP050114.1
	Xanthomonas oryzae pv. *oryzae* strain KXO85	CP033197.1
	Xanthomonas oryzae pv. *oryzae* strain MAI1	CP025609.1
	Xanthomonas oryzae pv. *oryzae* strain MAI68	CP019085.1
	Xanthomonas oryzae pv. *oryzae* strain MAI73	CP019086.1
	Xanthomonas oryzae pv. *oryzae* strain MAI95	CP019087.1
	Xanthomonas oryzae pv. *oryzae* strain MAI99	CP019088.1
	Xanthomonas oryzae pv. *oryzae* strain XM9	CP020334.1
	Xanthomonas oryzae pv. *oryzae* strain YC11	CP031464.1
	Xanthomonas oryzae pv. *oryzae* strain YN24	CP018089.1
	Xanthomonas oryzae pv. *oryzicola* BLS256	CP003057.2
	Xanthomonas oryzae pv. *oryzicola* strain 0-9	CP045912.1
	Xanthomonas oryzae pv. *oryzicola* strain B8-12	CP011955.1
	Xanthomonas oryzae pv. *oryzicola* strain BLS279	CP011956.1
	Xanthomonas oryzae pv. *oryzicola* strain BXOR1	CP011957.1
	Xanthomonas oryzae pv. *oryzicola* strain CFBP2286	CP011962.1
	Xanthomonas oryzae pv. *oryzicola* strain CFBP7331	CP011958.1
	Xanthomonas translucens pv. *undulosa* strain Xtu 4699	CP008714.1
	Xanthomonas vasicola pv. *arecae* strain NCPPB 2649	CP034653.1
	Xanthomonas vasicola pv. *vasculorum* strain SAM119	CP028127.1
	Xanthomonas vasicola pv. *vasculorum* strain Xv1601	CP025272.1
	Xanthomonas vasicola strain NCPPB 902	CP034657.1
	Xanthomonas vasicola strain NCPPB 1060	CP034649.1
	Xanthomonas vesicatoria ATCC 35937 strain LMG911	CP018725.1
	Xanthomonas vesicatoria strain LM159	CP018470.1
	Xanthomonas hortorum pv. *vitians* LM16734	CP060399.1
	Xanthomonas hortorum pv. vitians strain CFBP 498	LR828257.1
	Xanthomonas axonopodis pv. *phaseoli* strain CFBP6164	CP020967.1
	Xanthomonas axonopodis pv. *phaseoli* strain CFBP6546R	CP020971.1
	Xanthomonas axonopodis pv. *phaseoli* strain CFBP6982	CP020975.1
	Xanthomonas axonopodis pv. *phaseoli* strain ISO18C2	CP012048.1
	Xanthomonas axonopodis pv. *phaseoli* strain ISO18C8	CP012063.1

	Xanthomonas phaseoli pv. *phaseoli* strain ISO98C12	CP012057.1
	Xanthomonas axonopodis pv. *vasculorum* strain NCPPB 796	CP053649.1
	Xanthomonas campestris pv. badrii strain NEB122	CP051651.1
	Xanthomonas campestris pv. *campestris* MAFF106712	AP019682.1
	Xanthomonas campestris pv. *campestris* MAFF302021	AP019684.1
	Xanthomonas campestris pv. *campestris* complete genome, strain B100	AM920689.1
	Xanthomonas campestris pv. *campestris* strain 17	CP011946.1
	Xanthomonas campestris pv. *campestris* strain 3811	CP025750.1
	Xanthomonas campestris pv. *campestris* strain ICMP 4013	CP012146.1
	Xanthomonas campestris pv. *campestris* strain ICMP 21080	CP012145.1
	Xanthomonas campestris pv. *campestris* strain Xcc8004_Xcc1	CP029483.1
	Xanthomonas campestris pv. *campestris* strain Xcc8004_Xcc2	CP029484.1
	Xanthomonas citri pv. *phaseoli* var. *fuscans* strain CFBP6988R	CP020979.1
	Xanthomonas citri pv. *phaseoli* var. *fuscans* strain CFBP6989 CP020981.1	CP020981.1
	Xanthomonas citri pv. *phaseoli* var. *fuscans* strain CFBP6990	CP020983.1
	Xanthomonas citri pv. *phaseoli* var. *fuscans* strain CFBP6991	CP021015.1
	Xanthomonas citri pv. *phaseoli* var. *fuscans* strain CFBP6992	CP020985.1
	Xanthomonas citri pv. *phaseoli* var. *fuscans* strain CFBP6994R	CP020987.1
	Xanthomonas citri pv. *phaseoli* var. *fuscans* strain CFBP6996R	CP020989.1
	Xanthomonas citri pv. *punicae* strain BD0022	CP030159.1
	Xanthomonas citri pv. *punicae* strain BD0023	CP030161.1
	Xanthomonas citri pv. *punicae* strain BD0025	CP030169.1
	Xanthomonas citri pv. *punicae* strain LMG7439	CP030164.1
	Xanthomonas citri pv. *punicae* strain LMG7504	CP030166.1
	Xanthomonas citri pv. *punicae* strain LMG 859	CP030178.1
	Xanthomonas citri pv. *punicae* strain NCPPB 3563	CP030163.1
	Xanthomonas citri pv. *vignicola* strain CFBP7111	CP022263.1
	Xanthomonas citri pv. *vignicola* strain CFBP7112	CP022267.1
	Xanthomonas citri pv. *vignicola* strain CFBP7113	CP022270.1
	Xanthomonas oryzae pv. *oryzae* strain CFBP1952	CP033182.1
	Xanthomonas oryzae pv. *oryzae* strain CFBP7319	CP033181.1
	Xanthomonas oryzae pv. *oryzae* strain CFBP7320	CP033186.1
	Xanthomonas oryzae pv. *oryzae* strain CFBP7321	CP033180.1
	Xanthomonas oryzae pv. *oryzae* strain CFBP7322	CP033179.1
	Xanthomonas oryzae pv. *oryzae* strain CFBP7323	CP033178.1
	Xanthomonas oryzae pv. *oryzae* strain CFBP7324	CP033177.1

	Xanthomonas oryzae pv. *oryzae* strain CFBP7325	CP033176.1
	Xanthomonas oryzae pv. *oryzae* strain CFBP7337	CP033175.1
	Xanthomonas oryzae pv. *oryzae* strain CFBP7340	CP033174.1
	Xanthomonas oryzae pv. *oryzae* strain CFBP8172	CP033173.1
	Xanthomonas oryzae pv. *oryzae* strain CIAT	CP033194.1
	Xanthomonas oryzae pv. *oryzae* strain CIX298	CP036378.1
	Xanthomonas oryzae pv. *oryzae* strain CIX2374	CP036377.1
	Xanthomonas oryzae pv. *oryzae* strain Dak16	CP033172.1
	Xanthomonas oryzae pv. *oryzae* strain HuN37	CP031456.1
	Xanthomonas oryzae pv. *oryzae* strain ICMP3125	CP031697.1
	Xanthomonas oryzae pv. *oryzae* strain MAI106	CP019089.1
	Xanthomonas oryzae pv. *oryzae* strain MAI129	CP019090.1
	Xanthomonas oryzae pv. *oryzae* strain MAI134	CP019091.1
	Xanthomonas oryzae pv. *oryzae* strain MAI145	CP019092.1
	Xanthomonas oryzae pv. *oryzae* strain NX0260	CP033192.1
	Xanthomonas oryzae pv. *oryzae* strain OS198	CP031461.1
	Xanthomonas oryzae pv. *oryzae* strain PX079	CP031462.1
	Xanthomonas oryzae pv. *oryzae* strain PX086	CP031463.1
	Xanthomonas oryzae pv. *oryzae* strain PXO61	CP020942.1
	Xanthomonas oryzae pv. *oryzae* strain PXO61	CP021788.1
	Xanthomonas oryzae pv. *oryzae* strain PXO61	CP021789.1
	Xanthomonas oryzae pv. *oryzae* strain PXO61	CP033187.3
	Xanthomonas oryzae pv. *oryzae* strain PXO71	CP013670.1
	Xanthomonas oryzae pv. *oryzae* strain PXO83	CP012947.1
	Xanthomonas oryzae pv. *oryzae* strain PXO142	CP031698.1
	Xanthomonas oryzae pv. *oryzae* strain PXO145	CP013961.1
	Xanthomonas oryzae pv. *oryzae* strain PXO211	CP013674.1
	Xanthomonas oryzae pv. *oryzicola* strain CFBP7341	CP011959.1
	Xanthomonas oryzae pv. *oryzicola* strain CFBP7342	CP007221.1
	Xanthomonas oryzae pv. *oryzicola* strain GX01	CP043403.1
	Xanthomonas oryzae pv. *oryzicola* strain L8	CP011960.1
	Xanthomonas oryzae pv. *oryzicola* strain RS105	CP011961.1
	Xanthomonas oryzae pv. *oryzicola* strain YM15	CP007810.1
	Xanthomonas oryzae strain BAI23	CP036256.1
	Xanthomonas oryzae strain BB151-3	CP036255.1
	Xanthomonas oryzae strain BB156-2	CP036254.1
	Xanthomonas oryzae strain NCPPB 4346	CP036253.1
	Xanthomonas oryzae strain NJ611	CP036252.1
	Xanthomonas oryzae strain X11-5A	CP036251.1
	Xanthomonas perforans 91-118	CP019725.1
	Xanthomonas perforans strain LH3	CP018475.1
	Xanthomonas sacchari strain R1	CP010409.1
	Xanthomonas sp. CPBF 367 isolate 1	LR861803.1
	Xanthomonas sp. CPBF 426	LR861805.1
	Xanthomonas hortorum strain B07-007	CP016878.1
	Xanthomonas hortorum strain VT106	CP031607.1
	Xanthomonas hyacinthi strain CFBP 1156	CP043476.1
	Xanthomonas oryzae pv. *oryzae* KACC 10331	AE013598.1
	Xanthomonas oryzae pv. *oryzae* MAFF 311018	AP008229.1

	Xanthomonas oryzae pv. *oryzae* strain PXO524	CP013677.1
	Xanthomonas oryzae pv. *oryzae* strain PXO563	CP013678.1
	Xanthomonas oryzae pv. *oryzae* strain PXO602	CP013679.1
	Xanthomonas oryzae pv. *oryzae* strain SK2-3	CP019515.1
	Xanthomonas oryzae pv. *oryzae* strain ScYc-b	CP018087.1
	Xanthomonas oryzae pv. *oryzae* strain ScYc-b	CP031469.1
	Xanthomonas oryzae pv. *oryzae* strain T19	CP033171.1
	Xanthomonas oryzae pv. *oryzae* strain PXO364	CP033191.1
	Xanthomonas oryzae pv. *oryzae* strain PXO404	CP033190.1
	Xanthomonas oryzae pv. *oryzae* strain PXO421	CP033189.1
	Xanthomonas oryzae pv. *oryzae* strain PXO513	CP033188.1
	Xanthomonas citri pv. *malvacearum* strain AR81009	CP023155.1
	Xanthomonas campestris pv. *campestris* str. ATCC 33913	AE008922.1
	Xanthomonas campestris pv. *campestris* str. CN03	CP017308.1
	Xanthomonas campestris pv. *campestris* str. CN12	CP017310.1
	Xanthomonas campestris pv. *campestris* str. CN14	CP017317.1
	Xanthomonas campestris pv. *campestris* str. CN15	CP017323.1
	Xanthomonas campestris pv. *campestris* str. CN16	CP017389.1
	Xanthomonas campestris pv. *campestris* str. CN17	CP017307.1
	Xanthomonas campestris pv. *campestris* str. CN18	CP017319.1
	Xanthomonas campestris pv. *musacearum* NCPPB 4379	CP034655.1
	Xanthomonas campestris pv. *raphani* 756C	CP002789.1
	Xanthomonas campestris pv. *raphani* strain MAFF106181	CP058243.1
	Xanthomonas campestris pv. *vesicatoria*	AM039952.1
	Xanthomonas campestris pv. *vesicatoria* str. 85-10	CP017190.1
	Xanthomonas campestris strain M28	CP062066.1
	Xanthomonas citri pv. *anacardii* CFBP 2913	CP024057.1
	Xanthomonas citri pv. *citri* strain 03-1638-1-1	CP023285.1
	Xanthomonas citri pv. *citri* strain DAR72029	CP060446.1
	Xanthomonas citri pv. *citri* strain DAR73886	CP060465.1
	Xanthomonas citri strain UnB-Xtec2D	CP048044.1
	Xanthomonas citri strain UnB-XtecTG02-2	CP048712.1
	Xanthomonas citri subsp. *citri* A306	CP006857.1
	Xanthomonas citri subsp. *citri* Aw12879	CP003778.1
	Xanthomonas citri subsp. *citri* UI6	CP008992.1
	Xanthomonas citri subsp. *citri* strain 5208	CP009028.1
	Xanthomonas citri subsp. *citri* strain AW13	CP009031.1
	Xanthomonas citri subsp. *citri* strain AW14	CP009034.1
	Xanthomonas citri subsp. *citri* strain AW15	CP009037.1
	Xanthomonas citri subsp. *citri* strain AW16	CP009040.1
	Xanthomonas citri subsp. *citri* strain BL18	CP009025.1
	Xanthomonas citri subsp. *citri* strain FB19	CP009022.1
	Xanthomonas citri subsp. *citri* strain MN10	CP009004.1
	Xanthomonas citri subsp. *citri* strain MN11	CP009001.1
	Xanthomonas citri subsp. *citri* strain MN12	CP008998.1
	Xanthomonas citri subsp. *citri* strain NT17	CP008995.1
	Xanthomonas citri subsp. *citri* strain UI7	CP008989.1

	Xanthomonas citri subsp. *citri* strain gd2	CP009019.1
	Xanthomonas oryzae pv. *oryzae* strain ITCCBB0002	CP046148.1
	Xanthomonas oryzae pv. *oryzae* strain IXO704	CP040604.1
	Xanthomonas oryzae pv. *oryzae* strain IXO1088	CP040687.1
	Xanthomonas oryzae pv. *oryzae* strain IX-280	CP019226.1
	Xanthomonas oryzae pv. *oryzae* strain JL25	CP031457.1
	Xanthomonas oryzae pv. *oryzae* strain JL28	CP031458.1
	Xanthomonas oryzae pv. *oryzae* strain JL33	CP031459.1
	Xanthomonas oryzae pv. *oryzae* strain JP01	CP031460.1
	Xanthomonas oryzae pv. *oryzae* strain JW11089	CP033193.2
	Xanthomonas oryzae pv. *oryzae* strain K1	CP049205.1
	Xanthomonas oryzae pv. *oryzae* strain K2	CP050113.1
	Xanthomonas citri subsp. *citri* strain gd3	CP009016.1
	Xanthomonas citri subsp. *citri* strain jx4	CP009013.1
	Xanthomonas citri subsp. *citri* strain jx5	CP009010.1
	Xanthomonas citri pv. *citri* strain DAR73889	CP060470.1
	Xanthomonas citri pv. *citri* strain DAR73910	CP060476.1
	Xanthomonas citri pv. *citri* strain DAR84832	CP060460.1
	Xanthomonas citri pv. *glycines* strain 1018	CP041961.1
	Xanthomonas oryzae pv. *oryzae* strain PXO236	CP013675.1
	Xanthomonas oryzae pv. *oryzae* strain PXO282	CP013676.1
	Xanthomonas hortorum pv. *gardneri* strain JS749-3	CP018728.1
	Xanthomonas hortorum pv. *pelargonii* strain CFBP 2533	LR828261.1
	Xanthomonas citri pv. *citri* strain LH201	CP018858.1
	Xanthomonas citri pv. *citri* strain LH276	CP018854.1
	Xanthomonas citri pv. *citri* strain LJ207-7	CP018850.1
	Xanthomonas citri pv. *citri* strain LL074-4	CP018847.1
	Xanthomonas citri pv. *citri* strain TX160042	CP020882.1
	Xanthomonas citri pv. *citri* strain TX160149	CP020885.1
	Xanthomonas citri pv. *citri* strain TX160197	CP020889.1
	Xanthomonas citri pv. *citri* strain Xcc29-1	CP023661.1
	Xanthomonas citri pv. *citri* strain Xcc49	CP023662.1
	Xanthomonas citri pv. *citri* strain jx-6	CP011827.2
	Xanthomonas citri pv. *fuscans* CFBP 6988	CP026331.1
	Xanthomonas citri pv. *fuscans* strain Xff49	CP023294.1
	Xanthomonas citri pv. *glycines* strain 8ra	CP041781.1
	Xanthomonas citri pv. *fuscans* strain ISO118C5	CP012051.1
	Xanthomonas sp. GW	CP051189.1
	Xanthomonas sp. ISO98C4	CP012060.1
	Xanthomonas sp. SI	CP051261.1
	Xanthomonas sp. SS	CP051190.1
	Xanthomonas sp. WG16	CP062255.1
	Xanthomonas translucens pv. *cerealis* strain 01	CP038228.1
	Xanthomonas translucens pv. *translucens* DSM 18974 isolate peng1	LT604072.1
	Xanthomonas translucens pv. undulosa strain ICMP11055	CP009750.1
	Xanthomonas translucens pv. undulosa strain LW16	CP043540.1
	Xanthomonas translucens pv. undulosa strain P3	CP043500.1
	Xanthomonas citri pv. *glycines* strain K2	CP041967.1

	Xanthomonas citri pv. *glycines* str. 8ra	CP017188.2
	Xanthomonas citri pv. *glycines* strain 1157	CP041963.1
	Xanthomonas citri pv. *glycines* str. 12-2	CP015972.1
	Xanthomonas arboricola strain SL2098	CP041965.1
	Xanthomonas citri pv. *glycines* strain EB08	CP026334.1
	Xanthomonas fuscans subsp. *fuscans* strain ISO118C1	CP012053.1
	Xanthomonas fuscans subsp. *fuscans* strain ISO12C3	CP012055.1
	Xanthomonas translucens pv. *undulosa* strain Xtu 4699	CP008714.1
	Xanthomonas vasicola pv. *arecae* strain NCPPB 2649	CP034653.1
	Xanthomonas vasicola pv. *vasculorum* strain SAM119	CP028127.1
	Xanthomonas vasicola pv. *vasculorum* strain Xv1601	CP025272.1
	Xanthomonas vasicola strain NCPPB 902	CP034657.1
	Xanthomonas vasicola strain NCPPB 1060	CP034649.1
	Xanthomonas vesicatoria ATCC 35937 strain LMG911	CP018725.1
	Xanthomonas vesicatoria strain LM159	CP018470.1
	Xanthomonas hortorum pv. *vitians* LM16734	CP060399.1
	Xanthomonas hortorum pv. *vitians* strain CFBP 498	LR828257.1
	Xanthomonas hortorum strain B07-007	CP016878.1
	Xanthomonas hortorum strain VT106	CP031607.1
	Xanthomonas hyacinthi strain CFBP 1156	CP043476.1
	Xanthomonas oryzae pv. *oryzae* KACC 10331	AE013598.1
	Xanthomonas oryzae pv. *oryzae* MAFF 311018 DNA	AP008229.1
	Xanthomonas oryzae pv. *oryzae* strain PXO524	CP013677.1
	Xanthomonas oryzae pv. *oryzae* strain PXO563	CP013678.1
	Xanthomonas oryzae pv. *oryzae* strain PXO602	CP013679.1
	Xanthomonas oryzae pv. *oryzae* strain SK2-3	CP019515.1
	Xanthomonas oryzae pv. *oryzae* strain ScYc-b	CP018087.1
	Xanthomonas oryzae pv. *oryzae* strain ScYc-b	CP031469.1
	Xanthomonas oryzae pv. *oryzae* strain T19	CP033171.1
	Xanthomonas oryzae pv. *oryzae* strain PXO364	CP033191.1
	Xanthomonas oryzae pv. *oryzae* strain PXO404	CP033190.1
	Xanthomonas oryzae pv. *oryzae* strain PXO421	CP033189.1
	Xanthomonas oryzae pv. *oryzae* strain PXO421	CP033188.1
	Xanthomonas citri pv. *malvacearum* strain AR81009	CP023155.1
	Xanthomonas hortorum pv. *gardneri* strain ICMP 7383	CP018731.1
	Xanthomonas citri subsp. *citri* strain mf20	CP009007.1
	Xanthomonas cucurbitae strain ATCC 23378	CP033326.1
	Xanthomonas cynarae strain CFBP 2044	LR828251.1
	Xanthomonas euroxanthea CPBF 424	LR994544.1
	Xanthomonas euvesicatoria strain LMG930	CP018467.1
	Xanthomonas fragariae isolate Fap21	CP016830.1

	Xanthomonas fragariae isolate Fap29	CP016833.1
	Xanthomonas fragariae strain NBC2815	LT853880.1
	Xanthomonas fragariae strain PD885	LT853882.1
	Xanthomonas fragariae strain PD5205	LT853885.1
	Xanthomonas fuscans subsp. *fragariae* strain 1566	CP012002.1
	Xanthomonas fuscans subsp. *fragariae* strain FDC 1559	CP011160.1
	Xanthomonas fuscans subsp. *fragariae* strain FDC 1561	CP011250.1
	Xanthomonas fuscans subsp. *fragariae* strain FDC 1609	CP011163.1
	Xanthomonas fuscans subsp. *fuscans* str. 4834-R	FO681494.1
	Xanthomonas gardneri strain CFBP 8129	LR828253.1
	Xanthomonas hortorum pv. *taraxaci* strain NCPPB 940	LR828264.1

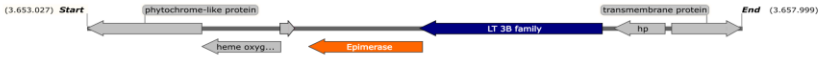
(3.653.027) Start
phytochrome-like protein
transmembrane protein
End (3.657.999)
LT 3B family
hp
heme oxyg...
Epimerase

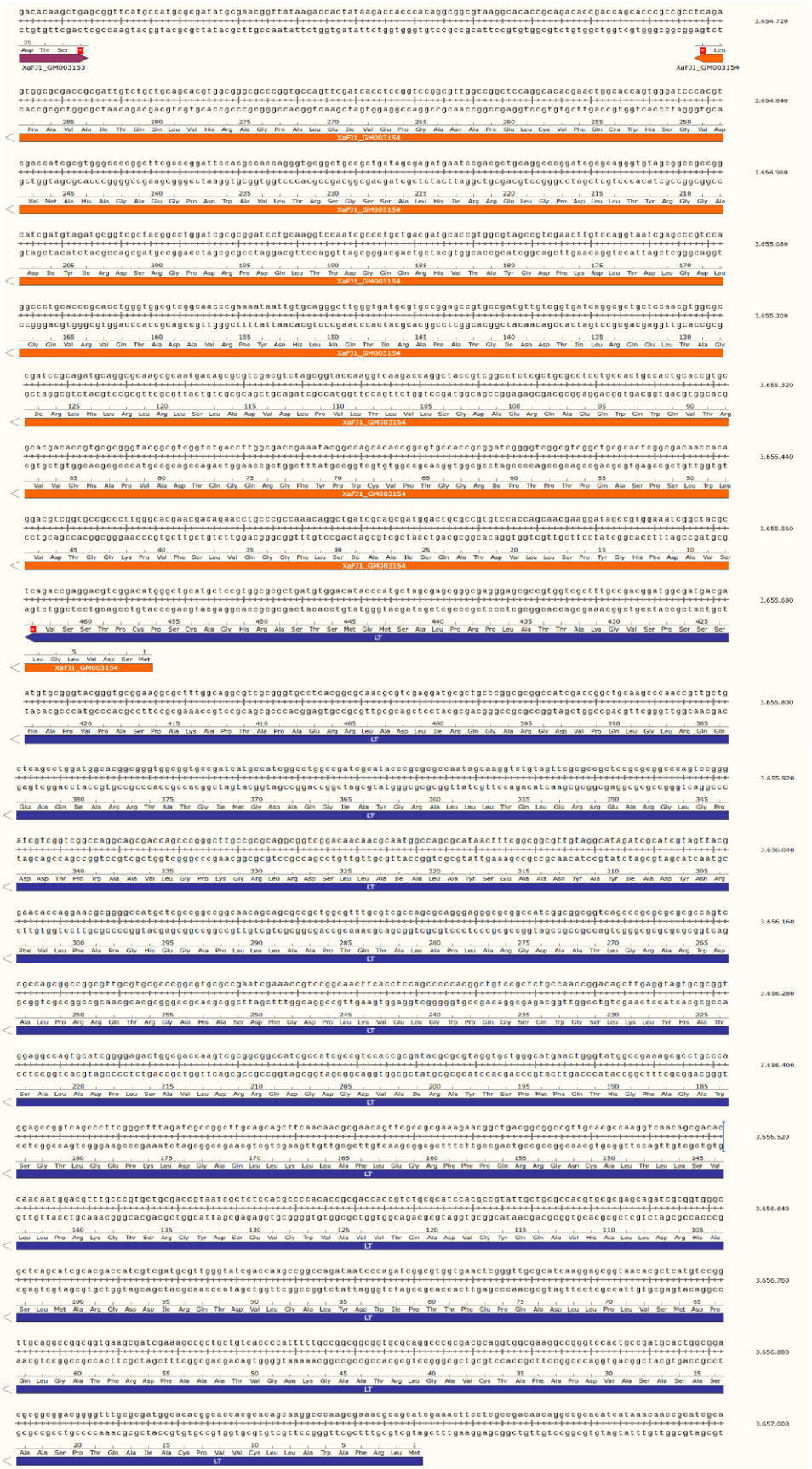
XaFJ1_GM003153
XaFJ1_GM003154
XaFJ1_GM003154
XaFJ1_GM003154
XaFJ1_GM003154
XaFJ1_GM003154
XaFJ1_GM003154
XaFJ1_GM003154
XaFJ1_GM003154
LT
LT
LT
LT
LT
LT
LT
LT
LT
LT

Figure S1. Comparative analyses of XAC4296 gene nucleotide structure and domains localization against the *Xanthomonas albilineans* strain Xa-FJ1 and GPE PC73 respective locus, showing the presence of the Epimerase and LT 3B as separated but overlapping genes.

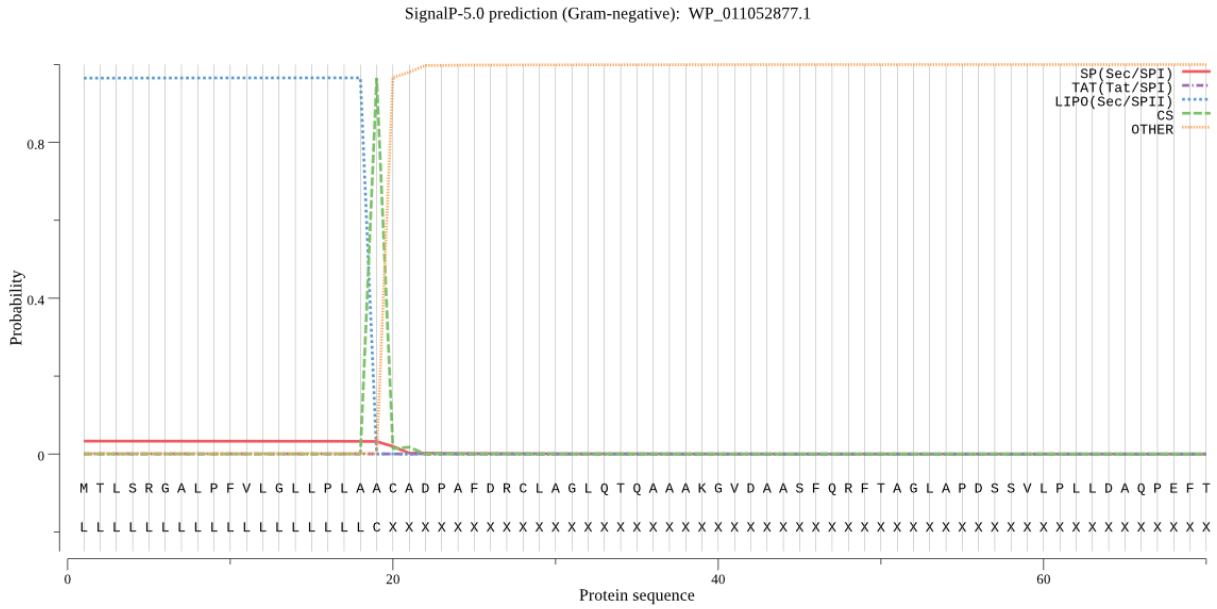

Figure S2. Predicted signal peptide for XAC4296 from *Xanthomonas citri*. The analysis was performed using the SignalP 5.0 Server (Armenteros et al., 2019).

microorganisms

MDPI

Article

XAC4296 is a multi-functional and exclusive *Xanthomonadaceae* gene containing a fusion of Lytic Transglycosylase and Epimerase domains

Amanda C. P. de Oliveira[1,3], Rafael M. Ferreira[2,3], Maria Inês T. Ferro[3], Jesus A. Ferro[3], Caio Zamuner[4], Henrique Ferreira[4] and Alessandro M. Varani[3]

1 Graduate Program in Agricultural and Livestock Microbiology, School of Agricultural and Veterinary Sciences, São Paulo State University (UNESP), Jaboticabal, SP, Brazil.
2 Graduate Program in Genetics and Plant Breeding, School of Agricultural and Veterinary Sciences, São Paulo State University (UNESP), Jaboticabal, SP, Brazil.
3 Department of Agricultural and Environmental Biotechnology, School of Agricultural and Veterinary Sciences, São Paulo State University (UNESP), Jaboticabal, SP, Brazil.
4 Department of General and Applied Biology, Institute of Biosciences, São Paulo State University (UNESP), Rio Claro, SP, Brazil.
* Correspondence: alessandro.varani@unesp.br

Abstract: Microorganisms have a limited and highly adaptable repertoire of genes capable of encoding proteins containing a single or variable multi-domains. The phytopathogenic bacteria *Xanthomonas citri* subsp. *citri* (*X. citri*) (*Xanthomonadaceae* family), the etiological agent of Citrus Canker (CC), presents a collection of multi-domain and multi-functional enzymes (MFEs) that remains to be explored. Recent studies have shown that multi-domain proteins belonging to the Lytic Transglycosylases (LTs) superfamily play an essential role in *X. citri* biology. One of these LTs, named XAC4296, apart from the Transglycosylase SLT_2 and Peptidoglycan binding-like domains, contains an unexpected aldose 1-epimerase domain linked to the central metabolism; therefore, resembling a canonical MFE. In this work, we experimentally characterized XAC4296 revealing its role as an MFE, demonstrating their probable gene fusion origin and evolutionary history. XAC4296 is expressed during plant-pathogen interaction, and the Δ4296 mutant shows an impact on CC progression. Moreover, Δ4296 exhibited chromosome segregation and cell division errors, and sensitivity to ampicillin, suggesting not only LT activity but also that XAC4296 may also contribute to resistance to β-lactams. However, both Δ4296 phenotypes can be restored when the mutant is supplemented with sucrose or glutamic acid as a carbon and nitrogen source, supporting the epimerase domain's functional relationship with the central carbon and cell wall metabolism. Taken together, these results elucidate the role of XAC4296 as an MFE in *X. citri*, also bringing new insights into the evolution of multi-domain proteins and antimicrobial resistance in the *Xanthomonadaceae* family.

Keywords: Citrus Canker; multi-domains enzymes; gene fusion; cell wall synthesis; antimicrobial resistance; and *Xanthomonas citri*

Citation: XAC4296 is a multi-functional and exclusive *Xanthomonadaceae* gene containing a fusion of Lytic Transglycosylase and Epimerase domains. *Microorganisms* **2022**, *9*, x. https://doi.org/10.3390/xxxxx

Academic Editor(s):

Received: date
Accepted: date
Published: date

1. Introduction

Many Gram-negative phytopathogens relevant to agriculture belong to the *Xanthomonadaceae* family (An et al., 2019). A critical species in this group is the *Xanthomonas citri* subsp. *citri* (*X. citri*), the causal agent of citrus canker (CC) (Rodriguez-R et al., 2012). The CC is a severe disease that affects citrus crops and decreases fruit production, leading to economic losses (Gottwald et al., 2002). Many efforts to understand CC mechanisms were made since the disease was discovered in the early 1900s (Boch and Bonas, 2010). One of the hallmarks that led to several new insights into the plant-pathogen interactions was the analyses of the *X. citri* genome, revealing the genetic basis of bacterial pathogenicity (Ryan et al., 2011). Since then, most studies have been focused on *Xanthomonas* pathogenicity mechanisms, such as regulation and secretion of virulence factors, such as the

Type 3 Secretion System (Büttner and Bonas, 2010; Ryan et al., 2011). Moreover, genetics studies were also conducted to understand chromosome segregation and cell division mechanism, aiming to better understand this phytopathogen's cellular biology (Lacerda et al., 2017; Ucci et al., 2014). However, other possible genetic mechanisms related to *X. citri* pathogenicity remain unknown. For instance, multi-domain and multi-functional enzymes (MFEs) are essential for bacterial cellular biology, virulence, and fitness.

The MFEs are ubiquitous in prokaryotes (Sriram et al., 2005). These proteins generally harbor more than one domain, each exhibiting distinct functions (Hult and Berglund, 2007). Therefore, the MFEs may simultaneously perform multiple physiologically biochemical or biophysical tasks in the cell (Moore, 2004; Vogel et al., 2004). These numerous functionalities might provide evolutionary advantages for the bacterium (Aharoni et al., 2005). For instance, combining multiple functions enables the enzyme to catalyze different steps of a single metabolic pathway (Jeffery, 2003). In addition, the MFEs can be considered a clever strategy for generating complexity from existing proteins without expanding the genome (Aharoni et al., 2005).

Besides MFEs, one interesting class of enzymes has gained attention by their relation to bacterial fitness and virulence. These are the Lytic Transglycosylases (LTs) related to peptidoglycan biosynthesis and recycling and cell-wall-antibiotic detection, also showing involvement with the bacterium septum division allowing cell separation and insertion of protein complexes like secretion systems, flagella, and pili (Alcorlo et al., 2017; Dik et al., 2017; Höltje, 1995; Koraimann, 2003; Scheurwater et al., 2008; Scheurwater and Burrows, 2011; Uehara and Park, 2008). Due to these features, LTs may also play a relevant role in the pathogenesis of many bacterial species, such as *Neisseria gonorrhoeae* (Rodriguez-R et al., 2012) and *Burkholderia pseudomallei* (Jenkins et al., 2019).

Recently, we described the LT's arsenal present in the *X. citri* genome (16 LTs from different families) (Oliveira et al., 2018). Among those, we functionally revealed that two LTs from the 3B family: MltB2.1 and MltB2.2, are directly implicated in *X. citri fitness* (Oliveira et al., 2018). We also identified another 3B-like LT, named as XAC4296 (NCBI locus_tag: XAC_RS21660). Notably, apart from the Transglycosylase SLT 2 (IPR031304) and Peptidoglycan binding-like (IPR002477) domains, XAC4296 contains an additional and unexpected aldose 1-epimerase domain (IPR015443) linked to carbohydrate metabolism, and potentially showing involvement with the bacterial cell wall metabolism and biosynthesis of a variety of cell surface polysaccharides (Sala et al., 1996). Interestingly, the XAC4296 gene was previously identified exclusively in the *Xanthomonas* genus (Oliveira et al., 2018). Moreover, *in silico* analyses revealed that XAC4296 appears to have been formed by a previous gene fusion event, originated by two independent genes (a 3B family LT and D-hexose-6-phosphate mutarotase gene), commonly separated in distinct loci in other non-*Xanthomonas* species (Oliveira et al., 2018). Therefore, XAC4296 resembles a canonical MFE, showing a multi-domain architecture.

In this work, we performed an *in silico,* fluorescence microscopy and pathogenicity assays to investigate the evolution and role of XAC4296 as a putative MFE. We also evaluated XAC4296 as a potential *X. citri* virulence and pathogenicity factor. Our results indicate that XAC4296 functions resemble a typical LT, mainly related to peptidoglycan biosynthesis. We also unveiled an additional role related to carbohydrate metabolism, compatible with epimerase domain's role, and chromosome segregation during cell division. Taken together, these results demonstrate that XAC4296 behaves like a classic MFE, showing at least two unrelated and mechanistically different roles, both impacting *X. citri fitness*: a primary role related to enzymatic catalysis and a secondary role related to cell structural function.

2. Material and Methods

2.1. *In silico and phylogenetic analysis*

Global comparisons were made based on sequenced *Xanthomonadaceae* genomes deposited in the National Center for Biotechnology Information (NCBI) repository. For XAC4296 homolog detection, we used as tblastn (Altschul et al., 1997) parameters a query coverage and identity >90% and >60%, respectively, and including all three characteristics domains (Table S1 show a complete list of genomes carrying XAC4296 homolog).

The XAC4296 three-dimensional structure was analyzed in two modules, the first considering the 420 amino acids located in the N-terminus of the protein, containing the SLT_2 (IPR031304) and PG_Binding 1 (IPR002477) domains, corresponding to the Lytic Transglycosylases from 3B family; the second module considering the last 309 amino acids located at the C-Terminus of the XAC4296 and corresponding to the D-hexose-6-phosphate mutarotase annotated gene, containing the aldose-1-epimerase domain (IPR015443). Molecular modeling was performed with the Robetta webserver (Kim et al., 2004). The Chimera Tool (Pettersen et al., 2004) was used to generate the three-dimensional structures and interactive visualization of the entire XAC4296 protein. The three-dimensional structures of the PDB (Protein Data Bank) used as models for the LT and epimerase modules were, respectively, 5AO8 and 2HTA. These proteins were selected according to the ranking established by the alignment performed by software MAFFT 7,309 (Katoh and Standley, 2013). The stereochemical quality of the generated models was evaluated by analyzing Ramachandran's plot, carried out by Chimera Tool.

The XAC4296 homolog sequences were aligned with MAFFT 7.309 (Katoh and Standley, 2013), and their best-fit evolutionary models were predicted with ProTest 3.2.4. A maximum-likelihood tree was reconstructed with RaxML 8.2.9 using a bootstrap value of 1000. The final tree was visualized in FigTree 1.4.4 (http://tree.bio.ed.ac.uk/software/figtree) and edited with Inkscape 0.92.4 (http://www.inkscape.org). The Integrated Microbial Genomes & Microbiomes (IMG/M) system (Markowitz et al., 2012) was used for comparative analyses.

2.2. Strains and growth conditions

Bacterial strains and plasmid strains used in this study are shown in Table S2. The *X. citri* strains were grown in three different culture media: nutrient broth (NB: 0.5% peptone, 0.3% beef extract), nutrient agar (NA: 0.5% peptone, 0.3% beef extract, 0.15% agar) supplemented with L-arabinose (0.05% w/v) and sucrose (5% w/v) when required or, XVM2 (20 mM NaCl, 10 mM (NH4)2SO4, 5 mM MgSO4, 1 mM CaCl2, 0.16 mM KH2PO4, 0.32 mM K2HPO4, 0.01 mM FeSO4, 10 mM fructose, 10 mM sucrose, 0.03% casaminoacids, pH 6.7) at 29ºC. *Escherichia coli* strains were cultivated in Luria-Bertani medium (LB: 1% tryptone, 0.5% yeast extract, 0.10 % NaCl, 0.15% agar; pH 7) and SOB media (Sambrook et al., 1989) at 37°C. Antibiotics were used as needed at the following concentrations: kanamycin (Kn), 30 μg/mL; carbenicillin (Carb), 50 μg/ml; streptomycin (Str), 50 μg/ml; gentamycin (Gen), 10 μg/mL; ampicillin (Amp), 100 μg/mL.

2.3. RNA extraction and cDNA synthesis from XAC4296

X. citri total RNA was extracted using RNeasy protect bacteria Mini kit (Qiagen) according to the manufacturer. The first strand of complementary DNA was synthesized from 1μg of total RNA using a qScript® cDNA SuperMix (Qiagen). Before cDNA synthesis, RNA samples were treated with DNaseI. The DNA and RNA quantification was performed using Qubit HS (High Sensitivity) (Thermo Fisher). Primers F4296 (F) and pMAJIIc (R) were used for PCR reaction using cDNA as template (Table S3). PCR products were checked by agarose gel electrophoresis.

2.4. Mutant construction

Mutant of gene XAC4296 was generated using homologous suicide plasmid (pNPTS138) (Bueno et al., 2021) integration through site-directed mutagenesis by PCR overlap extension approach (Lee et al., 2004). To construct the deletion mutant of XAC4296

ORF, we used *X. citri* genomic DNA as a template and primers described in Table S3. The first PCR amplifications were made separately using pairs of primers A(F)-B(R) and C(F)-D(R) and Phusion high fidelity DNA polymerase (Thermo Fischer Scientific) to generate the products A-B and C-D, with self-complementary tails. The second PCR was performed using primers A(F)-D(R) and the products A-B and C-D as template to obtain the A-D fragment, in which the XAC4296 sequence was deleted. The final PCR product A-D, and pNPTS138 suicide vector were double digested with *Nhe*I/*Hind*III enzymes (New England BioLabs inc®), and the ligation between vector and fragments was performed with T4 DNA Ligase (New England BioLabs inc®) according to the manufacturer's instructions. The recombinant vector Δ4296-pNPTS138 was transformed into chemically competent *E. coli* DH10B (Sambrook et al., 1989), and transformant colonies were selected using antibiotics and Lac-Z promoter. The constructions were checked by agarose gel electrophoresis and sequencing on a 3730xI DNA analyzer (Thermo Fisher Scientific) using primers A-D. Finally, the Δ4296-pNPTS138 recombinant plasmid was used for *X. citri* electroporation (Amaral et al., 2005), and colonies were selected by kanamycin resistance and sucrose susceptibility (Kaniga et al., 1991). Mutant Δ4296 was confirmed by sequencing.

The XAC4296 ORF was PCR amplified from *X. citri* genomic DNA using primers pMAJIIc (F)-pMAJIIc (R) (Table S3) and Phusion high fidelity DNA polymerase (Thermo Fisher Scientific). The PCR product and the integrative vector pMAJIIc (Pena et al., 2020) were double digested with *Nhe*I/*Xho*I enzymes (New England BioLabs inc®) and ligated with T4 DNA Ligase (New England BioLabs inc®), according to manufacturer's instructions. The recombinant vector 4296-pMAJIIc was transformed into chemically competent *E. coli* DH10B (Sambrook et al., 1989). Colonies were selected using kanamycin resistance. The recombinant plasmid DNA (pMAJIIc-XAC4296) was purified using Promega Wizard®Plus SV Minipreps DNA Purification System kit according to the manufacturer's instructions and the inserted XAC4296 DNA sequence was confirmed by sequencing. The recombinant plasmid was used to transform both mutant strain 4296 and *X. citri* wild type strain by electroporation (Amaral et al., 2005). Colonies were selected by kanamycin resistance and the integrative vector version was identified on NA plates supplemented with 0.2% soluble starch followed by iodine vapor crystals exposure (Pena et al., 2020). The strain Δ4296-pMAJIIc-4296 (named Δ4296c) was used as complemented strain in the following assays and the recombinant strain XccA-pMAJIIc-4296 was used for protein subcellular localization. The constructions were checked by agarose gel electrophoresis and DNA sequencing.

2.5. Pathogenicity assay

We used two methods for pathogenicity assays. In the first method, bacterial strains were inoculated into the leaves' surface only by spray (Li and Wang, 2011). *X. citri* and mutant Δ4296 were cultivated in NB medium for 16 hours to O.D. 600-nm ~0.8 and diluted in fresh NB medium to O.D. 600nm of 0.3. Cells were collected by centrifugation and resuspended in autoclaved tap water to an O.D. 600 nm of 0.3, equivalent to 10^8 CFU/mL. Three different "Pêra Rio" orange (*Citrus sinensis* L. Osbeck) plants were sprayed with each bacterial suspension until all leaves were thoroughly coated, then covered with a clear plastic bag for 24 h. After 25 days of inoculation (DAI), all leaves were quantified, and those presenting citrus canker (CC) symptoms were photographed, and the CC lesions were counted and the results analyzed and compared.

For pathogenicity assays by infiltration method, strains of *X. citri* and mutant Δ4296 were cultivated in NB medium for 16 hours to O.D. 600nm ~0.8 and diluted in fresh NB medium to O.D. 600nm of 0.3. Cells were collected by centrifugation and resuspended in autoclaved tap water to an O.D. 600 nm of 0.3, equivalent to 10^8 CFU/mL. This inoculum was diluted 100-fold (10^6 CFU/mL) and infiltrated on the abaxial surface of three young leaves (technical replicates) in three different plants (biological replicates) of "Pera Rio" orange (*C. sinensis* L. Osbeck) using 1 mL needleless hypodermic syringes (Laia et al.,

2009). Symptoms were observed for 25 days, and photos were taken at 4, 8, 12, 15, and 21 days after inoculation (DAI) (Laia et al., 2009).

Inoculated plants were kept in a high-efficiency particulate air (HEPA) filtered plant laboratory with controlled environmental conditions (28–30 °C, 55% humidity, 12 hours light cycle).

2.6. *Ex vivo growth curves*

X. citri and Δ4296 mutant were cultivated in NB medium for 16 hours and diluted in fresh NB medium to O.D. 600-nm of ~0.1. Cell cultures were distributed on 96 well plates and were incubated in a Synergy H1N1 microplate reader (BioTek®, Winooski, VT, USA) under constant agitation at 29 °C, and automated O.D. readings were taken every 30 min. Using GraphPad Prism 6 software, growth curves were generated based on three technical and three biological replicates (Lacerda et al., 2017).

2.7. *In planta growth curves*

X. citri and Δ4296 mutant were cultivated in NB medium for 16 hours until O.D. 600nm got around 0.8 and diluted in fresh NB medium to O.D. 600nm of 0.3. Cells were collected by centrifugation and resuspended in Falcon tubes containing 50 mL of autoclaved tap water to an O.D. 600 nm of 0.3, equivalent to 10^8 CFU/mL. This inoculum was diluted 100-fold (10^6 CFU/mL) and infiltrated on the abaxial surface of fifteen young leaves in four different plants (biological replicates) of "Pera Rio" orange (*C. sinensis* L. Osbeck) using 1 ML needleless hypodermic syringes. The strains were exuded from leaves at days 0, 1, 3, 6, and 10 DAI, and the number of cells per leave was achieved using the microculture strategy (Laia et al., 2009).

2.8. Microscopy

X. citri, Δ4296 mutant, and Δ4296c strains were cultivated in NB media until O.D. 600-nm reached around 0.3 ABS at 29 ºC. We performed analysis in different conditions: with ampicillin (20 μg/mL), sucrose 2% (w/v) and glutamic acid 2% (wv). For morphological analysis, strains were collected by centrifugation, and cells were resuspended in 0,85% NaCl. We used 4',6-diamidino-2-phenylindole DAPI staining at a final concentration of 0,01% to visualize chromosome organization. Cultures were treated with propidium iodide (IP) for cell viability investigations at a 0.001 mg/mL final concentration. Cells were immobilized in agarose-covered slides for microscope observation (Martins et al., 2010). We performed the assays three times and quantified cells individually (n=800). Following treatments, cells were immediately visualized using an Olympus BX61 microscope equipped with a monochromatic camera OrcaFlash 2.8 (Hamamatsu, Japan). The software CellSens Version 11 (Olympus) was used for data collection and analysis.

2.9. Data Analysis

All results obtained were submitted to Welch's ANOVA test - 0.05 using GraphPad Prism 8.0.1. Graphics were generated using Microsoft Office Excel for Windows.

3. **Results**

3.1. XAC4296 is conserved in Xanthomonas, Pseudoxanthomonas, and Stenotrophomonas, showing two distinct and independent domains modules

We first analyzed the XAC4296 gene (2,163 bp) using molecular modeling approaches. The Robetta software failed to generate a unique 3D structure corresponding to the complete protein containing LT and epimerase domains. Therefore, to understand the XAC4296 (720 aa) structure, both domains were modeled separately. While the LT located on the N-terminus of XAC4296, containing the SLT_2 and PG_Binding 1 domains were modeled based on a sequence of 408 amino acids, the XAC4296 C-terminus, having the

epimerase bearing the aldose-1-epimerase domain, was modeled based on 312 amino acids sequence (Figure 1A and 1B).

The first module resembles a classic 3B LT showing the 3D structure composed mainly by alpha-helices (Figure 1 C). In contrast, the second module shows mainly beta-sheets, exhibiting high identity to other well-characterized D-hexose-6-phosphate mutarotase (Figure 1 C). Therefore, it is presumed that the aldose 1-epimerase domain might perform the epimerization by ring-opening or mutarotation (Allard et al., 2001). The confidence value for both models was 0.86 and 0.81, respectively, supporting a reasonable quality of both 3D structure predictions. Taken together, these findings suggest that XAC4296 may have two completely independent domains that might preserve the transglycosylase and epimerase activities separately.

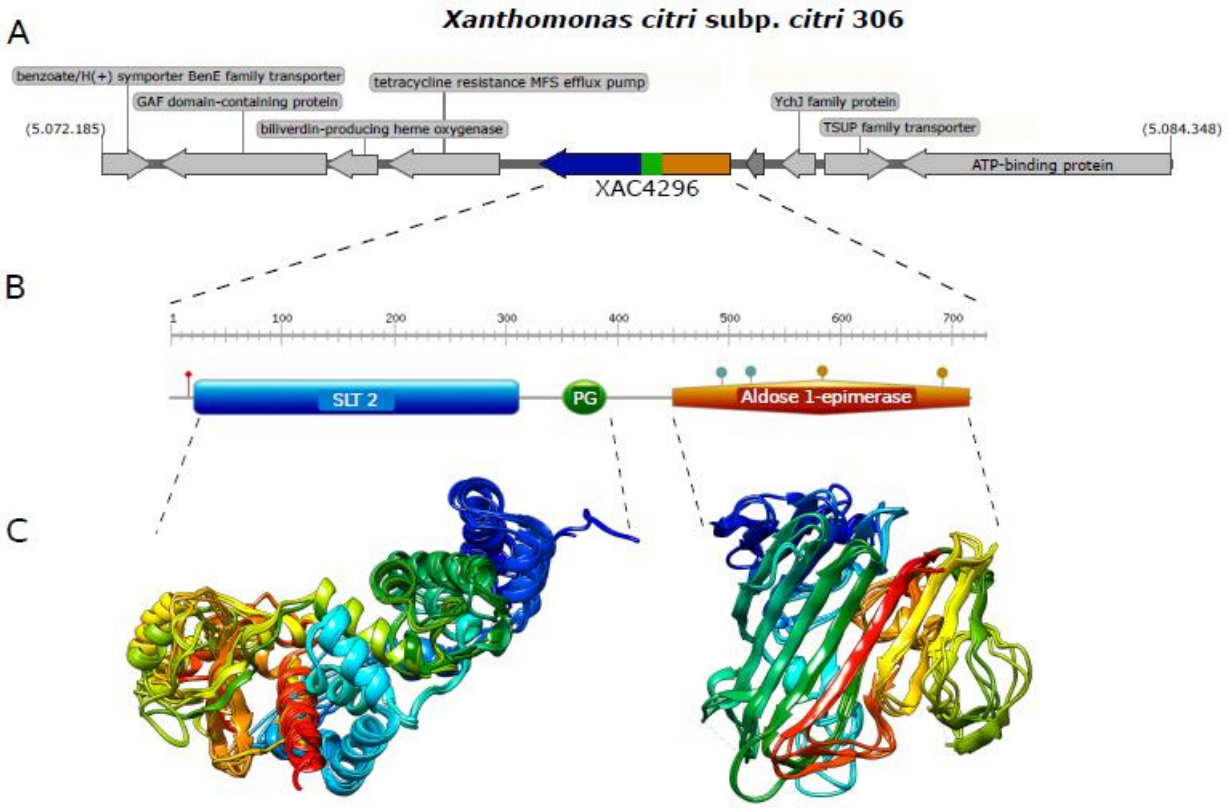

Figure 1. Genome context, protein domain, and structure of XAC4296. **A.** Genome context of XAC4296 from X. citri genome. **B.** Protein domain and structure of XAC4296. XAC4296 has 720 aa with the LT domain associated with 3B family: Transglycosylase SLT domain (SLT_2) (IPR031304.) and Peptidoglycan binding (PG_binding_1) (IPR002477) domains, and the Aldose 1-epimerase (IPR015443) domain. **C.** Molecular modeling cartoon representation of the LT and epimerase XAC4296 domains.

We also investigated the origin and evolution of XAC4296, revealing that apart from different species from *Xanthomonas*, this gene can also be found in different members from the *Xanthomonadaceae family*, such as *Pseudoxanthomonas* and *Stenotrophomonas*, accounting for at least 308 complete sequenced genomes available in the GenBank database (Figure 2 A, and Table S1). Moreover, considering these three genera, the XAC4296 homologs are generally located in a conserved genomic context (Figure S1) and are not associated with common mobile genetic elements, such as prophages, Insertion Sequences, Transposons, Integrons and Genomic Islands. Therefore, strongly supporting that the XAC4296 origin is not associated to common lateral gene transfer mechanisms. It is noteworthy to mention that the XAC4296 homolog is not present in the *Xanthomonas albilineans* and in the phylogenetically closely-related *Xylella* genus (Figure 2 A). *Xylella* carries an independent

epimerase gene (i.e. WP_010894718.1) and a least 4 LTs genes, all located at distant genomic loci. Conversely, in addition to an aldose 1-epimerase domain containing gene (i.e. XALC_0947 and XaFJ1_GM000925), the *X. albilineans* species (e.g. GPE PC73 and Xa-FJ1 strains), also carries the two modules (LT and Epimerase) as separated and overlapping genes (21 nt of overlapping), each gene showing the domains modules in different frames, and resembling a degenerated XAC4296 homolog (Figure S2). Moreover, the other *Xanthomonas* species, *Pseudoxanthomonas* and *Stenotrophomonas* carry their own set of LTs (varying in number and diversity of families); however, the aldose-1-epimerase domain is exclusive for each XAC4296 homolog, and thus, do not exist as an alone or duplicated feature, such as D-hexose-6-phosphate mutarotase gene in these genomes, as observed in *Xylella* and *X. albilineans*.

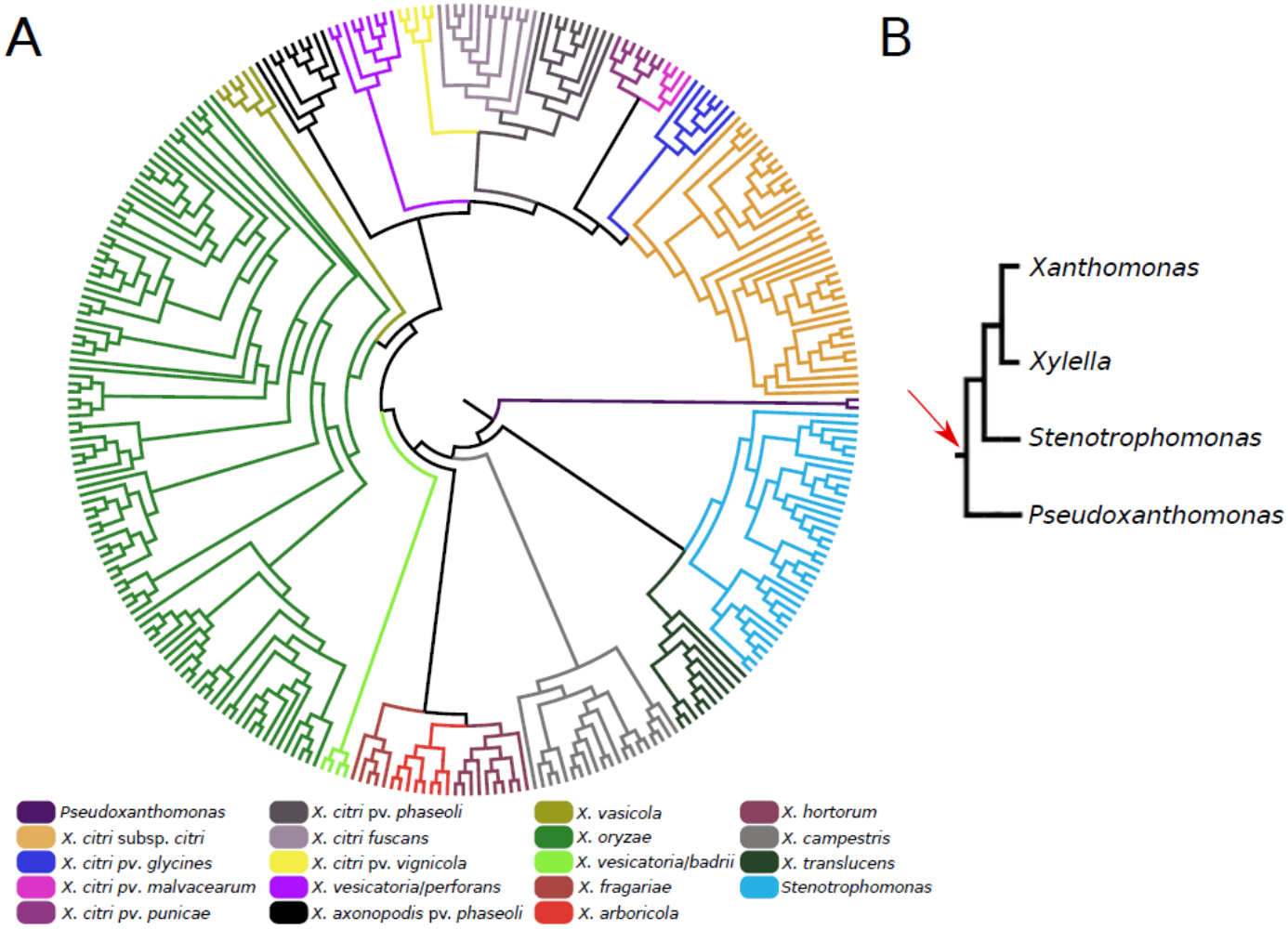

***Figure* 2. A.** Maximum-likelihood phylogenetic tree of XAC4296 homologs across Xanthomonadaceae family supports the XAC4296 potential origin before Xanthomonas, Xylella, Pseudoxanthomonas and Stenotrophomonas differentiation. The closely-related Xylella genus lost the XAC4296 homolog. **B.** Phylogenetic construction of the Xanthomonadaceae family phylogroup formed by Xanthomonas, Xylella, Pseudoxanthomonas and Stenotrophomonas (based on (Bansal et al., 2021). The red arrow indicates the potential gene fusion event that originated the XAC4296 ancestor. .

3.2. X. citri expresses XAC4296 in Citrus sinensis L. Osbeck, and Δ4296 mutant does not affect bacterial growth but impacts the CC progression

We further investigated the role of XAC4296 on *Xanthomonas citri* virulence and pathogenicity. To confirm the XAC4296 expression during plant-pathogen interaction, *Citrus sinensis* L. Osbeck (considered a moderately resistant host) was inoculated with *X. citri*,

and the pathogen was exuded five days after inoculation. The synthesis of double-stranded cDNA from total RNA was performed and used as a template for PCR reaction. The fragment with approximately 2,200 pb was obtained, indicating that XAC4296 is entirely expressed during plant-pathogen interaction (Figure S3).

Furthermore, the XAC4296 gene was deleted by site-directed mutagenesis to generate mutant *X. citri* Δ4296, and the integrative plasmid pMAJIIc (Pena et al., 2020) was employed to construct the complemented strain Δ4296c. Different bacterial inoculation methods (spray and infiltration methods) (Table 1 and Figure S4) and growth curves analyses (Figure S5) indicated that the wild-type and mutant exhibited a similar growth pattern; however, pointing that XAC4296 can be related to CC symptoms enhancement in different hosts (e.g., *Citrus latifolia* Tan, *Citrus sinensis*, and *Citrus reticulata*) considering only the spray method.

Table 1. Citrus canker quantification of "Pera Rio" orange leaves (Citrus sinensis L. Osbeck) by spray method. Strains were inoculated in a total of 65 leaves. The number of lesions was quantified in the abaxial surface of the leaves.

Strain	Number of leaves with CC lesions	Number of leaves without CC lesions	Total CC lesions	Average of CC lesions per leaf
X. citri	19	46	884[a]	46,52[a]
Δ4296	24	41	395[b]	19,42[b]

According to the Tukey test, different letters mean significant differences – p = 0.05.

3.3Δ4296. cells displayed abnormal nucleoid distribution, chains, and short filaments

To evaluate the potential role of the XAC4296 LT domain with bacterial *peptidoglycan* metabolism, the cell morphology and the chromosome organization of wild-type *X. citri* and the Δ4296 mutant were investigated using DAPI-staining (Figure 3, Table 2). The wild-type *X. citri* displays an average cell length of approximately 1,44 ± 0.31 μm (Ucci et al., 2014). Moreover, in standard growth conditions, *X. citri* exhibits a bilobed nucleoid centrally located in a single compartment (newborn or not-dividing rods) (Figure 3A), or evenly distributed, one per cell half, when division constriction is present.

Different from the wild type, the Δ4296 mutant formed chains and sometimes a phenotype resembling short filaments, accompanied by irregular distribution of the chromosomal mass (Figure 3B, white arrows). The proportions of short filaments and chains measured in a given mutant culture were 30,6% and 15%, respectively (Table 3). Close inspection of the chains with clear septal constrictions (red arrows in Figure 3) showed no apparent nucleoid bisection. However, the Δ4296 mutant seems perfectly competent in chromosome segregation because many cells in a culture display normal nucleoid distribution (Figure 3B). However, it seems that in successive cellular cycles, errors in late cell division lead to the accumulation of chromosomal mass generated by subsequent events of replication. The short filaments morphotype that happened nearly twice as much as the chains could be caused by triggering the division error in an early stage of the cell cycle or converting chains into short filaments. At the moment, we cannot pinpoint which of these options is taking place. Finally, complementation of *X. citri* Δ4296 with pMAJIIc (Δ4296c) expressed from an ectopic site completely restored the wild-type phenotype (Figure 3C).

These findings suggest that the first cell error probably occurs mainly during late cell division. The filamentation seems to happen due to the cell losing the ability to form septa in successive cellular cycles.

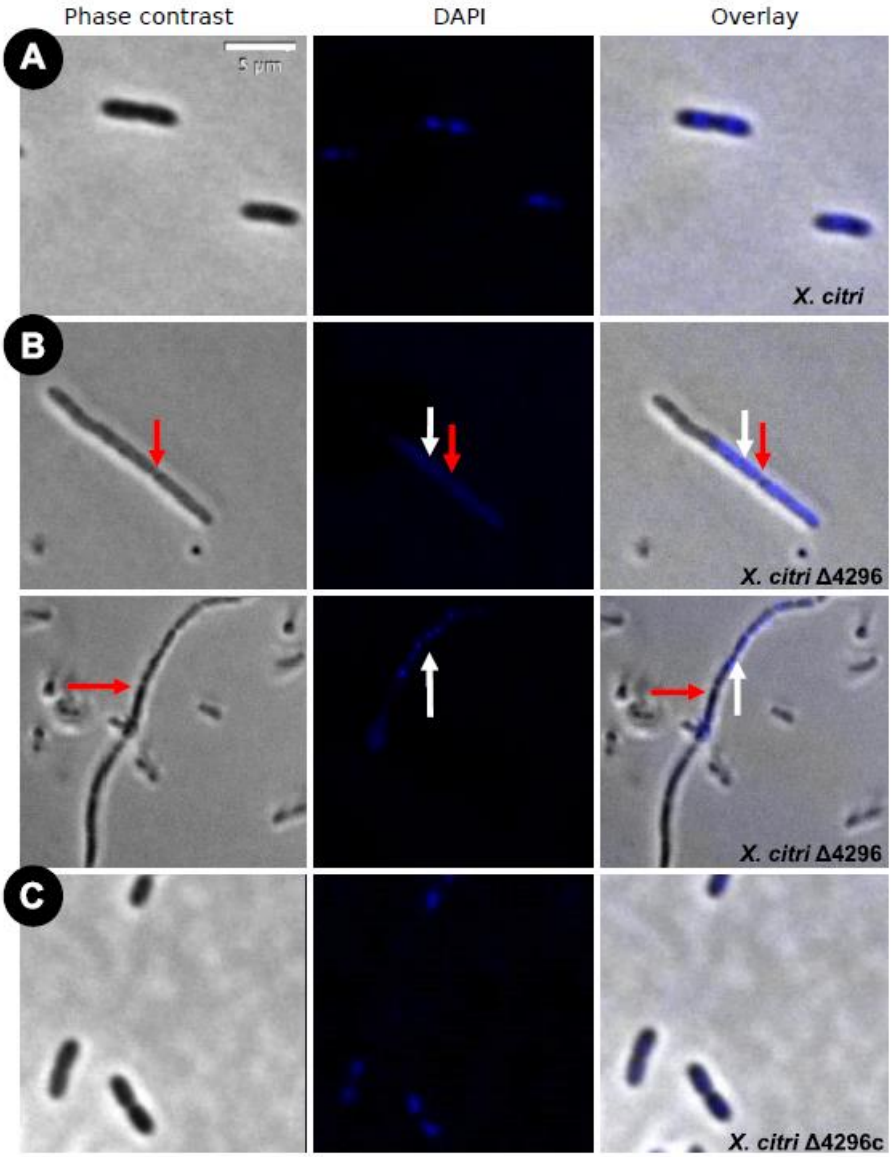

Figure 3. Morphological analysis and errors/aberrant nucleoid distribution of *X. citri*, Δ4296, and Δ4296c strains. Short filaments, chain phenotype, and errors/unusual nucleoid distribution were intensified without XAC4296. The figure shows microscopy phase contrast, DAPI, and overlay of the two filters for **A:** *X. citri* WT; **B:** Δ4296, and **C:** Δ4296c (pMAJIIc-XAC4296) (magnification of 100X). White arrows indicate nucleoid distribution; red arrows indicate septum constriction (magnification of 100X)—scale=5 µm. .

Table 3. Statistics of morphotypes and nucleoid distribution of cells cultivated in rich medium (NB).

	Short filaments %	Chain %	Nucleoid %
X. citri	0.50^{a}	0^{a}	0^{a}
Δ4296	30.625^{b}	15.75^{b}	37.125^{b}
Δ4296c	0.25^{a}	0^{a}	0.5^{a}

Total n= 800 cells measured. Data correspond to the average cell morphology—different letters mean significant difference according to Welch's ANOVA test- p =0.05.

3.4. XAC4296 is required for proper cell wall synthesis and β-lactam resistance

Considering that *X. citri* is naturally resistant to ampicillin (the XAC_RS19350/XAC3833 gene provides the resistance) (Weng et al., 2004), we evaluate the

cell morphology and the chromosome organization of wild type *X. citri* and the Δ4296 mutant in the presence of ampicillin antibiotic using DAPI-staining (Figure 4, Table 3). The Δ4296 mutant showed a significant growth delay in the presence of ampicillin, suggesting that antibiotic sensitivity is pronounced (Figure 4A). All cells of the Δ4296 cultures displayed short filaments and chains with the abnormal distribution of the nucleoids (Figure 4B, Table 3). Permeability analysis showed that membrane disruption was not detected (Figure S6, Table S4).

Table 3. Statistics of morphotypes and nucleoid distribution of cells cultivated in rich medium (NB) and ampicillin.

	Short filaments (%)	Chain (%)	Nucleoid (%)
X. citri	0^a	$0{,}25^a$	0^a
Δ4296	100^b	50^b	100^b
Δ4296c	0^a	0^a	0^a

Total n= 800 cells measured. Data correspond to the average cell morphology. According to Welch's ANOVA test, different letters mean a significant difference – 0.05.

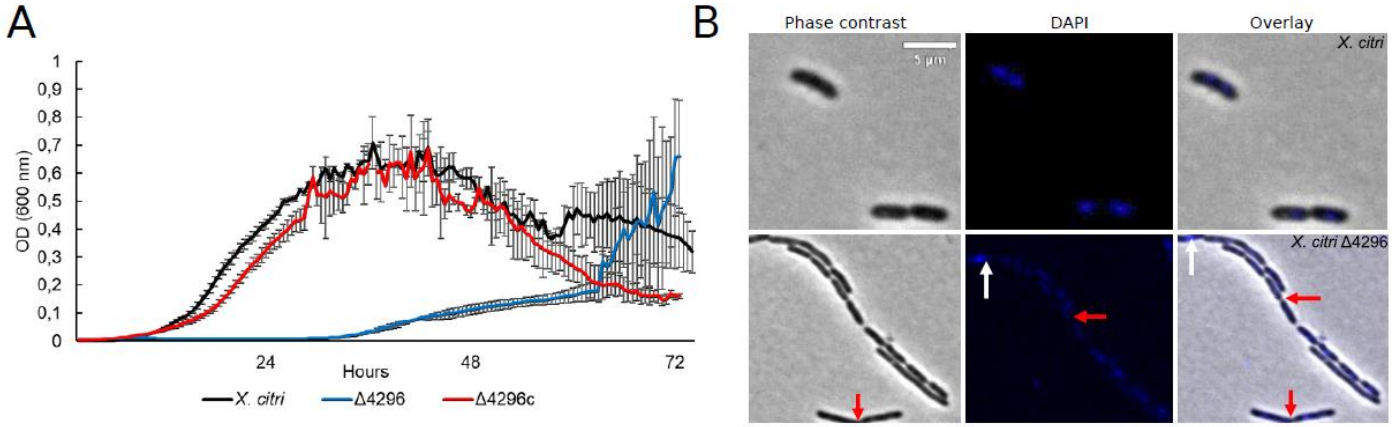

Figure 4. XAC4296 may be related to β-lactam antibiotic resistance in *X. citri* **(A)** *Ex planta* bacterial growth curves performed on rich medium and ampicillin 20 µg/mL for *X. citri*, Δ4296, and Δ4296c. Δ4296 growth is affected in the presence of ampicillin. Error bars indicate the standard error of three independent biological and technical replicates. **(B)** Morphological analysis and errors/aberrant nucleoid distribution of *X. citri*, Δ4296, and Δ4296c strains of *X. citri* and Δ4296 strains on NB supplemented with ampicillin 20 µg/mL. All cultures of mutant Δ4296 exhibit short filaments and chain phenotype. The figure shows the phase contrast, DAPI, and overlay of the two images, respectively, for *X. citri* and Δ4296 (magnification of 100X). White arrows indicate the chromosome position, and red arrows indicate septum constriction (magnification of 100X)—scale=5 µm.

3.5. XAC4296 is related to bacterial central carbon metabolism

To evaluate the potential role of the XAC4296 epimerase domain, two different carbon and nitrogen sources were used to supplement the NB medium with ampicillin. In the presence of sucrose, the Δ4296 mutant cell-shape and chromosome organization was partially restored (Figure 5, Table 4), cells still showed short filaments, chains, and unusual chromosome organization/segregation (Figure 5A and B, Table 4, Figure S7). In contrast, the addition of glutamic acid-enhanced Δ4296 growth to the point where it matches that of the wild type *X. citri* and fully reversing back to normal chromosome organization/segregation and cell division (Figure 6A and 6B, Table 4, Figure S7). Considering that: (a) D-hexose-6-phosphate mutarotase gene containing the aldose 1-epimerase domain can be related to epimerization by ring-opening or mutarotation acting in the central carbon metabolism and impacting the cell-wall metabolism, and (b) the supplementation with different carbon sources restores the Δ4296 mutant to the wild-type *X. citri* phenotype;

these results supports that XAC4296 epimerase domain might have an essential relation with the central carbon metabolism.

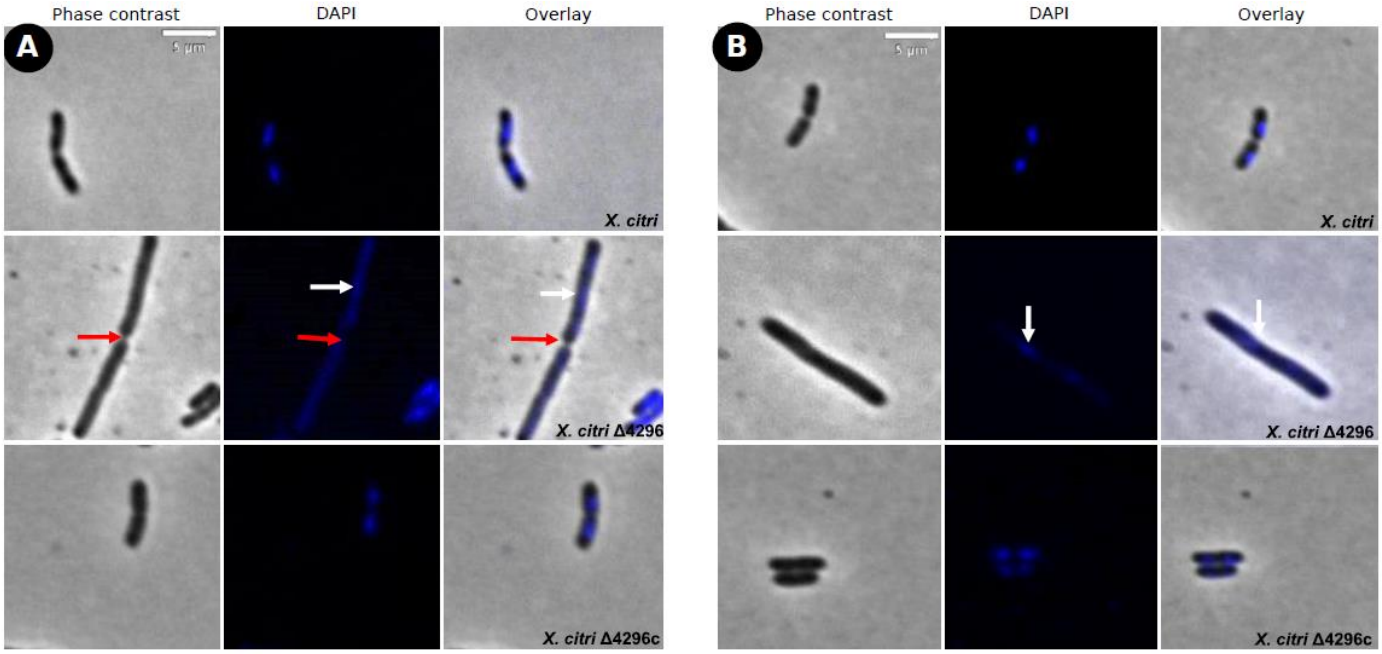

Figure 5. Short filaments and chain phenotype show partial reversion in sucrose's presence as carbon source **(A)** Morphological analysis of *X. citri*, Δ4296, and Δ4296c strains on NB supplemented with sucrose 0.1% (w/v). **(B)** NB supplemented with sucrose 0.1% (w/v) and ampicillin 20 μg/mL. The figure shows the phase contrast, DAPI, and overlay of the two filters, respectively, for *X. citri*; Δ4296 and Δ4296c. White arrows indicate the chromosome distribution, and red arrows indicate septum constriction (magnification of 100X)—scale=5 μm.

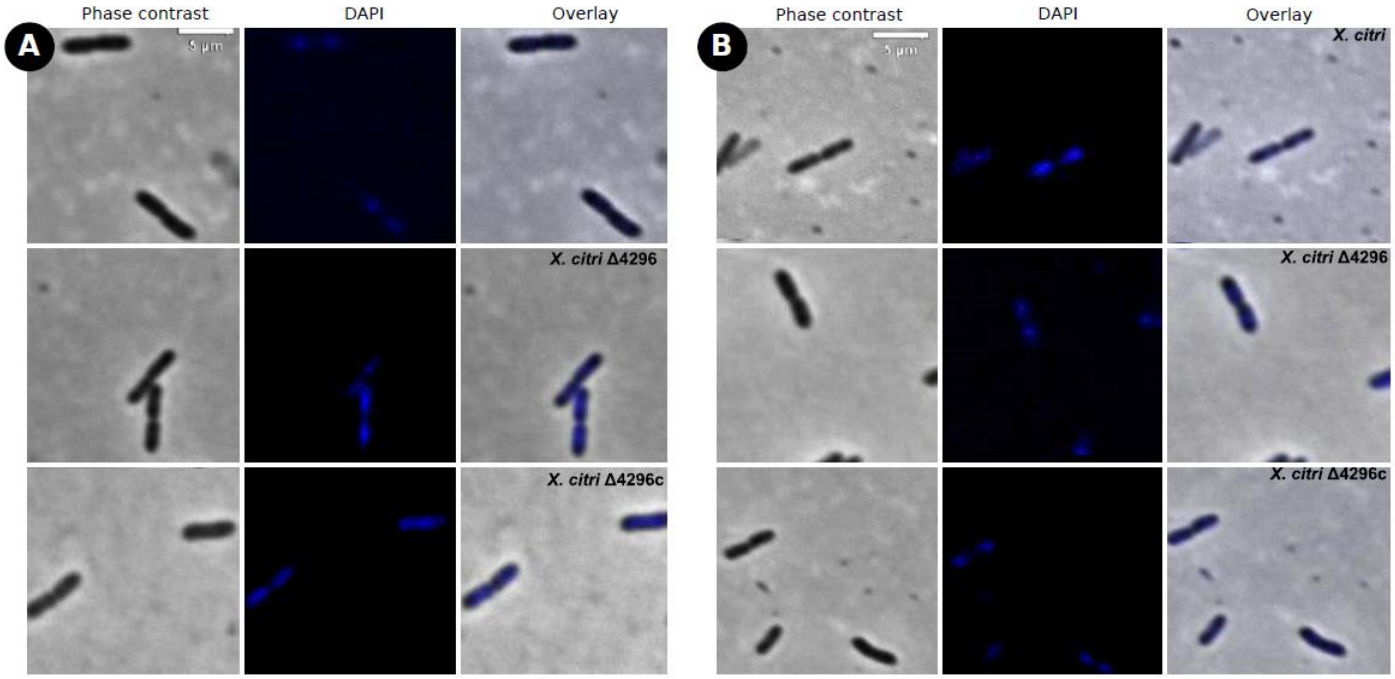

Figure 6. Short filaments, chain phenotype, and nucleoid organization show full reversion in glutamate's presence as carbon source **(A)** Morphological analysis of *X. citri*, Δ4296, and Δ4296c strains on NB supplemented with glutamic acid 0.1% (w/v). **(B)** NB supplemented with glutamic acid 0.1% (w/v) and ampicillin 20 μg/mL. The figure shows the phase contrast, DAPI, and overlay of the two filters, respectively, for *X. citri*, Δ4296 and Δ4296c (magnification of 100X) Scale=5μm.

Table 4. Short filaments, chain, and aberrant nucleoid organization phenotype were restored to normal on NB medium with sucrose or ampicillin and NB medium with glutamic acid or ampicillin.

		Short filaments (%)	Chain (%)	Nucleoid (%)
NB medium sucrose 0,1%	*X. citri*	1[a]	0,38 [a]	0 [a]
	Δ4296	1,75 [a]	0,75 [a]	0,5 [a]
	Δ4296c	0,25 [a]	0,38 [a]	0 [a]
NB medium sucrose 0,1% ampicillin 20μg/mL	*X. citri*	0,13 [a]	1,25 [a]	0,5 [a]
	Δ4296	2,25 [a]	1,88 [a]	1 [a]
	Δ4296c	0,25 [a]	0,13 [a]	0 [a]
NB medium glutamic acid 0,1%	*X. citri*	0[a]	0 [a]	0 [a]
	Δ4296	0 [a]	0 [a]	0 [a]
	Δ4296c	0 [a]	0 [a]	0 [a]
NB medium glutamic acid 0,1% ampicillin 20μg/mL	*X. citri*	0,13 [a]	0 [a]	0 [a]
	Δ4296	0 [a]	1 [a]	0 [a]
	Δ4296c	0 [a]	0 [a]	0 [a]

Total n= 800 cells measured. Data correspond to the average cell morphology — same letters meaning no significant difference according to Welch's ANOVA test- p =0.05.

4. **Discussion**

In this work, we investigate the role of the XAC4296 in *Xanthomonas citri* metabolism and virulence using *in silico* and molecular approaches. The XAC4296 protein contains two distinct modules: the first containing the SLT_2 (IPR031304) and PG_Binding1 (IPR002477) domains, homologs to LTs 3B Family. The second module contains the aldose-1-epimerase domain (IPR015443), classified as an epimerase superfamily. Proteins belonging to the LTs (Lytic Murein Transglycosylases) family cleave the polysaccharide of the peptidoglycan at the NAM-NAG glycosidic bond by intramolecular cyclization of the N-acetylmuramyl moiety to yield a 1,6-anhydro-N-acetyl-β-D-muramyl (1,6-anhydroMurNAc) product during the peptidoglycan biosynthesis (Dik et al., 2017). On the other hand, epimerases are usually involved in metabolic pathways such as inversion of D-alanine and D-glutamate for bacterial cell wall metabolism (Sala et al., 1996); biosynthesis of a variety of cell surface polysaccharides; biosynthesis of LPS and capsular sugar precursors (McNeil et al., 1990); and complex biosynthetic pathways, such as Glycolysis, Entner-Doudoroff, Leloir and others that present several chemical steps (Nowitzki et al., 1995; Teige et al., 1995). Epimerases are also involved in the oxidation, acetylation, dehydration, and carbohydrate reduction (reviewed by Allard et al., 2001). Our molecular modeling results also support that the LT and epimerase modules can act independently and may synergistically function as a canonical MFE, thus, performing multiple physiologically biochemical or biophysical functions simultaneously in the cell.

Previous studies revealed that the XAC4296 modules exist as separate and independent genes in other γ-proteobacteria (Oliveira et al., 2018). Our results indicate that XAC4296 homolog is widespread in different *Xanthomonas* species and exists in other members from the *Xanthomonadaceae* family, *such as Stenotrophomonas and Pseudoxanthomonas. It is worthy of mentioning that the Xanthomonas, Stenotrophomonas, Xylella and Pseudoxanthomonas. genus from the Xanthomonadaceae family are closely related and form a phylogroup (Bansal et al., 2021). Therefore, our results support that the* XAC4296 origin may be related with a previous gene fusion origin before or during this *phylogroup differentiation*. However, *Xylella* and *Xanthomonas albilineans* does not have the XAC4296 homolog. For instance, *Xylella* carries an independent D-hexose-6-phosphate mutarotase gene containing the aldose-1-epimerase domain and their LT gene repertoire is in a distinct genomic loci,

whereas the *X. albilineans* shows both protein modules, the LT and epimerase, homologs to XAC4296, as separated but overlapping genes, in addition to an independent D-hexose-6-phosphate mutarotase gene. It is known that the *Xylella* genus has undergone drastic genome reduction since diverging from the *Xanthomonas* genus (Firrao et al., 2021; Pieretti et al., 2009), and that *X. albilineans* has experienced significant genomic erosion, having unique genomic features in comparison to other *Xanthomonas* species (Pieretti et al., 2015). Therefore, the most parsimonious hypothesis to explain these absences of XAC4296 homologs in *Xylella* and *X. albilineans* is that while *Xylella* lost their XAC4296 homolog during the genome reduction process, but maintaining their epimerase gene alone, and their own LTs repertoire, the *X. albilineans* genome is accumulating mutations and nucleotide deletions that led to the formation of two separated genes, and thus, suggesting a current process of gene decay. Both hypothesis are based on the current knowledge that the genome reduction or erosion process is currently shaping *Xyella* and *X. albilineans* in order to adapt both pathogens to a restricted host range .

This work further evaluated XAC4296 role in *X. citri fitness*, virulence, and pathogenicity. Our results indicate that the XAC4296 gene is not essential for *X. citri* survival or *in planta* CC development but may play a role in bacterial *fitness*. Our findings also support XAC4296 direct relationship with *X. citri* pathogenicity, particularly CC progression. However, this result is not surprising since previous studies revealed a role of the LT from the 3B family with *X. citri* pathogenicity and *fitness* (Oliveira et al., 2018).

To explore the involvement of the XAC4296 LT domain with the peptidoglycan metabolism, the cell morphology was examined under the microscope using DAPI-staining. *X. citri* lacking XAC4296 formed chains related to late cell division errors. In these cells, the early division is normal, forming constriction but does not progress until complete closure of the septum and cell separation. This is not an unexpected result since many studies based on LTs mutants (from different families) reported similar phenotypes (Cloud and Dillard, 2004; Heidrich et al., 2002; Jorgenson et al., 2015; Lommatzsch et al., 1997). Indeed, cell-wall biosynthesis stays in a homeostatic balance between construction and demolition (Johnson et al., 2014). In the absence of the activity of the LT domain provided by XAC4296, the peptidoglycan maintenance is perturbed, leading to these morphological defects observed in *X. citri*. This finding supports the hypothesis that XAC4296 function is related to the 1,6-anhydroMurNAc-containing muropeptides production, the hallmark of LT catalysis (Dik et al., 2017). These muropeptides may be transported from the periplasm to the cytoplasm through the transmembrane protein AmpG (Jacobs et al., 1994). Next, these muropeptides are degraded in the cytoplasm, and their components are used for Lipid II biosynthesis that is assembled in the cytoplasm and, again, delivered to the periplasm for *de novo* synthesis of the peptidoglycan (Barreteau et al., 2008; Bouhss et al., 2008; Butler et al., 2013; Kuk et al., 2017; Leclercq et al., 2017; Meeske et al., 2015; Mohammadi et al., 2014; Scheffers and Tol, 2015; Sham et al., 2014; Sieger et al., 2013; Vollmer and Bertsche, 2008). Therefore, our results support XAC4296 LT role, acting in the peptidoglycan synthesis and dynamics, consequently influencing cell shape as previously described for this class of enzymes (Dik et al., 2017).

In this work, we observed that the short filaments phenotype intensified when ampicillin was added to the Δ4296 mutant culture, impacting cell growth. Ampicillin is a β-lactam antibiotic that blocks the activity of penicillin-binding proteins (Delcour, 2009). Although *X. citri* appears to express β-lactamase constitutively (XAC_RS19350/ XAC3833) (Weng et al., 2004), in the Δ4296 strain, the absence of XAC4296 protein seems to hinder their ability to reconstruct cell wall making the bacteria susceptible to this antibiotic. Indeed, the bacterial exposure to β-lactams leads to disturbs in peptidoglycan recycling and accumulates MurNAc-peptides in the cytoplasm (Jacobs and Fre, 1997). In addition, during LT catalysis, the product 1,6-anhydroMurNAc-containing muropeptides are transported from the periplasm to the cytoplasm (Jacobs et al., 1994). These muropeptides are transported through the transmembrane protein AmpG (Jacobs et al., 1994). The muropeptides may be metabolized further through multiple routes to yield UDP-MurNAc-

pentapeptide, a precursor of peptidoglycan biosynthesis (Gisin et al., 2013; Uehara and Park, 2008) or may bind to AmpR and converts it into an activator of *ampC* transcription. (Dietz et al., 1997; Jacobs and Fre, 1997). Here, we hypothesize that the observed behavior of Δ4296 may be explained due to bacterial decreasing of the pool of muropeptides in the periplasm, consequently in the cytoplasm, leading to peptidoglycan synthesis imbalance and interrupting *ampC* transcription, and consequently, increasing β-lactams susceptibility. Therefore, our results strongly support that XAC4296 protein may also contribute to β-lactam antibiotic resistance in *X. citri*.

However, the morphological defects observed in the XAC4296 mutant (with or without the addition of ampicillin) can be directly related to the epimerase domain, since our results also indicate that the late cell division errors observed in the chain and short filaments phenotypes can be wholly restored with sucrose and glutamate supplementation. One possible way to interpret these results is that the XAC4296 epimerase domain may contribute to many reactions in carbohydrate metabolism, such as the D-hexose-6-phosphate mutarotase. Its absence leads to an imbalance of metabolic precursors related to anabolism pathways, indirectly affecting bacterial cell division and chromosome segregation in *X. citri*. In the absence of XAC4296, glutamate and sucrose supplement may probably provide substrate for alpha-glucose-6-phosphate production for the central carbon source metabolism, and together with the activity of the other LTs from the 3B family present in the *X. citri* genome and their known functional redundancy mechanism (Dik et al., 2017; Oliveira et al., 2018) restored the bacterial metabolism and, consequently, the cell cycle. In addition, the glucose-6 phosphate is the primary metabolic substrate present for the glycolysis, phosphogluconate, and Entner–Doudoroff pathways. Nonetheless, the glutamate and sucrose supplement may provide a comprehensive carbon source to the bacteria, facilitating energy metabolism and bacterial adaptation and survival to a stressful condition, free living, and wide host ranges. However, further studies such as protein purification and *in vitro* tests to check XAC4296 enzymatic activity are still needed to determine its role thoroughly.

Finally, previous studies raised the possibility of combining an LT inhibitor with β-lactam antibiotics as an alternative for future antibiotic development (Williams et al., 2017). For example, the possible interaction between the LT Slt35 (3B family) and Bulgecin A (Van Asselt et al., 1999), a potent LTs inhibitor, which restores the efficiency of β-lactam antibiotics against resistant bacteria (Williams et al., 2017). Taken together, our results strongly support these previous studies, suggesting future development of 3B LT and epimerase inhibitors as potential new tools, not only for the control of the disease caused by *Xanthomonas* and other phytopathogens but also for antimicrobial resistance in general.

5. **Conclusion**

The XAC4296 protein seems to be related to late cell division leading to chromosome segregation errors and ampicillin susceptibility. Moreover, we have shown that XAC4296 mutants display a metabolism-dependent phenotype, resulting from the imbalance of metabolic precursors related to anabolism pathways, suggesting that XAC4296 also acts in central carbon metabolism. In conclusion, our results strongly indicate that XAC4296 is a multi-functional protein, playing a role as a transglycosylase as much as an epimerase, impacting bacterial *fitness,* and bringing new insights into *X. citri* and other *Xanthomonadaceae* metabolism, evolution, and antimicrobial resistance emergence.

Author Contributions: Amanda C.P. Oliveira conceived and designed the experiments, performed the experiments, analyzed the data, prepared figures and/or tables, authored or reviewed drafts of the paper, approved the final draft. Rafael M. Ferreira conceived and designed the experiments, performed the experiments, analyzed the data, prepared figures and/or tables, authored or reviewed drafts of the paper, approved the final draft. Maria Inês T. Ferro contributed reagents/materials/analysis tools, authored or reviewed drafts of the paper, approved the final draft. Jesus A. Ferro conceived and designed the experiments, contributed reagents/materials/analysis tools,

authored or reviewed drafts of the paper, approved the final draft. Henrique Ferreira conceived and designed the *ex planta* growth curves and microscopy assays experiments and approved the final draft. Alessandro M. Varani conceived and designed the experiments, performed the experiments, analyzed the data, contributed reagents/materials/analysis tools, prepared figures and/or tables, authored or reviewed drafts of the paper, approved the final draft.

Acknowledgments: This study was financed in part by Coordenação de Aperfeiçoamento de Pessoal de Nível Superior - Brasil (CAPES) - Finance Code 001. We thank the Center for Biological Resources and Genomic Biology (CREBIO) from São Paulo State University (UNESP) at Jaboticabal Campus, Brazil for the laboratory and molecular biology support. We also thanks to the lab team at the Laboratory of Bacterial Genetics of the Department of General and Applied Biology, Biosciences Institute, of São Paulo State University (UNESP) at Rio Claro Campus, Brazil, and all the members of the Laboratory of Molecular Biology of the Department of Agricultural and Environmental Sciences of São Paulo State University (UNESP) at Jaboticabal Campus, Brazil for all the laboratory support. AMV, HF, JAF and MITF are recipients of productivity fellowship from the Brazilian National Research Council (CNPq) and RMF is recipient of a post-doctoral PNPD fellowship from CAPES provided by the Agronomy (Genetics and Plant Breeding) Graduate Program of the Faculty of Agricultural and Veterinary Sciences (FCAV-UNESP-Jaboticabal).

References

Aharoni, A., Gaidukov, L., Khersonsky, O., Gould, S.M.Q., Roodveldt, C., Tawfik, D.S., 2005. The "evolvability" of promiscuous protein functions. Nat. Genet. 37, 73–76. https://doi.org/10.1038/ng1482

Alcorlo, M., Martínez-Caballero, S., Molina, R., Hermoso, J.A., 2017. Carbohydrate recognition and lysis by bacterial peptidoglycan hydrolases. Curr. Opin. Struct. Biol. 44, 87–100. https://doi.org/10.1016/j.sbi.2017.01.001

Allard, S.T.M., Giraud, M.F., Naismith, J.H., 2001. Epimerases: Structure, function and mechanism. Cell. Mol. Life Sci. 58, 1650–1665. https://doi.org/10.1007/PL00000803

Altschul, S.F., Madden, T.L., Schäffer, A.A., Zhang, J., Zhang, Z., Miller, W., 1997. Gapped BLAST and PSI-BLAST: a new generation of protein database search programs. Nucleic Acids Res. 25, 3389–3402. https://doi.org/10.1093/nar/25.17.3389

Amaral, A.M. do, Toledo, C.P., Baptista, J.C., Machado, M.A., 2005. Transformation of Xanthomonas axonopodis pv. citri by electroporation. Fitopatol. Bras. 30, 292–294. https://doi.org/10.1590/s0100-41582005000300013

An, S.Q., Potnis, N., Dow, M., Vorhölter, F.J., He, Y.Q., Becker, A., Teper, D., Li, Y., Wang, N., Bleris, L., Tang, J.L., 2019. Mechanistic insights into host adaptation, virulence and epidemiology of the phytopathogen Xanthomonas. FEMS Microbiol. Rev. 44, 1–32. https://doi.org/10.1093/femsre/fuz024

Bansal, K., Kumar, S., Kaur, A., Singh, A., Patil, P.B., 2021. Deep phylo-taxono genomics reveals Xylella as a variant lineage of plant associated Xanthomonas and supports their taxonomic reunification along with Stenotrophomonas and Pseudoxanthomonas. Genomics 113, 3989–4003. https://doi.org/10.1016/j.ygeno.2021.09.021

Barreteau, H., Kovač, A., Boniface, A., Sova, M., Gobec, S., Blanot, D., 2008. Cytoplasmic steps of peptidoglycan biosynthesis. FEMS Microbiol. Rev. 32, 168–207. https://doi.org/10.1111/j.1574-6976.2008.00104.x

Boch, J., Bonas, U., 2010. Xanthomonas AvrBs3 family-type III effectors: Discovery and function. Annu. Rev. Phytopathol. 48, 419–436. https://doi.org/10.1146/annurev-phyto-080508-081936

Bouhss, A., Trunkfield, A.E., Bugg, T.D.H., Mengin-Lecreulx, D., 2008. The biosynthesis of peptidoglycan lipid-linked intermediates. FEMS Microbiol. Rev. 32, 208–233. https://doi.org/10.1111/j.1574-6976.2007.00089.x

Bueno, D., Pedrolli, D.B., Martins, P.M.M., Bocchini, D.A., Moraes, K.C.M., Facincani, A.P., Ferro, J.A., Varani, A.M., Pena, M.M., Ferreira, H., 2021. Riboswitch theo/mete as a transcription regulation tool for Xanthomonas citri subsp. citri. Microorganisms 9, 1–15. https://doi.org/10.3390/microorganisms9020329

Butler, E.K., Davis, R.M., Bari, V., Nicholson, P.A., Ruiz, N., 2013. Structure-Function Analysis of MurJ Reveals a Solvent-Exposed Cavity Containing Residues Essential for Peptidoglycan Biogenesis in Escherichia coli. https://doi.org/10.1128/JB.00731-13

Büttner, D., Bonas, U., 2010. Regulation and secretion of Xanthomonas virulence factors. FEMS Microbiol. Rev. 34, 107–133. https://doi.org/10.1111/j.1574-6976.2009.00192.x

Cloud, K.A., Dillard, J.P., 2004. Mutation of a Single Lytic Transglycosylase Causes Aberrant Septation and Inhibits Cell Separation of Neisseria gonorrhoeae 186, 7811–7814. https://doi.org/10.1128/JB.186.22.7811

Delcour, A.H., 2009. Outer membrane permeability and antibiotic resistance. Biochim. Biophys. Acta - Proteins Proteomics 1794, 808–816. https://doi.org/10.1016/j.bbapap.2008.11.005

Dietz, H., Pfeifle, D., Wiedemann, B., 1997. The Signal Molecule for β -Lactamase Induction in Enterobacter cloacae Is the Anhydromuramyl-Pentapeptide 41, 2113–2120.

Dik, D.A., Marous, D.R., Fisher, J.F., Mobashery, S., 2017. Lytic transglycosylases: concinnity in concision of the bacterial cell wall. Crit. Rev. Biochem. Mol. Biol. 52, 503–542. https://doi.org/10.1080/10409238.2017.1337705

Firrao, G., Scortichini, M., Pagliari, L., 2021. Orthology-based estimate of the contribution of horizontal gene transfer from distantly related bacteria to the intraspecific diversity and differentiation of Xylella fastidiosa. Pathogens 10, 1–17. https://doi.org/10.3390/pathogens10010046

Gisin, J., Schneider, A., Nägele, B., Borisova, M., Mayer, C., 2013. A cell wall recycling shortcut that bypasses peptidoglycan de novo biosynthesis 9. https://doi.org/10.1038/nchembio.1289

Gottwald, T.R., Graham S. J, Schubert, T.S., 2002. Citrus canker: The Pathogen and Its Impact. APS Publ. 3, 36. https://doi.org/10.1094/PHP-2002-0812-01-RV

Heidrich, C., Ursinus, A., Berger, J., Schwarz, H., Höltje, J.V., 2002. Effects of multiple deletions of murein hydrolases on viability, septum cleavage, and sensitivity to large toxic molecules in Escherichia coli. J. Bacteriol. 184, 6093–6099. https://doi.org/10.1128/JB.184.22.6093-6099.2002

Höltje, J.V., 1995. From growth to autolysis: the murein hydrolases in Escherichia coli. Arch. Microbiol. 164, 243–254. https://doi.org/10.1007/BF02529958

Hult, K., Berglund, P., 2007. Enzyme promiscuity: mechanism and applications. Trends Biotechnol. 25, 231–238. https://doi.org/10.1016/j.tibtech.2007.03.002

Jacobs, C., Fre, J., 1997. Cytosolic Intermediates for Cell Wall Biosynthesis and Degradation Control Inducible ◎ -Lactam Resistance in Gram-Negative Bacteria 88, 823–832.

Jacobs, C., Huang, L.J., Bartowsky, E., Normark, S., Park, J.T., 1994. Bacterial cell wall recycling provides cytosolic muropeptides as effectors for β-lactamase induction. EMBO J. 13, 4684–4694. https://doi.org/10.1002/j.1460-2075.1994.tb06792.x

Jeffery, C.J., 2003. Multifunctional proteins: Examples of gene sharing. Ann. Med. 35, 28–35. https://doi.org/10.1080/07853890310004101

Jenkins, C.H., Wallis, R., Allcock, N., Barnes, K.B., Richards, M.I., Auty, J.M., Galyov, E.E., Harding, S. V., Mukamolova, G. V., 2019. The lytic transglycosylase, LtgG, controls cell morphology and virulence in Burkholderia pseudomallei. Sci. Rep. 9, 1–13. https://doi.org/10.1038/s41598-019-47483-z

Johnson, J.W., Fisher, J.F., Mobashery, S., 2014. Bacterial cell-wall recycling 1277, 54–75. https://doi.org/10.1111/j.1749-6632.2012.06813.x.Bacterial

Jorgenson, M.A., Chen, Y., Yahashiri, A., Popham, D.L., Weiss, D.S., 2015. The Bacterial Septal Ring Protein RlpA is a Lytic Transglycosylase that Contributes to Rod Shape and Daughter Cell Separation in Pseudomonas aeruginosa 93, 319–335. https://doi.org/10.1111/mmi.12643.The

Kaniga, K., Delor, I., Cornelis, G.R., 1991. A wide-host-range suicide vector for improving reverse genetics in Gram-negative bacteria: inactivation of the blaA gene of Yersinia enterocolitica. Gene 109, 137–141. https://doi.org/10.1016/0378-1119(91)90599-7

Katoh, K., Standley, D.M., 2013. MAFFT multiple sequence alignment software version 7: Improvements in performance and usability. Mol. Biol. Evol. 30, 772–780. https://doi.org/10.1093/molbev/mst010

Kim, D.E., Chivian, D., Baker, D., 2004. Protein structure prediction and analysis using the Robetta server. Nucleic Acids Res. 32, 526–531. https://doi.org/10.1093/nar/gkh468

Koraimann, G., 2003. Lytic transglycosylases in macromolecular transport systems of Gram-negative bacteria. Cell. Mol. Life Sci. 60, 2371–2388. https://doi.org/10.1007/s00018-003-3056-1

Kuk, A.C.Y., Mashalidis, E.H., Lee, S., Carolina, N., 2017. conformation 24, 171–176. https://doi.org/10.1038/nsmb.3346.Crystal

Lacerda, L.A., Cavalca, L.B., Martins, P.M.M., Govone, J.S., Bacci, M., Ferreira, H., 2017. Protein depletion using the arabinose promoter in Xanthomonas citri subsp. citri. Plasmid 90, 44–52. https://doi.org/10.1016/j.plasmid.2017.03.005

Laia, M.L., Moreira, L.M., Dezajacomo, J., Brigati, J.B., Ferreira, C.B., Ferro, M.I.T., Silva, A.C.R., Ferro, J. a, Oliveira, J.C.F., 2009. New genes of Xanthomonas citri subsp. citri involved in pathogenesis and adaptation revealed by a transposon-based mutant library. BMC Microbiol. 9, 1–17. https://doi.org/10.1186/1471-2180-9-12

Leclercq, S., Derouaux, A., Olatunji, S., Fraipont, C., Egan, A.J.F., Vollmer, W., Breukink, E., Terrak, M., 2017. Interplay between Penicillin-binding proteins and SEDS proteins promotes bacterial cell wall synthesis. Sci. Rep. 7, 1–13. https://doi.org/10.1038/srep43306

Lee, J., Lee, H.J., Shin, M.K., Ryu, W.S., 2004. Versatile PCR-mediated insertion or deletion mutagenesis. Biotechniques 36, 398–400. https://doi.org/10.2144/04363bm04

Li, J., Wang, N., 2011. The wxacO gene of Xanthomonas citri ssp. citri encodes a protein with a role in lipopolysaccharide biosynthesis, biofilm formation, stress tolerance and virulence. Mol. Plant Pathol. 12, 381–396. https://doi.org/10.1111/j.1364-3703.2010.00681.x

Lommatzsch, R., Templin, M.F., Kraft, A.R., Vollmer, W., Biochemie, A., 1997. Outer Membrane Localization of Murein Hydrolases : MltA , a Third Lipoprotein Lytic Transglycosylase in Escherichia coli 179, 5465–5470.

Markowitz, V.M., Chen, I.M.A., Palaniappan, K., Chu, K., Szeto, E., Grechkin, Y., Ratner, A., Jacob, B., Huang, J., Williams, P., Huntemann, M., Anderson, I., Mavromatis, K., Ivanova, N.N., Kyrpides, N.C., 2012. IMG: The integrated microbial genomes database and comparative analysis system. Nucleic Acids Res. 40, 115–122. https://doi.org/10.1093/nar/gkr1044

Martins, P.M.M., Lau, I.F., Bacci, M., Belasque, J., Do Amaral, A.M., Taboga, S.R., Ferreira, H., 2010. Subcellular localization of proteins labeled with GFP in Xanthomonas citri ssp. citri: Targeting the division septum. FEMS Microbiol. Lett. 310, 76–83. https://doi.org/10.1111/j.1574-6968.2010.02047.x

McNeil, M., Daffe, M., Brennan, P.J., 1990. Evidence for the nature of the link between the arabinogalactan and peptidoglycan of mycobacterial cell walls. J. Biol. Chem. 265, 18200–18206. https://doi.org/10.1016/s0021-9258(17)44738-7

Meeske, A.J., Sham, L., Kimsey, H., Koo, B., Gross, C.A., Bernhardt, T.G., 2015. MurJ and a novel lipid II flippase are required for cell wall biogenesis in Bacillus subtilis 112, 6437–6442. https://doi.org/10.1073/pnas.1504967112

Mohammadi, T., Sijbrandi, R., Lutters, M., Verheul, J., Martin, N.I., Blaauwen, T. Den, Kruijff, B. De, Breukink, E., 2014. Specificity of the Transport of Lipid II by FtsW in Escherichia coli *. J. Biol. Chem. 289, 14707–14718. https://doi.org/10.1074/jbc.M114.557371

Moore, B.D., 2004. Bifunctional and moonlighting enzymes: Lighting the way to regulatory control. Trends Plant Sci. 9, 221–228. https://doi.org/10.1016/j.tplants.2004.03.005

Nowitzki, U., Wyrich, R., Westhoff, P., Henze, K., Schnarrenberger, C., Martin, W., 1995. Cloning of the amphibolic Calvin cycle/OPPP enzyme d-ribulose-5-phosphate 3-epimerase (EC 5.1.3.1) from spinach chloroplasts: functional and evolutionary aspects. Plant Mol. Biol. 29, 1279–1291. https://doi.org/10.1007/BF00020468

Oliveira, A.C.P., Ferreira, R.M., Ferro, M.I.T., Ferro, J.A., Chandler, M., Varani, A.M., 2018. Transposons and pathogenicity in Xanthomonas: Acquisition of murein lytic transglycosylases by TnXax1 enhances Xanthomonas citri subsp. citri 306 virulence and fitness. PeerJ 2018, 1–23. https://doi.org/10.7717/peerj.6111

Pena, M.M., Teper, D., Ferreira, H., Wang, N., Sato, K.U., Ferro, M.I.T., Ferro, J.A., 2020. mCherry fusions enable the subcellular localization of periplasmic and cytoplasmic proteins in Xanthomonas sp. PLoS One 15, 1–15. https://doi.org/10.1371/journal.pone.0236185

Pettersen, E.F., Goddard, T.D., Huang, C.C., Couch, G.S., Greenblatt, D.M., Meng, E.C., Ferrin, T.E., 2004. UCSF Chimera - A visualization system for exploratory research and analysis. J. Comput. Chem. 25, 1605–1612. https://doi.org/10.1002/jcc.20084

Pieretti, I., Pesic, A., Petras, D., Royer, M., Süssmuth, R.D., Cociancich, S., 2015. What makes Xanthomonas albilineans unique amongst xanthomonads? Front. Plant Sci. 6, 1–7. https://doi.org/10.3389/fpls.2015.00289

Pieretti, I., Royer, M., Barbe, V., Carrere, S., Koebnik, R., Cociancich, S., Couloux, A., Darrasse, A., Gouzy, J., Jacques, M.A., Lauber, E., Manceau, C., Mangenot, S., Poussier, S., Segurens, B., Szurek, B., Verdier, V., Arlat, M., Rott, P., 2009. The complete genome sequence of Xanthomonas albilineans provides new insights into the reductive genome evolution of the xylem-limited Xanthomonadaceae. BMC Genomics 10, 1–15. https://doi.org/10.1186/1471-2164-10-616

Rodriguez-R, L.M., Grajales, A., Arrieta-Ortiz, M.L., Salazar, C., Restrepo, S., Bernal, A., 2012. Genomes-based phylogeny of the genus Xanthomonas. BMC Microbiol. 12. https://doi.org/10.1186/1471-2180-12-43

Ryan, R.P., Vorhölter, F.J., Potnis, N., Jones, J.B., Van Sluys, M.A., Bogdanove, A.J., Dow, J.M., 2011. Pathogenomics of Xanthomonas: Understanding bacterium-plant interactions. Nat. Rev. Microbiol. 9, 344–355. https://doi.org/10.1038/nrmicro2558

Sala, R.F., Morgan, P.M., Tanner, M.E., 1996. Enzymatic formation and release of a stable glycal intermediate: The mechanism of the reaction catalyzed by UDP-N-acetylglucosamine 2-epimerase. J. Am. Chem. Soc. 118, 3033–3034. https://doi.org/10.1021/ja960266z

Sambrook, J., Fritsch, E.R., Maniatis, T., 1989. Molecular Cloning: A Laboratory Manual, in: Molecular Cloning: A Laboratory Manual. Cold Spring Harbor, NY: Cold Spring Harbor Laboratory Press.

Scheffers, D.J., Tol, M.B., 2015. LipidII: Just Another Brick in the Wall? PLoS Pathog. 11, 1–12. https://doi.org/10.1371/journal.ppat.1005213

Scheurwater, E., Reid, C.W., Clarke, A.J., 2008. Lytic transglycosylases: Bacterial space-making autolysins. Int. J. Biochem. Cell Biol. 40, 586–591. https://doi.org/10.1016/j.biocel.2007.03.018

Scheurwater, E.M., Burrows, L.L., 2011. Maintaining network security: How macromolecular structures cross the peptidoglycan layer. FEMS Microbiol. Lett. 318, 1–9. https://doi.org/10.1111/j.1574-6968.2011.02228.x

Sham, L.-T., Butler, E.K., D, M.L., Kahne, D., Bernhardt, T.G., Ruiz, N., 2014. Bacterial cell wall. MurJ is the flippase of lipid-linked precursors for peptidoglycan biogenesis 220, 220–222. https://doi.org/10.1126/science.1254522

Sieger, B., Schubert, K., Donovan, C., Bramkamp, M., 2013. The lipid II flippase RodA determines morphology and growth in Corynebacterium glutamicum 90, 966–982. https://doi.org/10.1111/mmi.12411

Sriram, G., Martinez, J.A., McCabe, E.R.B., Liao, J.C., Dipple, K.M., 2005. Single-gene disorders: What role could moonlighting enzymes play? Am. J. Hum. Genet. 76, 911–924. https://doi.org/10.1086/430799

Teige, M., Kopriva, S., Bauwe, H., Süss, K.H., 1995. Chloroplast pentose-5-phosphate 3-epimerase from potato: cloning, cDNA sequence, and tissue-specific enzyme accumulation. FEBS Lett. 377, 349–352. https://doi.org/10.1016/0014-5793(95)01373-3

Ucci, A.P., Martins, P.M.M., Lau, I.F., Bacci, M., Belasque, J., Ferreira, H., 2014. Asymmetric chromosome segregation in Xanthomonas citri ssp. citri. Microbiologyopen 3, 29–41. https://doi.org/10.1002/mbo3.145

Uehara, T., Park, J.T., 2008. Growth of Escherichia coli: Significance of peptidoglycan degradation during elongation and septation. J. Bacteriol. 190, 3914–3922. https://doi.org/10.1128/JB.00207-08

Van Asselt, E.J., Dijkstra, A.J., Kalk, K.H., Takacs, B., Keck, W., Dijkstra, B.W., 1999. Crystal structure of Escherichia coli lytic transglycosylase Slt35 reveals a lysozyme-like catalytic domain with an EF-hand. Structure 7, 1167–1180. https://doi.org/10.1016/S0969-2126(00)80051-9

Vogel, C., Bashton, M., Kerrison, N.D., Chothia, C., Teichmann, S.A., 2004. Structure, function and evolution of multidomain proteins. Curr. Opin. Struct. Biol. 14, 208–216. https://doi.org/10.1016/j.sbi.2004.03.011

Vollmer, W., Bertsche, U., 2008. Murein (peptidoglycan) structure, architecture and biosynthesis in Escherichia coli. Biochim. Biophys. Acta - Biomembr. 1778, 1714–1734. https://doi.org/10.1016/j.bbamem.2007.06.007

Weng, S.F., Lin, J.W., Chen, C.H., Chen, Y.Y., Tseng, Yi Hsuan, Tseng, Yi Hsiung, 2004. Constitutive Expression of a Chromosomal Class A (BJM Group 2) β-Lactamase in Xanthomonas campestris. Antimicrob. Agents Chemother. 48, 209–215. https://doi.org/10.1128/AAC.48.1.209-215.2004

Williams, A.H., Wheeler, R., Thiriau, C., Haouz, A., Taha, M.K., Boneca, I.G., 2017. Bulgecin a: The key to a broad-spectrum inhibitor that targets lytic transglycosylases. Antibiotics 6, 1–14. https://doi.org/10.3390/antibiotics6010008